Exploring the potential function of dimethylsulfoniopropionate and its by-product acrylate within the coral holobiont

Submitted by

Geoffrey D. Yau

In fulfilment of the requirements for the degree of

Master of Philosophy

(Natural and Physical Sciences)

College of Science and Engineering

James Cook University

August, 2023

Dedicated to my parents,

who taught me to insist on the righteous cause

擇善固執

zaak^{6} sin^{6} gu^{3} zap^{1}

Declaration

I hereby affirm that the research entitled "Exploring the potential function of dimethylsulfoniopropionate and its by-product acrylate within the coral holobiont" is an original work and does not contain any material that has been submitted for the award of any other degree or diploma, except where proper references are duly cited within the text of the examinable outcome. To the best of my knowledge, this research does not include any content previously published or authored by another individual, except where appropriate references have been provided within the text of the examinable outcome. In cases of collaborative research or joint publications, this work transparently acknowledges the respective contributions of all contributing researchers or authors.

Every reasonable effort has been undertaken to secure permissions and appropriately acknowledge the copyright owners of any included materials. I am open to receiving communication from any copyright holder who might have been inadvertently omitted or inaccurately acknowledged. This declaration serves to uphold the principles of academic integrity and responsible research conduct.

Geoffrey D. Yau

Acknowledgements

I would like to acknowledge the Australian Aboriginal and Torres Strait Islander peoples as the first inhabitants of the nation and acknowledge the Bindal and Wulgurukaba peoples as Traditional Owners of the land and waters on where much of the research for this thesis was conducted. I pay respect to Elders past, present, and future, and value the traditions, cultures, and aspirations of the First Australians of this land.

I would have never thought that Prof. David Bourne would bring me onboard this project when I emailed him seeking a volunteering opportunity during my undergraduate summer break. He offered me this project, allowing me to combine my knowledge in chemistry with coral research, which eventually became the focus of my Master's research. Completing this thesis would have been impossible without the care and support from my supervisory team: Prof. David Bourne, Dr. Cherie Motti, and Prof. David Miller. I am grateful to have all of you on my supervisory panel, for providing guidance, and most importantly, for always being there for me in both the project and in life.

I appreciate how patient David Bourne has been with my numerous questions, always offering guidance for me to find the answers myself. Your prompt one-business day feedback never ceases to amaze me. There are not enough words to express my gratitude for Cherie's dedicated effort in helping me improve my scientific writing and for her encouragement when I doubt myself. Thank you for the comprehensive training on various analytical instruments; I have learned so much about being a chemist from you. David Miller, I am thankful for your guidance in the genetic module and your consistent proactive support, especially since I am away from my home country.

Dr. Felicity Kuek and Dr. Jean-Baptiste Raina, I am deeply grateful for generously sharing your expertise throughout the project, from experiment planning to statistical analysis and result interpretation. Thank you, Rachel Johns, for letting me be involved in your minor project which became the foundation of this thesis. I would not have been able to complete the chemical analysis without Dr. Mark Robertson kindly agreeing to let me use their liquid chromatography–mass spectrometer.

The extensive experiments would not have been possible without the guidance and support from the AIMS chemistry lab, including Peter Thomas-Hall, Dr. Marina Santana, Dr. Amanda Dawson, Dr. Michaela Miller, and of course, Cherie's morning tea. A big thank you to Lauren Beattie, Paris Raynes, Clare Grimm, Coraline Marot, and Jihun Kim for assisting with coal settlements, photo imagery, and chemical extractions. Sarah Kwong and Vilde

Snekkevik, your last-minute assistance was a lifesaver, and I truly appreciate your kind help. Tia Ngo Nguyen, Millie Larkey, Michael Guyt, and Bonnie Allen, thank you for your contributions to the coral recruit counts.

I extend my sincere appreciation to Dr. Lone Hoj and Dr. Carlos Alvarez Roa for their invaluable guidance and expertise in the fields of Symbiodiniaceae inoculation and microscopy. Furthermore, I am deeply grateful to Dr. Matthew Nitschke, Dr. Nadine Boulotte, and Hugo Scharfenstein for their generous assistance and support in the process of Symbiodiniaceae identification.

Annam Raza, your assistance with graphic illustration and your companionship as a friend and housemate have been invaluable in keeping me sane throughout this journey.

My time in Townsville would have been very different if I hadn't met Kynan Hartog-Burnett, Curtis Werrett, Ella Smyth, Sam Crisp, Gina Karnasch, Tess Jenkins, Skye Thomas, Ellie Corne, Edwin Corne, Laura Missen, Casey Mitchell, Kate Malloy, Léa Breistroff, Christian O' Dea, Riley Large, Rachel Neil, Christopher and Ramona Brunner, Eryn Chang, Tony Lin, Ellen Clark, Iris Lai, and Christy Kong. Thank you all for being amazing friends and colleagues, sharing both joy and sadness with me. I am truly grateful to have you all as my friends, turning Townsville into my second home. These lifelong memories will never fade.

Lastly, I would like to express my heartfelt gratitude to my family and friends in Hong Kong, especially my parents, for raising me in the remarkable manner that you did. Thank you, Daniel Yau, for imparting scuba diving lessons when I was merely 10 years old, and to Carmen Cheung, for instilling within me the profound importance of giving my utmost in every moment and for your unwavering support in the pursuit of my dreams. Felice Yau, your determined efforts to visit me during the challenging times of the pandemic hold immeasurable significance in my heart. Uncle CK Lee, I extend my sincere appreciation for sparking my passion for marine biology and for constantly urging me to explore the vastness of the world. Tommy Man and Benny Chan, your unwavering moral support has been nothing short of invaluable. To all of you, I want to express my deep love and gratitude.

Statement of the Contribution of Others

Research and travel funding:

- James Cook University (JCU)
- ARC Centre of Excellence for Coral Reef Studies (ARC CoE)
- Australian Institute of Marine Science (AIMS)
- AIMS@JCU

Supervision:

- Dr. Cherie A. Motti (AIMS)
- Prof. David G. Bourne (JCU, AIMS)
- Prof. David J. Miller (JCU, ARC CoE)

Experimental set-up and instrumentation:

- Dr. Cherie A. Motti (AIMS; Chapters 2 and 3)
- Prof. David G. Bourne (JCU, AIMS; Chapters 2 and 3)
- Prof. David J. Miller (JCU, ARC CoE; Chapter 2)
- Dr. Mark Robertson (JCU; Chapters 2 and 3)
- Staff of the National Sea Simulator (SeaSIM, AIMS; Chapter 2 and 3)

Illustrations:

- Dr. Felicity Kuek (JCU, AIMS; Figure 1.4)
- Annam Raza (Figure 4.1)

Editorial assistance:

- Dr. Cherie A. Motti, Prof. David G. Bourne, Prof. David J. Miller (whole thesis)

Thesis Abstract

Dimethylsulfoniopropionate (DMSP) is an organic sulfur compound that plays important ecological roles in marine ecosystems. It serves as a nutrient for marine bacteria and acts as a signalling molecule for a diverse range of organisms from seabirds to fish. DMSP is central to the global sulfur cycle as it bridges the marine and atmospheric sulfur cycles by releasing its breakdown product, dimethylsulfide (DMS) gas, into the atmosphere, which can induce cloud formation. Corals are one of the largest DMSP producers in the ocean. In the coral holobiont, endosymbiotic algae of the family Symbiodiniaceae contribute the majority of DMSP production, though the coral host and coral-associated bacteria are also capable of producing this compound, adding to the coral pool. DMSP is catabolised via cleavage pathways to DMS and acrylate and these metabolites play a crucial role in coral health as they act as antioxidants and stress indicators. High levels of DMSP and acrylate are present in fast-growing Acroporids, with other genera containing considerably less. This observation suggests a potential direct relationship that may provide an advantage to Acroporids compared to other slower-growing taxa.

This study investigates the potential roles that DMSP and acrylate may have within the coral holobiont. I review (Chapter 1) aspects of coral chemistry, specifically focusing on the underlying coral calcification process before discussing the potential function of DMSP and acrylate in enhancing coral growth through aiding calcification. I then examine if supplementation with exogenous DMSP or acrylate can increase the pool of DMSP and enhance the growth of aposymbiotic coral juveniles (Chapter 2). I also investigate whether hosting different Symbiodiniaceae species can increase this pool of DMSP and enhance the growth of coral juveniles (Chapter 3). Finally, I provide a broad overview (Chapter 4) discussing in detail the evidence for and against a role of DMSP and acrylate in promoting calcification in fast growing Acroporids, in addition to other putative roles in the coral holobiont.

The ability of coral to uptake exogenous DMSP and acrylate to enhance the pool of DMSP in coral tissues and utilize it for growth is unknown. In Chapter 2, exogenous DMSP or acrylate was supplemented to newly settled aposymbiotic fast-growing *Acropora kenti* juveniles and slow-growing *Goniastrea retiformis*. DMSP concentrations in *A. kenti* tissues supplemented with DMSP were similar to those of aposymbiotic control juveniles, indicating that this species has the capacity to endogenously produce DMSP. DMSP was not detected

within aposymbiotic *G. retiformis* juvenile tissue; however, these juveniles were able to take up exogenous DMSP, as confirmed with liquid chromatography-mass spectrometry (LC-MS). Growth of both *A. kenti* and *G. retiformis* was not enhanced by exogenous supplementation of DMSP, and therefore there was no evidence that DMSP or acrylate supplementation promoted coral growth, suggesting that in *G. retiformis* the uptake of DMSP may support other ecological functions.

Different species of isolated Symbiodiniaceae cultures exhibit varying intracellular DMSP concentrations. In Chapter 3, newly settled recruits of *A. kenti* and *G. aspera* were inoculated with two different clades of symbionts. *A. kenti* juveniles hosting *Durusdinium* displayed higher DMSP concentrations within coral tissue and experienced greater growth during early ontogeny (days 4 - 37) compared to juveniles hosting *Cladocopium*. However, by the end of the experiment (day 51), corals with *Cladocopium* achieved similar DMSP concentrations and growth as juveniles hosting *Durusdinium*. Although higher growth correlated with higher DMSP concentrations in *Acropora* juveniles inoculated with Symbiodiniaceae, suggesting DMSP might be involved in coral calcification, no direct link between DMSP levels and enhanced coral growth could be established. In addition, though this study identified that *Goniastrea* aspera juveniles could uptake DMSP derived from the Symbiodiniaceae, their coral growth was not enhanced in this slow growing genus.

In summary, this study investigated the functions of DMSP and acrylate in a fast-growing *Acropora* and slow-growing *Goniastrea* recruits through exogenous DMSP supplementation and Symbiodiniaceae inoculation. The biosynthesis of DMSP in aposymbiotic *Acropora* coral juveniles was demonstrated, whereas aposymbiotic *Goniastrea* did not exhibit this capability. It reveals that *Goniastrea* juveniles have the mechanism to uptake and maintain tissue DMSP concentrations through either exogenous DMSP supplementation or Symbiodiniaceae inoculation and achieve a similar concentration as aposymbiotic *Acropora* juveniles. Additionally, this study identifies genus-specific responses to DMSP enhancement from hosting Symbiodiniaceae, where *Acropora* growth was enhanced, though *Goniastrea* juvenile growth did not differ from that of the aposymbiotic controls. These studies did not find conclusive evidence for the role of DMSP and acrylate in coral calcification, yet it is possible the promoted DMSP concentrations in coral could be fuelling other non-calcifying processes. However, these studies do highlight the complexity when investigating DMSP and acrylate metabolic pathways within the coral holobiont and have provided valuable insights into the fundamental understanding of DMSP production in

coral recruits. Multiple research directions are suggested to further the understanding of the potential functions of DMSP and acrylate in coral calcification.

Table of Contents

List of Tables

List of Figures

Chapter 1 General introduction

1.1 Ocean acidification and marine carbon chemistry

The oceans absorb nearly a third of the annual carbon dioxide (CO_2) released into the atmosphere (Gruber et al. 2019), in doing so buffering the Earth's greenhouse effect (Doney et al. 2009). This CO_2 is absorbed by seawater in the form of carbonic acid (H_2CO_3) (Doney et al. 2009), and, through the dissociation of hydrogen ions (H^+), can form bicarbonate ions (HCO_3^-) and carbonate ions (CO_3^{2-}). The dissociation of H^+ and the respective concentrations of H_2CO_3, HCO_3^- and CO_3^{2-} determine the pH of the seawater and, under normal conditions, an equilibrium between these ions is maintained (Figure 1.1). Ocean acidification (OA) occurs when large amounts of atmospheric CO_2 enters the marine system, increasing seawater CO_2 concentrations and elevating H_2CO_3 levels. This forces the equilibrium to favour H^+ dissociation and formation of HCO^{3-}. Consequently, the available CO_3^{2-} in the ocean reacts with the excess H^+ to form more HCO^{3-}, resulting in fewer CO_3^{2-} ions available for calcifying organisms shifting the equilibria, leading to an overall decrease in ocean pH.

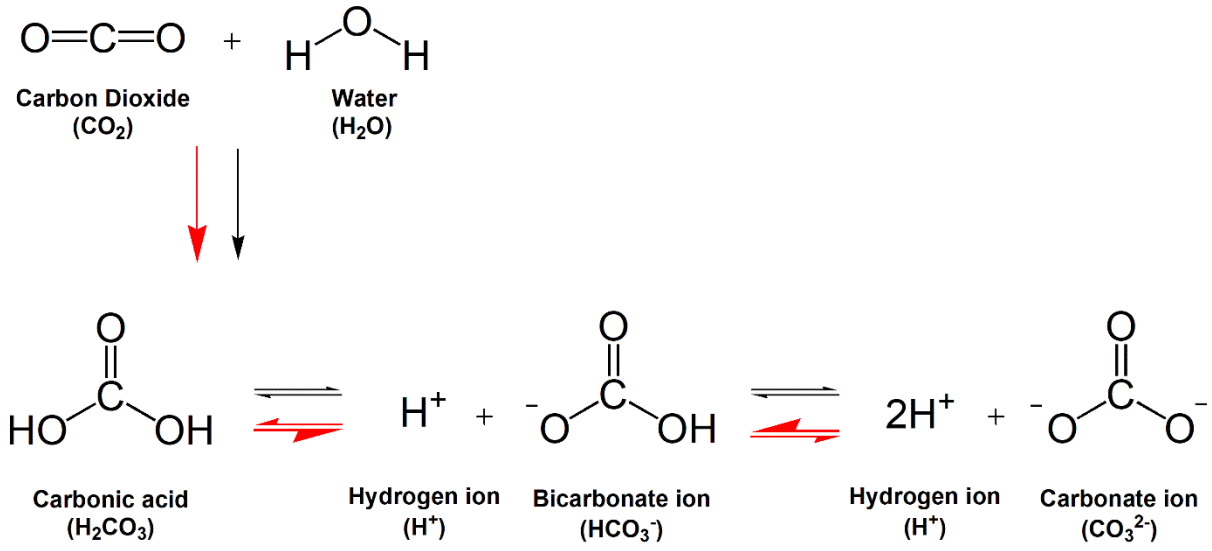

Figure 1.1 Illustration of the ocean carbonate equilibrium under normal conditions (black arrow), and the shift under ocean acidification (red arrow)

Calcifying organisms form calcium carbonate ($CaCO_3$) via an enzyme-mediated ionic reaction between calcium ions (Ca^{2+}) and CO_3^{2-} (Drake et al. 2013; Mass et al. 2013; Ramos-Silva et al. 2013; Von Euw et al. 2017). In essence, the calcification process is determined by the availability of these ions in the surrounding seawater. Under OA, less CO_3^{2-} is available in the seawater, ultimately reducing the ocean's $CaCO_3$ saturation state (Hoegh-Guldberg et al.

2007; Morse et al. 2007; Chua et al. 2013). As such, OA introduces significant challenges to coral and other calcifying marine organisms that require CO_3^{2-} for skeletal formation. The effect of OA is likely to amplify under future predicted climate scenarios of increasing atmospheric CO_2 (Jiang et al. 2019), raising concerns about future calcification rates of many marine organisms. Scleractinian corals are considered foundation reef-building species (Bellwood et al. 2003; Rocha and Bowen 2008; Inoue et al. 2013; Foster et al. 2016); the calcified skeletal structure of corals supports many marine organisms by providing habitat and nutrients (Cole et al. 2011). Therefore, any reduction in coral calcification will ultimately have wide-reaching impacts for coral reefs.

Coral skeleton is primarily composed of orthorhombic $CaCO_3$ crystal structures, known as aragonite, and while it is physically robust it is also chemically unstable (Ni and Ratner 2008; Antao and Hassan 2009). Aragonite solubility increases with acidity; therefore, OA not only reduces its saturation state and accretion rate, but also increases $CaCO_3$ dissolution, further adversely impacting coral calcification processes (Morse et al. 2007). According to modelling predictions of OA, even pre-existing coral skeletons may be at risk of dissolution (Marubini et al. 2008; Jokiel 2011; Steiner et al. 2018a). Therefore, OA represents a real and current threat to the future of coral reefs (Hoegh-Guldberg et al. 2007; Chua et al. 2013). As such, an improved understanding of the calcification process in Scleractinia coral, including the chemical pathways that mediate it, is necessary to formulate mitigation strategies to protect coral reefs into the future.

1.2 Dimethylsulfoniopropionate and the marine sulfur cycle

The CLAW hypothesis postulates that sulphated atmospheric aerosols, produced from marine algae-derived gaseous sulfur, induces cloud formation and creates a negative feedback loop to control local climate (Charlson et al. 1987) The volatile gas dimethyl sulfide (DMS), notable by its distinct smell of the sea, is produced through the enzymatic conversion of dimethylsulfoniopropionate (DMSP) (Stefels 1997). As DMS permeates through the water column it can either be oxidized to dimethyl sulfoxide (DMSO) or released into the atmosphere where it is converted to methanesulphonic acid (MSA) and sulfur dioxide (SO_2), the SO_2 further oxidizing to sulphated aerosols (Ayers and Gillett 2000; Carpenter et al. 2012). In high light conditions marine plankton produce more DMS, with more released into atmosphere; the increased concentrations of derived sulfate aerosols induce cloud formation which consequently also increases the reflectivity of solar radiation and cools ocean surface

waters, relieving temperature stress. Hence, DMSP plays an important role in the atmospheric sulfur cycle (Sievert et al. 2007).

Acrylate, a 3-carbon compound produced during the conversion of DMSP to DMS, is present in many marine organisms, including bacteria (Kirkwood et al. 2010; Todd et al. 2010), algae (Sunda et al. 2002; Alcolombri et al. 2015), diatoms (Kettles et al. 2014; Kageyama et al. 2018) and phytoplankton (Sieburth 1960; Yoch 2002). The biological function of acrylate has been investigated in numerous different biological systems (Wolfe et al. 1997a; Simó 2001a; Yoch 2002; Todd et al. 2010; Curson et al. 2011a, 2014; Moran et al. 2012) and all three compounds (acrylate, DMS and DMSP) have crucial roles in many marine ecosystems. For example, reef fish larvae which are spawned into oceanic currents, follow the distinct chemical odour of DMS to relocate back to reefs (Foretich et al. 2017). Antarctic *Procellariiform* seabirds use DMS as an olfactory foraging cue to locate their prey krill and other zooplankton that are rich in DMS (Nevitt et al. 1995; Nevitt 2000). Pygoscelid penguins feed on an algal rich diet which emits DMS and accumulates the algal-derived acrylate within their gut (Sieburth, 1961), even though in high concentrations acrylate is toxic to many organisms (Wang et al. 2002). The marine coccolithophore *Emiliania huxleyi* uses acrylate as a deterrent against grazing by microzooplankton *Oxyrrhis marina* (Wolfe et al. 1997a; Simó 2001a), while a subsequent study identified that DMSP added to seawater reduced the grazing of *Amphidinium longum* on *E. huxleyi* (Strom et al. 2003). This suggests some macrozooplankton recognize nontoxic DMSP as a signalling compound for the presence of toxic acrylate. In marine algae, DMSP, DMS and acrylate all function as antioxidants by scavenging hydroxyl radicals and reactive oxygen species (ROS) generated by the excessive photosynthetic activity induced under ultraviolet stress or other environmentally challenging conditions (Sunda et al. 2002). Indeed, acrylate is 20 times more reactive to hydroxyl radicals than DMSP (Sunda et al. 2002). Overall, these metabolically interrelated compounds have many biological functions and, in addition to contributing to the cycling of sulfur, are considered important signalling compounds in the marine environment (Strom et al. 2003).

1.2.1 The metabolism and function of DMSP in the coral holobiont

Acrylate, along with DMSP, are also produced in high quantities in fast growing hard corals of the *Acroporidae* family (Tapiolas et al. 2010). In the coral holobiont, studies investigating DMSP function have established it to be a stress response indicator (Gardner et al. 2016, 2017b; Hopkins et al. 2016). For example, the hard coral *Acropora millepora* produces high levels of DMSP, when exposed to thermal stress, hypo-saline conditions or

nutrient enrichment, which activates antioxidant mechanisms (Raina et al. 2013; Deschaseaux et al. 2014b; Jones and King 2015; Gardner et al. 2016; Aguilar et al. 2017; Westmoreland et al. 2017). The production of this DMSP was initially attributed to the Symbiodiniaceae (Broadbent et al. 2002; Oduro et al. 2012), however, studies on the other members of the coral holobiont have since confirmed the coral host (Raina et al. 2013) and several bacteria species isolated from corals (Kuek et al. 2022) are also capable of producing DMSP. Raina et al (2013) specifically demonstrated that newly settled *Acropora millepora* and *A. kenti* (formerly *A. tenuis* (Bridge et al. 2023)) juveniles, produce DMSP in the absence of their algal symbionts (Raina et al. 2013; Bridge et al. 2023). These aposymbiotic *Acropora* were capable of heightened DMSP production to combat thermal stress. In a related study, DMSP was also found to structure the coral microbial community, acting as a bacterial signalling molecule, attracting microbial communities that support coral health (Raina et al. 2010, 2013).

The amount of DMSP produced by Symbiodiniaceae is species-specific and varies depending on environmental conditions. For example, free-living *Cladocopium*, commonly found in corals, can produce higher levels of DMSP and DMS than *Durusdinium* under normal conditions. In contrast, when *Cladocopium* is thermally stressed, DMSP levels decrease to concentrations similar to those observed in *Durusdinium*, suggesting the less thermally tolerant *Cladocopium* utilises the sulfur compounds as an antioxidant to combat thermal stress (Deschaseaux et al. 2014a). However, the influence of hosting different species of Symbiodiniaceae on coral holobiont DMSP concentrations is unknown. Importantly, the Symbiodiniaceae species type has a strong effect on the host coral traits and responses to environmental conditions (Cantin et al. 2009). The endosymbiotic algal partner acquires CO_2 and water from the coral host allowing photosynthesis, in return providing photosynthates and oxygen to the coral host, supporting energy acquisition and growth (Hughes and Grottoli 2013). *A. tenuis* coral juveniles from reefs in Okinawa Japan (taxonomy currently under revision (Bridge et al. 2023)) which hosted *Durusdinium* exhibited significantly higher skeletal development in their early life stages (first 4 months) compared to those hosting *Cladocopium* (Yuyama and Higuchi 2014). However, when subjected to thermal stress, juveniles hosting *Cladocopium* displayed higher photosynthetic activity compared to *Durusdinium,* though also had a higher mortality (Yuyama et al. 2016). Collectively, this evidence implies that hosting distinct Symbiodiniaceae species could potentially impact coral traits and the concentration of DMSP within the coral holobiont. This begs the question: **can**

coral calcification be enhanced through a greater pool of DMSP made available by the symbionts?

All members of the coral holobiont (i.e., coral host, Symbiodiniaceae and bacteria) have the genetic machinery to degrade DMSP via the cleavage pathways catalysed by DMSP lyase converting DMSP into DMS and acrylate in a 1:1 ratio (Cantoni and Anderson 1956; Todd et al. 2010; Curson et al. 2011a, 2014; Shinzato et al. 2021). In the coral host, the cleavage of DMSP to DMS and acrylate is facilitated by DMSP lyase like (DL-L) genes, similar to the *Alma1* lyase enzymes that have been identified in *Emiliania huxleyi* algae (Alcolombri et al. 2015; Chiu and Shinzato 2022). These eukaryotic DMSP lyases exhibit distinct homology compared to bacterial DMSP lyases (Alcolombri et al. 2015). A genus-specific expansion of the DL-L genes have been reported in *Acropora* genera, and it is likely that these genes are actively expressed (Chiu and Shinzato, 2022; Shinzato et al., 2021), facilitating the high levels of acrylate observed in this genus (Tapiolas et al. 2010). Conversely, other coral genera such as *Galaxea*, *Goniastrea*, and *Porites* only possess a single copy of the DL-L genes (Shinzato et al. 2021; Chiu and Shinzato 2022). Genetic analyses have revealed that the DL-L genes in *Acropora* share similarities with those identified in Symbiodiniaceae and hence the endosymbiotic dinoflagellates are also equipped with the capacity for cleaving DMSP to DMS and acrylate. Interestingly, this similarity suggests that the ancestor of Scleractinian corals might have acquired DL-L genes through horizontal gene transfer from their endosymbiotic Symbiodiniaceae partner (Shinzato et al. 2021).

In coral associated bacteria, DMSP lyase encoded by the *ddd*'s genes (*dddL*, *dddP*, *dddQ*, *dddW*, *dddK*, *dddY*) have been identified and shown to be responsible for the cleavage of DMSP to DMS and acrylate (Todd et al. 2009; Raina et al. 2010; Curson et al. 2011a; Bullock et al. 2017; Tandon et al. 2020a; Kuek et al. 2022; Li et al. 2022). In addition, coral microbes are capable of cleaving DMSP with a coenzyme A (CoA) transferase (encoded by the *dddD* gene) to produce 3-hydropropionate and DMS. These bacteria utilize DMSP as carbon source to support growth and survival (Curson et al. 2008; Tandon et al. 2020a). Alternatively, DMSP can be degraded through the demethylation pathway, a process facilitated by the *dmdA* enzyme common in coral associated bacteria (Todd et al. 2007). This enzymatic activity leads to the production of 3-methyl-propionate (MMPA), which subsequently undergoes further metabolization to yield methanethiol (MeSH). MeSH is hypothesised to be further metabolised to acrylate, although the metabolic pathway is unclear (Howard et al. 2008). Furthermore, the key coral metabolites fumaric acid, glycerol and lactic

acid have been hypothesized, though yet to be confirmed, to produce acrylate (Westmoreland et al. 2017).

This compound serves as a source of organic carbon and sulfur, contributing to microbial energy production and protein synthesis (Kiene et al. 1999; Kiene and Linn 2000). In marine bacteria, the DMSP metabolism pathways are regulated based on DMSP availability and environmental condition (Gao et al. 2020). Under thermal stress, when DMSP concentrations are high, coral associated bacteria upregulate the cleavage pathway activity to produce more antioxidant DMS and acrylate (Gardner et al. 2022). However, the machinery that regulates the activity of the DMSP breakdown pathways is unknown in the coral host and Symbiodiniaceae.

1.2.2 Acrylate as a potential antioxidant and indicator of environmental stress

While both DMSP and DMS have received considerable attention and been found to have important consequences for coral health, i.e., acting as antioxidants (Sunda et al. 2002; Jones et al. 2007; Gardner et al. 2022), few studies have investigated the function of acrylate in corals (Tapiolas et al. 2010, 2013; Westmoreland et al. 2017). Acrylate has been shown to be present in high concentrations in both the coral tissues (Raina et al. 2010; Tapiolas et al. 2010) and the associated mucus layer (Raina et al. 2009; Todd et al. 2010), though is toxic to many marine organisms (Wang et al. 2002), this suggests acrylate plays a particularly important role as chemical defence in these corals.

The role of acrylate in scavenging hydroxyl radicals and ROS in coral has been investigated. As acrylate is a potential effective ROS scavenger (Sunda et al. 2002), the observed reduction in acrylate levels (Raina et al. 2013) may reflect a role in ROS elimination and hence be an indicator that corals have experienced oxidative stress. Exposure of *Acropora* juveniles to hypo-saline conditions for 24 hours also resulted in lower levels of acrylate (Aguilar et al. 2017). Similar to thermal stress, the reduction of acrylate levels may reflect scavenging excess ROS resulting from hypo-osmotic conditions. In contrast, nutrient enrichment (i.e., high ammonium and phosphate) and low calcium conditions, as occurs from agricultural runoff (GESAMP 2001; Ajikumar et al. 2005), resulted in an increase in acrylate concentrations in corals (Westmoreland et al. 2017). This suggests acrylate production is a direct response to oxidative stress, i.e., from ammonia (Sunda et al. 2002). These responses to environmental stressors indicate acrylate is an important coral stress indicator.

1.3 Skeleton formation: a chemical and biological mediated process

Significant research effort has focused on the mechanisms that drive coral skeleton formation, and it is widely acknowledged that calcification is a complex process under both physicochemical and biological control. Under the physicochemical theory, the calcification rate is dictated by CO_3^{2-} availability according to the marine carbonate equilibrium and pH of seawater (Marshall et al. 2007; Venn et al. 2011; Allison et al. 2014). However, a recent study investigating the ratio of elemental calcium to strontium and magnesium (elements that influence the crystal structure of $CaCO_3$) in the coral skeleton revealed that ratios were not thermodynamically equivalent to that in seawater (Mass et al. 2017). This equilibrium divergence indicates that the physicochemical availability of CO_3^{2-} in the environment does not reflect the calcification process of coral (Von Euw et al. 2017) and is not simply passive. Recent evidence suggests calcification is primarily biologically driven (Mass et al. 2017; Von Euw et al. 2017), with the incorporation of CO_3^{2-} into coral tissue during calcification being mediated by the organic matrix and its component proteins (Drake et al. 2013; Mass et al. 2013; Ramos-Silva et al. 2013). This finding proposes that biomacromolecules are central to the calcification process (Von Euw et al. 2017), but this does not exclude the effect of physicochemical conditions. Low CO_3^{2-} availability in seawater, as a result of OA, would still limit the calcification rate, therefore, coral skeleton formation is influenced by both physicochemical and biological factors.

1.3.1 Calcium ion (Ca^{2+}) transport mechanism for coral calcification

The calcification site in the coral organic matrix is isolated from the seawater by the epithelial tissue layer (Findlay et al. 2011). Specific mechanisms are necessary to transport calcifying materials to the calcification site through various tissues. Corals are believed to acquire Ca^{2+} for skeleton formation from the surrounding seawater through passive diffusion via Ca^{2+} channels located on the external surface of the cell membrane (Zoccola et al. 1999; Allemand et al. 2004a, 2011). Calcium ions are passively (or paracellularly) transported through the oral and coelenteron tissues and then actively into the calicoblastic epithelium cells via L-type voltage-dependent Ca^{2+} channels (Ip et al. 1991; Zoccola et al. 1999; Furla et al. 2000; Allemand et al. 2004a; Tambutté et al. 2011; Hohn and Merico 2012). Finally, plasma membrane Ca^{2+} adenosine triphosphatase (PMCA) actively pumps Ca^{2+} into the extracellular calcification site (Zoccola et al. 2004; Sevilgen et al. 2019). This process is also documented in other marine calcifying organisms, such as foraminifera and sea urchins (Khalifa et al. 2016; Vidavsky et al. 2016). However, alternate paracellular pathways that

enable passive diffusion of Ca^{2+} through the subectodermal space of the calicoblastic cells and entry into the calcification site have been proposed (Constantz 1986; Allemand et al. 2011). The potential for passive diffusion of Ca^{2+} was determined based on permeability of the calicoblastic cellular membrane (Tambutté et al. 2011). Nevertheless, there is still no definitive evidence regarding the preferred route of Ca^{2+} incorporation in corals, primarily due to the relative contribution of paracellular and transcellular transportation routes likely varying between species (Hohn and Merico 2012; Sevilgen et al. 2019). Further effort is required to truly understand Ca^{2+} permeability through the calicoblastic cell layer (Allemand et al. 2011; Tambutté et al. 2011; Sevilgen et al. 2019) and how it influences the deposition of $CaCO_3$ (i.e., calcification).

1.3.2 Carbonate ion (CO_3^{2-}) transport mechanism for coral calcification

Initially, the acquisition of CO_3^{2-} for skeleton formation in corals was thought to happen through passive diffusion of CO_2 (Pearse 1970). However, subsequent studies revealed that CO_2 concentrating mechanisms in coral cells were not the primary source of CO_3^{2-} for calcification. Instead, research demonstrated that HCO_3^- from seawater plays a crucial role in coral calcification (Herfort et al. 2008; Marubini et al. 2008; Allemand et al. 2011). A membrane bound carbonic anhydrase is responsible for actively converting seawater-derived HCO_3^- to CO_2 which then diffuses into the ectodermal cells of coral (Zoccola et al. 2015). Inside these cells, intracellular CO_2 is converted back to HCO_3^- by another carbon anhydrase and transported into the calicoblastic cells through a solute carrier bicarbonate type 4 transporter known as SLC4γ (Zoccola et al. 2015; Sevilgen et al. 2019). Alternatively, HCO_3^- can also diffuse paracellularly from the coelenteron to the outer surface of the calicoblastic tissue where it crosses the calicoblastic membrane via another SLC4γ transporter (Furla et al. 2000; Zoccola et al. 2015). Therefore, HCO_3^- is supplied to the calicoblastic tissue through both active and passive transport mechanisms. Similarly, HCO_3^- within the calicoblastic cells, regulated by carbonic anhydrase, is transported to the calcification site by SLC4γ. Additionally, CO_2, produced through mitochondrial respiration, diffuses across the membrane, and is converted to HCO_3^- by yet another carbonic anhydrase enzyme. However, the relative contribution of paracellular and transcellular HCO_3^- transport mechanisms to the calcification site is unclear and requires further investigation (Barott et al. 2015). Finally, in the presence of biomacromolecules, intracellular Ca^{2+} and HCO_3^- at the calcification stie undergoes nucleation to form $CaCO_3$ (Equation 1).

$$Ca^{2+} + 2\ HCO_3^- \rightarrow CaCO_3 + CO_2 + H_2O$$

1.4 Physical and chemical properties of calcium carbonate in aragonite formation

The shells and skeletons of various calcifying marine organisms, such as molluscs and echinoderms, consist of a combination of orthorhombic (aragonite) and rhombohedral (calcite) $CaCO_3$ crystals (Hossain et al. 2009; McDougall and Degnan 2018). In contrast, corals exclusively secrete $CaCO_3$ in the form of orthorhombic crystals (aragonite) (Higuchi et al. 2014; Falini et al. 2015). This provides corals with an ecological advantage in terms of growth, as the precipitation rate of aragonite is three times faster than calcite in seawater under the same concentrations of Ca^{2+} and CO_3^{2-} (Cohen 2003; Lemarchand et al. 2004). Furthermore, the formation of aragonite and calcite are dependent on the elemental ratios of magnesium to calcium (Mg:Ca) in the marine environment (Raz et al. 2000). In corals, high Mg:Ca ratios at the calcification site promote the formation of aragonite (Meibom et al. 2004). However, despite its fast precipitation rate, the higher Mg content distorts the aragonite atomic structure and weakens the bonding. Consequently, aragonite is chemically unstable and more susceptible to dissolution at low pH compared to calcite and vaterite (Morse et al. 2007; Ni and Ratner 2008; Ries et al. 2009).

1.5 The Skeletal Organic Matrix

The skeletal organic matrix (SOM) plays a crucial role in coral skeletogenesis (Allemand et al. 1998). It facilitates the nucleation of Ca^{2+} and HCO_3^- and is involved in the precipitation and deposition of the aragonite $CaCO_3$ (Wheeler and Sikes 1984). Coral calicoblastic cells secrete the SOM into the extracellular space between the calicoblastic epithelium layer and the skeleton (Goldberg 2001; Puverel et al. 2005; Mass et al. 2014; Falini et al. 2015). The site for $CaCO_3$ deposition is known as the scaffold, which acts as the three-dimensional blueprint for the SOM (Addadi et al. 2006; Falini et al. 2013). Comprised of biomacromolecules including proteins and lipids, the SOM captures, aligns, and binds Ca^{2+} and HCO_3^- (Allemand et al. 2011; DeCarlo et al. 2018). Extensive studies employing gas chromatography mass spectrometry (GC-MS), amino acid sequencing, and Fourier transform infrared spectroscopy (FTIR) techniques have confirmed the presence of these biomacromolecules in the SOM (Adamiano et al. 2014; Falini et al. 2015). The proteins within the SOM initiate the calcification of $CaCO_3$ by buffering the pH of the calcifying fluid medium and regulating the size and arrangement of $CaCO_3$ aggregates before crystallization (Barnes 1970; Puverel et al. 2005; DeCarlo et al. 2018).

1.6 Amorphous calcium carbonate

There has been debate in the literature as to whether aragonite is directly precipitated or gradually transformed into aragonite. Under normal conditions, $CaCO_3$ is initially precipitated in a highly unstable phase comprised of randomly arranged, spherical, nanoparticles ca. 100 nm in diameter (Gal et al. 2015), referred to as amorphous $CaCO_3$ (ACC). For sea urchins, accretion of this amorphous phase has been shown to play a crucial role in the crystallization of $CaCO_3$ into calcite (Albéric et al. 2019). In mature *Stylophora sp.*, ACC is transported to the calcification site through the transportation vesicle after which, it is deposited as ACC nanoparticles at the calcification centre near the growing skeleton surface (Mass et al. 2017). Nanoparticles aggregate, facilitating accretion and crystallization into aragonite (Mass et al. 2017; Walker et al. 2017). Akiva (2018a) presented Raman spectroscopic evidence for the presence of ACC on the outer edge of the *Stylophora* skeleton (Mass et al. 2017; Akiva et al. 2018a). However, a subsequent study also using Raman spectroscopy, was unable to detect ACC in either *Stylophora* coral tissue or the skeleton (DeCarlo et al. 2019), instead the signal previously attributed to ACC was reassigned to aragonite (Mass et al. 2017; Akiva et al. 2018a; DeCarlo et al. 2018), strengthening the case for direct deposition of aragonite (Barron et al. 2018). More recently, Drake et al (2020) has shown that ACC nanoparticles at the coral calcification site attach to one another through ion-to-ion attachment, effectively providing a scaffold that promotes aragonite crystal formation. Although the mechanism that drives this transformation in corals remains to be fully established, ACC is thought to be a contributing factor in the rapid growth of some hard coral species (Akiva et al. 2018b).

1.7 The function of aspartic acid in coral calcification

Coral acid-rich proteins (CARPs) are rich in polyaspartic acid and polyglutamic acid domains, with their carboxyl functional groups (-COOH) playing a major role in calcification (Ajikumar et al. 2005; Gotliv et al. 2005; Zhou et al. 2011; Mass et al. 2013). CARPs are found in the SOM at the interface of coral tissue and skeleton (Mann 1993; Rahman and Oomori 2008) and are intricately involved in coral calcification as a process-directing agent (Gower 2008). CARPs can represent up to 50 mol % of organic matrix making them a key component for the formation of the SOM, a prerequisite of coral skeletogenesis (Allemand et al. 1998). The level of incorporation of labelled aspartic acid into the SOM and the skeleton was greatly reduced when corals were exposed to the protein synthesis inhibitors, emetine and cycloheximide (Allemand et al. 1998). The presence of labelled aspartic acid in the coral

skeleton in the absence of inhibitors also provides direct evidence for its involvement in coral biomineralization (Mann 1993; Rahman and Oomori 2008).

CARPs 1-4 extracted from Symbiodiniaceae-free *Stylophora pistillata* cells have been shown to catalyse the deposition of $CaCO_3$ *in vitro* (Mass et al. 2013). The sequence of CARP1 is similar to the calumenins, Ca^{2+} binding proteins that have a wide distribution across the Metazoa, while CARPs 2-4 have high similarity to other acidic proteins in Scleractinian, suggesting they perform a similar function in coral calcification. CARPs that are dominate in polyaspartic acid catalyse the precipitation of $CaCO_3$ with its carboxyl functional group. The oxygen atoms on the negatively charged carboxylate group ($-COO^-$) form coordinate bonds with Ca^{2+} (Gotliv et al. 2005; Verch et al. 2011; Zhou et al. 2011), creating metal-ligands and localizing Ca^{2+} at the calcification surface (Holm et al. 1996). This drives an increase in the ionic strength thereby elevating the local dielectric constant (that is, the amount of electric potential energy in the form of induced polarization) ultimately decreasing the acid dissociation constant (pKa) (Bashford and Karplus 1990). Under these conditions electrostatic displacement can readily occur, with the negatively charged oxygen atom on the CARP carboxylate group displacing a proton (H^+) from HCO_3^- and converting it to CO_3^{2-} (Mass et al. 2013). Subsequently, the CO_3^{2-} competitively replaces the weaker carboxylate coordination bond and forms a stronger ionic bond with Ca^{2+} (Silva and Williams 2001), which results in the precipitation of $CaCO_3$ at the calcification site (Greenfield et al. 1984) (Figure 1.2).

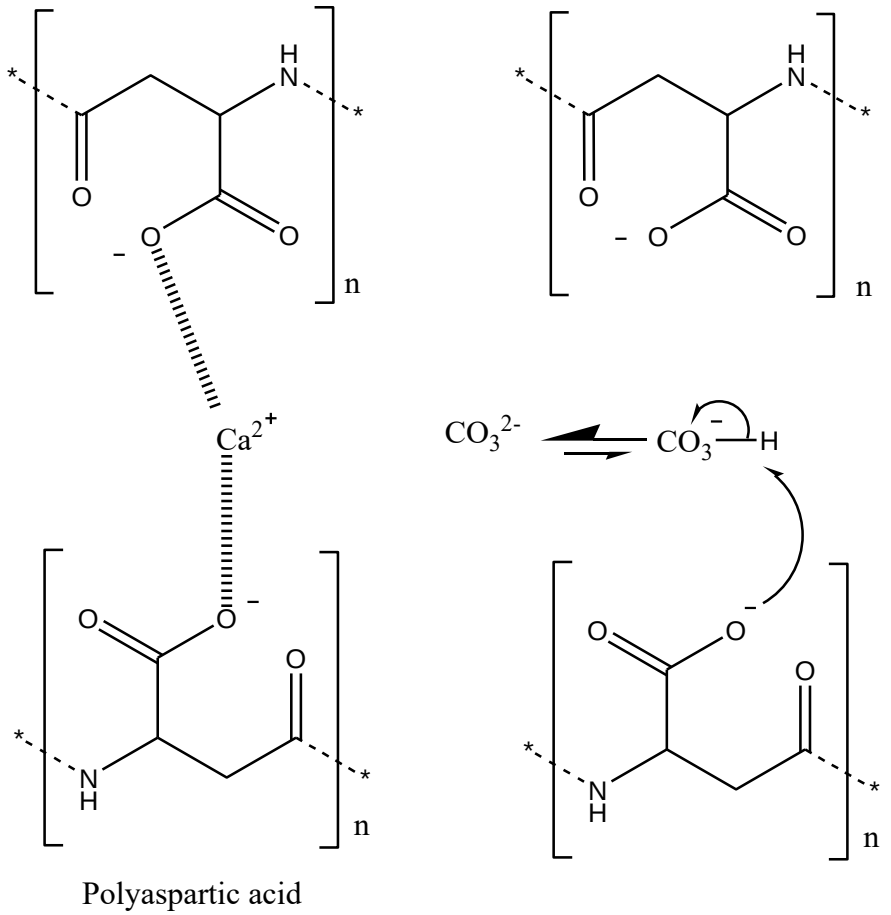

Figure 1.2 Illustration of an acidic protein rich in aspartic acid residues and the mechanism of calcification through the binding (i.e., capture) of calcium ions, adapted from (Kuek 2021) with modification; and the release of protons to produce carbonate ions, adapted from (Mass et al. 2013).

Akiva et al. (2018a) demonstrated the *in vitro* role of CARPs in coral calcification described by Mass et al. (2013) *in vivo*. Gene expression analysis indicated that CARP2 is rich in glutamic acid and is highly expressed immediately before larval settlement (Akiva et al. 2018a). By contrast, expression of CARPs 1,3 and 4, which encode proteins rich in aspartic acid domains, occurs predominantly after coral settlement (Akiva et al. 2018a). Solid state nuclear magnetic resonance (ssNMR) analysis confirmed an increase in $CaCO_3$ carboxyl group concentrations in newly settled 3-day old polyps, while genetic analysis revealed an increase in the expression of CARPs 1, 3 and 4 encoding genes (Akiva et al. 2018a). This suggests glutamic acid rich proteins may delay the calcification process before settlement (Mass et al. 2016), while aspartic acid rich proteins promote $CaCO_3$ precipitation post settlement (Aizenberg et al. 2002; Mass et al. 2013). A distinct distribution of CARPs was found in the coral skeleton, embedded with aragonite crystals in a unique fan like arrangement that is consistent with the calcification patterns observed (Mass et al.

2013).Together, the data suggests that upregulation of CARPs 1, 3 and 4 after settlement promotes the physical contact between proteins and the mineral phase facilitating crystal nucleation and calcification that ultimately result in aragonite formation (Drake et al. 2013; Akiva et al. 2018a).

1.8 Structural similarity of polyacrylic acid to polyaspartic acid and its potential role in coral

Acrylate can be readily protonated to acrylic acid, a monomer which can be polymerized to form polyacrylic acid (Llauro et al. 2004) (Figure 1.3).

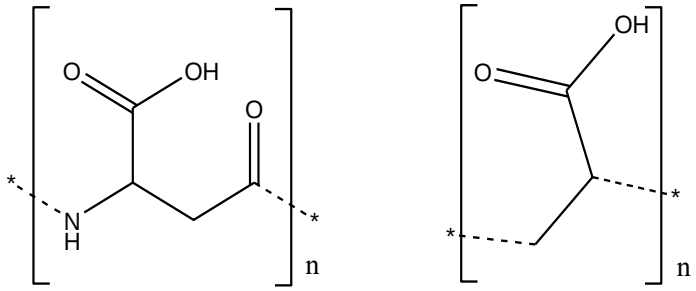

Polyaspartic acid Polyacrylic acid

Figure 1.3 Molecular structures of polyacrylic acid and polyaspartic acid

Polyacrylic acid is used as an additive in the industrial production of $CaCO_3$, and greatly enhances the mineralization rate (Cantaert et al. 2013b). Polyacrylic acid stabilizes the crystalline precursor and controls the deposition of $CaCO_3$ via a polymer-induced liquid precursor (PILP) phase into small membrane pores, enabling fine control over the *in vitro* crystal orientation of $CaCO_3$ fibres (Kim et al. 2009; Zhou et al. 2011; Cantaert et al. 2013a, 2013b). The possible involvement of polyacrylic acid in biomineralization has been recently documented (Liu et al. 2011; Nudelman et al. 2013). Polyacrylic acid induces the formation of long apatite crystals in the intermolecular space of collagen fibrils derived from calfskin. These intrafibrillar collagen zones appear to be associated to some degree with mammal skeleton formation ($Ca_3(PO_4)_2$). The wide industrial application of polyacrylic acid and its association with biomineralization processes raises questions regarding its contribution to $CaCO_3$ skeleton formation in fast-growing hard corals containing high levels of acrylate (Tapiolas et al. 2013).

A recent Raman Spectroscopy study has revealed signals reminiscent of polyacrylic acid at the growing edge of the newly deposited *Acropora* juvenile skeleton (Kuek 2021) (Figure 1.4). Polyacrylic acid possesses carboxyl functional groups (-COOH) and structurally resembles polyaspartic acid (Ajikumar et al. 2005) (Figure 1.3). Hence, polyacrylic acid may mimic the chemical functionality of polyaspartic acid. These recent findings justify further investigation into the possible role of polyacrylic acid in biologically-controlled coral calcification.

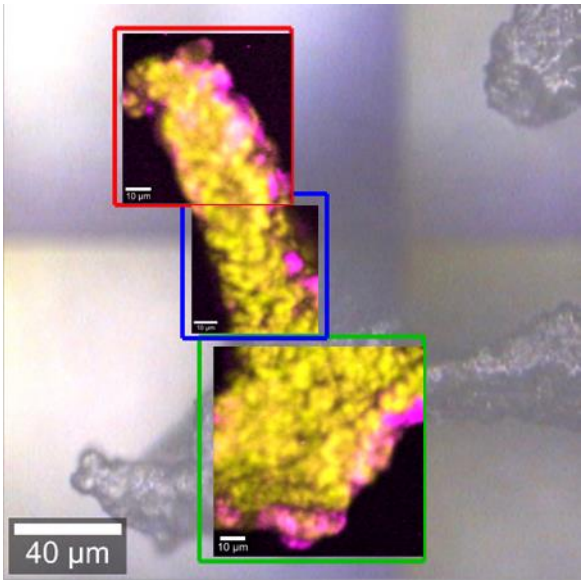

Figure 1.4 Confocal Raman microscopy of the skeleton of aposymbiotic *Acropora millepora* juveniles adapted from (Kuek 2021). Expanded view of a single septum (coloured boxes), with the false colour composite maps of aragonite (in yellow) and polyacrylic acid (in pink) (scale bar = 10 µm).

1.9 The impacts of nutrients on corals

A study examining the impact of exogenous seabird-derived nitrogen-rich nutrients to *Acropora formosa* demonstrated a four-fold growth increase in coral skeletal growth (Savage 2019). This uptake highlights the possibility of using exogenous supplementation to support coral growth, particularly in aquaria. Both DMSP and acrylate are present in seawater (Giordano et al. 2005; Xue and Kieber 2021), and the ability for corals to uptake dissolved nutrients has raised the question: **does the uptake of dissolved seawater-derived DMSP and acrylate contribute to the elevated pools of DMSP and acrylate within Acroporid corals**? One avenue to investigate this is to provide exogenous DMSP and acrylate supplements to newly settled aposymbiotic *Acropora* juveniles, then monitor for changes in the concentration of DMSP and acrylate in host tissues and compare this with recruit growth. Additionally, supplementing slow-growing taxa with DMSP or acrylate will provide a

comparison to *Acropora* treatments and, if growth is enhanced, support a possible relationship between high DMSP and acrylate content and enhanced skeleton formation. However, the use of supplements needs to be carefully considered as it may inadvertently impart an ecological disadvantage to coral. For instance, corals deficient in phosphate are more likely to experience tissue bleaching (Rosset et al. 2017). Supplementation with phosphate to improve coral bleaching resilience promotes skeleton growth, however, excessive concentrations can also adversely affect skeletal density (Dunn et al. 2012). Hence, when considering supplementation with DMSP and acrylate it is crucial to ensure the concentrations are within the normal biological range and do not compromise the health and survival of corals.

1.10 Measurement of coral growth: methods and limitations

Most Scleractinian corals have a thin tissue layer (approx. 5 mm) that covers the exterior of the $CaCO_3$ skeleton (Barnes and Lough 1992) with the skeleton often having a highly complex three-dimensional structure and variable growth form. The skeletal morphology can also vary with environmental conditions (Kramer et al. 2022). As such estimates of coral growth are often inferred from measurements such as geometric approximation of size, wax dipping, weight measurements or planar photography (Naumann et al. 2009b). Geometric approximation measures the geometry of the entire coral is derived from basic dimensional parameters such as radius and height (Naumann et al. 2009a). This method is simple, non-destructive, and can be applied to most coral taxa. It does not require complex instrumentation and allows for repeated measurements over time (Naumann et al. 2009a). However, it introduces bias in height measurements of corals with complex morphology, including highly branched species such as the Acroporids, and does not account for the change in volume or surface area (SA) (Ferrari et al. 2017). This limitation has mostly been overcome by the wax dipping method, which applies a wax cast for SA estimation (Naumann et al. 2009a). Not only is this method destructive, which limits its application in longer-term growth studies, errors resulting from wax surface tension are introduced for corals smaller than 5 cm^2 (Veal et al. 2010). Weight estimates of the coral can also be combined with SA estimates to calculate skeleton density (Dodge and Brass 1984). Unfortunately, none of these methods are suitable for measuring the growth of newly settled coral recruits with sizes significantly <5 cm^2 and having low biomass. Planar photography has been successfully employed for coral that are both small and large in size (Raina et al. 2013; Aguilar et al. 2017). This non-destructive method measures the coral surface area from photographic images taken directly above the specimen by tracing the outline of the coral

structure and calculating the approximate SA (Naumann et al. 2009a). Inherently, this method is limited to two-dimensional growth measurements and does not account for any vertical growth (DeCarlo et al. 2017). Despite this limitation, and given it is non-destructive, this method remains reliable for measuring coral juvenile growth during the first six months post-settlement, when coral skeleton vertical extension is minimal. Planar photography can be combined with the technique of structure form motion (SfM) to capture a photogrammetric measurement with higher resolution enabling a more accurate estimation of coral juvenile SA. SfM requires similar photographic equipment (House et al. 2018) with the ability to acquire images from various angles. Hemispheric image processing software combines all images and creates a 3-dimensional model of the coral surface from which the SA is then calculated. A recent study has also shown that the three-dimensional morphological structure of coral juveniles can be accurately modelled using a dental scanner (Quigley and Vidal Garcia 2022).

1.11 Measurement of DMSP and acrylate in corals

As all members of the coral holobiont, i.e., the coral host, Symbiodiniaceae and associated bacteria, can produce DMSP and acrylate (Raina et al. 2010, 2013, 2017; Tapiolas et al. 2010; Kuek et al. 2022) it is first necessary to decouple the contribution made by each partner to the acrylate pool. Metabolism of Symbiodiniaceae can be studied *in vitro* by extracting the symbionts from their coral host (Lesser et al. 1990). Similarly, coral-associated bacteria can be isolated and, in some instances, cultured to enable metabolic investigation (Raina et al. 2017). In contrast, metabolic studies of the coral host are considerably more challenging to undertake, especially as the coral is heavily dependent on its symbiont partners for nutrients and energy (Hughes and Grottoli 2013). The contribution of DMSP and acrylate from Symbiodiniaceae will interfere with the estimate of coral host-derived DMSP and acrylate concentrations. The use of aposymbiotic (symbiont-free) coral recruits can, to some degree, overcome this limitation. Under normal conditions newly settled juvenile corals acquire Symbiodiniaceae within 7-days post-settlement (Nitschke et al. 2016), however, they can be maintained in aquaria for several weeks in the absence of their symbiotic partner (Raina et al. 2013), providing an opportunity to study the coral host in isolation. Unfortunately, aposymbiotic coral juveniles are only viable for short-term experiments, hence the study of DMSP and acrylate metabolism across different life stages remains limited. Moreover, this method does not apply to coral taxa for which symbionts are maternally inherited.

A wide variety of chemical analytical techniques are available to profile coral metabolites. The application of these techniques largely depends on the chemistry (i.e., DMSP, DMS, acrylate and downstream by-products) and the coral compartment being investigated (i.e., tissue, symbionts and skeleton). For example, GC-MS is a well-established method for the **indirect** quantification of DMSP via the detection and quantification of DMS gas released by coral tissue under alkaline conditions (Sulyok et al. 2001; Broadbent and Jones 2004; Deschaseaux et al. 2014b, 2014a, 2016; Swan et al. 2017). GC-MS is capable of detecting DMS at very low concentrations (~1 nmol) due to its high sensitivity (Yost and Mitchelmore 2010). However, as acrylate can be produced in corals via metabolic pathways other than through DMSP metabolism (Westmoreland et al. 2017), GC-MS quantification of DMS is not suitable for the indirect quantification of acrylate.

Ultra-performance liquid chromatography coupled with mass spectrometry (LC-MS) with a hydrophilic interaction liquid chromatography phase (HILIC) has been used for the selective and direct detection of DMSP and acrylate in coral tissue extracts (Spielmeyer and Pohnert 2010). With the advantage of low detection limits (~20 nM), LC-MS does not require purification or derivatization prior to analysis and has permitted direct quantification of the acrylate in extracts not only of coral tissue but also of microalgae and phytoplankton (Spielmeyer and Pohnert 2010). Therefore, considering the relative low detection limit of this technique, LC-MS is well suited to the quantification of DMSP and acrylate within coral recruit tissues.

Quantitative proton nuclear magnetic resonance (^{1}H-qNMR) can provide precise quantification of target molecules (Pauli 2001), and allows direct simultaneous quantification of both DMSP and acrylate in coral tissue (Tapiolas et al. 2013). While ^{1}H-qNMR is non-destructive with respect to the chemistry, its higher detection limit means sample mass becomes a limiting factor and is therefore not the most suitable method for analysing low biomass coral recruits.

Previous studies have confirmed DMSP biosynthesis pathways in cultures of Symbiodiniaceae and bacteria using nano-scale secondary ion mass spectrometry (NanoSIMS) imaging (Raina et al. 2017). This method revealed the distribution of stable sulfur isotope markers in Symbiodiniaceae, following the enzymatic conversion of inorganic labelled sulfate ($^{34}SO_4^{2-}$) into labelled ^{34}S-DMSP within cells. The subsequent degradation of ^{34}S-DMSP by bacteria was surmised by the drop in ^{34}S-DMSP concentration over time,

however, as NanoSIMS is unable to capture the volatile ^{34}S-DMS, this method was not able to confirm which DMSP degradation pathway was followed. Regardless, Raina et al. (2017), demonstrate the possibility of using NanoSIMS and a labelled sulfur marker to identify the DMSP uptake in the coral holobiont.

Investigation of coral skeleton chemistry requires different approaches. FTIR coupled with X-ray diffraction (XRD) has been used to detect the presence of $CaCO_3$ within the intact coral skeleton and establish the crystalline phase as aragonite (Mansur et al. 2005). Solid state NMR (ssNMR) with magical angle detection has been applied to establish the presence of $CaCO_3$ in the form of aragonite crystals in the SOM of ^{13}C-labelled pre-settled coral planula (Akiva et al. 2018a). Raman spectrometry has similarly been used for the detection of crystalline structures of $CaCO_3$ in coral skeletons and other marine calcifiers (Akiva et al. 2018a; DeCarlo et al. 2019). Raman has more recently been used to detect polyacrylic acid at the growing edge of the newly deposited skeleton in *Acropora* juveniles, suggesting that polyacrylic acid may play a role in the coral calcification process, similar to that of polyaspartic acid-rich proteins (Kuek 2021) (Figure 1.4).

1.12 Conclusions and Study Aims

DMSP and acrylate are present in high concentrations in several fast-growing Acroporid species, with both compounds potentially having important roles in the health of the coral holobiont. These high metabolite levels in Acroporids and their relatively fast growth rates suggest there may also be a direct relationship that affords an advantage over slower growing taxa. Hence, a thorough understanding of coral chemistry, and specifically the underlying coral calcification process is required. Although the pool of DMSP and acrylate in the coral holobiont is predominantly controlled by Symbiodiniaceae juvenile corals are capable of synthesising DMSP. Currently, little is understood regarding the potential for exogeneous uptake of DMSP or acrylate or the contribution of different Symbiodiniaceae species (noting free-living *Cladocopium* has a higher DMSP production per cell than *Durusdinium*) to the pool of these metabolites within the coral holobiont. Furthermore, the link between DMSP and acrylate tissue concentrations and growth rates remain to be established. Therefore, the primary aims of this study are:

1. To examine whether supplementation with exogenous DMSP or acrylate can increase the pool of DMSP and enhance the growth of aposymbiotic coral juveniles.

Changes in the surface area and the concentration of DMSP in *Acropora* and non-*Acropora* juveniles will be examined in response to DMSP and acrylate supplements to determine whether they have the capacity to take up and utilise exogenous DMSP and acrylate.

2. To investigate whether inoculation of coral juveniles with different Symbiodiniaceae species can increase the pool of DMSP and enhance recruit growth. Changes in the surface area and the concentration of DMSP in *Acropora* and non-*Acropora* juveniles will be examined after inoculation with common *Cladocopium* or *Durusdinium* symbionts to determine which, if either, species affords an early life stage advantage.

Together these studies can offer valuable insights into the health and resilience of coral.

Chapter 2: Supplementation of aposymbiotic recruits with DMSP and acrylate induces species-specific responses in *Acropora kenti* and *Goniastrea retiformis*

2.1 Abstract

Corals are one of the largest producers of dimethylsulfoniopropionate (DMSP) in the ocean. DMSP concentrations within coral tissues fluctuate under different environmental stresses. In some coral genera, DMSP and its breakdown products dimethyl sulfide (DMS) and acrylate likely serve as antioxidants in response to stress. High levels of DMSP and acrylate are found in fast-growing *Acropora* while, in contrast, only low or undetectable levels of DMSP and acrylate are observed in slow-growing non-Acroporid species. It is postulated that the high DMSP and acrylate levels in *Acropora* aid calcification and the formation of the coral skeleton. This study aimed to address this through supplementation of newly settled aposymbiotic *Acropora kenti* and *Goniastrea retiformis* juveniles with exogenous DMSP or acrylate. Supplementation of juveniles with 1 mM DMSP resulted in similar survival profiles to that of non-supplemented controls and there was no enhancement of growth for either species. DMSP concentrations in *A. kenti* tissues supplemented with DMSP were similar to those of aposymbiotic control juveniles, indicating this species has the capacity to endogenously produce DMSP. DMSP was not detected within aposymbiotic *G. retiformis* juvenile tissue, though juveniles were able to take up exogenous DMSP. Supplementation with acrylate demonstrated a toxicity effect to juveniles of both species with no enhancement of growth. No evidence was found to support a role for DMSP or acrylate in early life stage coral calcification. Nevertheless, this study provides valuable knowledge towards the genus-specific metabolism of DMSP and acrylate within the coral holobiont.

2.2 Introduction

Dimethylsulfoniopropionate (DMSP) is an abundant organic sulfur compound in the oceans (Gregory et al. 2021) and, along with its volatile breakdown product dimethyl sulfide (DMS), has been included in recent climate models to account for their contribution to the global atmospheric sulfur cycle (Aumont et al. 2002; Bopp et al. 2004; Hoffmann et al. 2021). Scleractinian corals are one of the largest producers of DMSP in marine ecosystems (Broadbent and Jones 2004; Fischer and Jones 2012). Although the coral host and its associated bacteria are capable of DMSP production (Raina et al. 2013; Kuek et al. 2022), the majority of DMSP within the coral holobiont is derived from the endosymbiotic algal partner, Symbiodiniaceae (Hill et al. 1995; Broadbent et al. 2002), that are located within the coral gastrodermal tissue layer. DMSP is associated with the coral stress response, which suggests that the fluctuation of DMSP concentrations within coral tissues is a good indicator of overall environmental stress. When corals are exposed to thermal or osmotic changes or nutrient enrichment, DMSP concentrations increase (Raina et al. 2013; Gardner et al. 2016, 2017a; Aguilar et al. 2017; Westmoreland et al. 2017). DMSP also functions as an antioxidant to protect coral from oxidative damage through scavenging reactive oxygen species (ROS) and oxygen radicals produced during coral respiration and photosynthesis (Sunda et al. 2002; Deschaseaux et al. 2014b; Gardner et al. 2016). In addition, DMSP can structure the microbial community associated with the coral holobiont, as it represents an abundant carbon source for bacterial metabolism and functions as a signalling molecule to attract bacteria that support coral health (Raina et al. 2009, 2010; Tandon et al. 2020b). Overall, DMSP serves various important roles in the coral holobiont.

DMSP can be broken down through two different metabolic pathways, demethylation and cleavage. In the demethylation pathway, the *dmdA* enzyme catabolises DMSP breakdown into methylmercaptopropionate (MMPA), methanethiol, acetaldehyde, CO_2 and acetate (Howard et al. 2006; Todd et al. 2007; Reisch et al. 2011b). Methanethiol (MeSH) is a source of organic sulfur and carbon and serves as an energy source, supporting protein synthesis in coral associated bacteria (Kiene et al. 1999; Raina et al. 2010). Alternatively, through the cleavage pathway, DMSP lyase catalyses the formation of DMS and acrylate (Cantoni and Anderson 1956; Yoch 2002; Alcolombri et al. 2015; Zhang et al. 2019; Shinzato et al. 2021). Acrylate has a three-carbon (C3) backbone and has structural similarity to other C3 molecules involved in energy production in cellular cycles (Preuß et al. 1989). Acrylate likely plays other roles in the coral and while it is toxic to some marine organisms and inhibits bacterial

growth (Sieburth 1960; Wang et al. 2002), within corals, it is postulated to control microbial community structure and function as an antioxidant (Sunda et al. 2002; Jones et al. 2007; Raina et al. 2009).

It is not clear what regulates the DMSP catabolism activity of the demethylation and cleavage breakdown pathways, though both likely occur simultaneously within the coral holobiont (Reisch et al. 2011b, 2013). This process has been described in bacteria, with activation of the pathways dependent on the DMSP concentration and cellular sulfur demand (Kiene et al. 2000; Gao et al. 2020). In bacteria, DMSP undergoes demethylation when concentrations are low, while the cleavage pathway is activated at high DMSP concentrations (Gao et al. 2020). For example, when bacteria isolated from the coral microbiome were subjected to environmental stressors, i.e., thermal or oxidative stress, DMSP was predominantly metabolised through the cleavage pathway to produce high levels of DMS and acrylate, these molecules likely functioning as antioxidants to harvest the resulting ROS produced (Gardner et al. 2022; Kuek et al. 2022; Wang et al. 2022). High concentrations of DMSP and acrylate have also been found in the tissues of the fast-growing coral *Acropora* under ambient, non-stress conditions (Tapiolas et al. 2010, 2013). Furthermore, DMSP-like lyases that catalyse the cleavage pathway are duplicated in the *Acropora* genome (Shinzato et al. 2021; Chiu and Shinzato 2022). The high concentrations of DMSP and acrylate in the tissues of some coral species, specifically members of the Acroporids, suggest that these compounds could have ancillary functions within the coral holobiont.

Acrylate can be readily protonated to acrylic acid and polymerized to polyacrylic acid. Polyacrylic acid is often used as an additive to enhance mineralization rates during the industrial production of calcium carbonate ($CaCO_3$) (Cantaert et al. 2013b). The acid function in stabilizing the $CaCO_3$ intermediate and controlling the structural orientation of $CaCO_3$ with a polymer-induced liquid precursor (Donnet et al. 2005; Kim et al. 2009; Zhou et al. 2011; Cantaert et al. 2013b). Polyacrylic acid has also been used to promote biomineralization through the precipitation of apatite (calcium phosphate) along collagen fibrils, mimicking natural cellular processes that are controlled by polyaspartic acid (Liu et al. 2011; Nudelman et al. 2013). In coral, acidic-rich proteins (i.e., aspartic and glutamic acids with carboxyl functional groups [$RCOO^-$]) in the organic matrix, catalyses the coral skeleton calcification process (Ajikumar et al. 2005; Gotliv et al. 2005; Zhou et al. 2011; Cantaert et al. 2013b; Mass et al. 2013; Mummadisetti et al. 2021). Specifically, they catalyse the precipitation of $CaCO_3$ which is initiated by stabilizing the calcium ion (Ca^{2+}) at the calcification site (Mass et

al. 2013; Akiva et al. 2018a). In polyaspartic acid-rich proteins the negatively charged resonance $RCOO^-$ establishes a coordinate bond with Ca^{2+}, forming metal-ligand bonds that deliver Ca^{2+} to the calcification surface (Holm et al. 1996). This Ca^{2+} localisation increases the ionic strength of the complex, raising the local dielectric constant and reducing the acid dissociation constant (pKa) (Bashford and Karplus 1990). In addition, the negatively charged resonance stabilised $RCOO^-$, facilitates electrostatic displacement of the hydrogen ion (H^+) associated with the bicarbonate anion (HCO_3^-), thereby forming the carbonate ion (CO_3^{2-}). The CO_3^{2-} anions bind preferentially to Ca^{2+}, replacing the weak coordination bond between polyaspartic acid-rich protein and Ca^{2+} with a stronger ionic bond, facilitating the controlled precipitation of $CaCO_3$ and formation of highly structured and uniform aragonite calcified crystals. Under these conditions calcite precipitation is inhibited (Greenfield et al. 1984; Cantaert et al. 2013b; Drake et al. 2013; Von Euw et al. 2017; Laipnik et al. 2020). In coral juveniles, the expression of coral acidic-rich proteins dominant in the polyaspartic acid domain is upregulated in the post-settlement stage (Drake et al. 2013; Akiva et al. 2018a), suggesting that polyaspartic acid-rich proteins are critical for skeleton formation in the early life stages. However, the polyaspartic acid-rich protein induced aragonite precipitation is inhibited at low pH, which could reduce coral reef calcification rates in the future with ocean acidification (Kellock et al. 2020). The presence of high levels of acrylate in fast-growing coral (Tapiolas et al. 2010), and the revelation that newly settled aposymbiotic juveniles of *A. millepora* and *A. kenti* (formerly *A. tenuis*) in the Great Barrier Reef region are capable of its production (Raina et al. 2013), suggests that acrylate may also play a role in coral calcification; i.e. its polymer, polyacrylic acid (capable of promoting industrial calcification) may provide the same $RCOO^-$ functionality as aspartic acid-rich protein in catalysing coral calcification (Miller and Holcombe 2001; Cantaert et al. 2013b). Acrylate may prove especially relevant for Acroporids with rapid skeletal calcification rates.

To examine the potential contribution of DMSP and its breakdown product acrylate to coral growth and calcification, aposymbiotic *Acropora* juveniles were supplemented with exogenous DMSP or acrylate. The survival and growth characteristics of juveniles were measured and compared with those of the slow growing species *Goniastrea retiformis*, which was expected not to produce DMSP and to contain comparatively low levels of acrylate, based on results from adult corals of the same genus (*Goniastrea aspera*) (Tapiolas et al. 2013). To assess the physiological responses of different taxa to DMSP and acrylate supplements, DMSP concentrations within tissues of juvenile corals were also measured. This

study contributes to the understanding of the physiological responses of aposymbiotic coral juveniles to chemical supplements and the potential function of DMSP and acrylate in the growth of early life stage corals of different taxa.

2.3 Methods

2.3.1 Chemical Synthesis

DMSP was synthesized in the same batch with Kuek (2021) following the published method in Chambers et al. (1987) with some modifications. Briefly, 98% sulfuric acid (H_2SO_4; Ajax Chemicals; CAS: 7664-93-9) was added dropwise onto sodium chloride (NaCl; Fisher scientific; CAS: 7647-14-5) within a sealed flask to produce hydrogen chloride gas [$HCl_{(g)}$]. After that $HCl_{(g)}$ was bubbled slowly into a mixture of dichloromethane (CH_2Cl_2; 20 mL; Fisher Scientific; CAS: 75-09-2), DMS (5 mL; Sigma Aldrich; CAS: 75-18-3) and acrylic acid (CH_2=CHCOOH; 4 mL; Sigma Aldrich; CAS: 79-10-7) that had been distilled over copper wool. This reaction formed a white precipitate that was then filtered and recrystallized with ice bath chilled ethanol and then freeze-dried overnight. The final yield of DMSP was 27%, the low yield being a consequence of losses during the final filtering step in which the product was washed away by cold ethanol when removing the unreacted acrylic acid. A standard 1 mM DMSP solution was made up with Milli-Q water. Similarly, a 1mM Acrylate standard was prepared by dissolving sodium acrylate (Sigma Aldrich; CAS 7446-81-3) in Milli-Q water.

2.3.2 Coral Sample Collection

Four gravid colonies of *Acropora kenti* (formerly *Acropora tenuis*) (Bridge et al. 2023) were collected on the 25th of October 2020 from Yunbenun, Magnetic Island, Townsville (19°07'45.6"S 146°52'39.5"E) in the inshore central Great Barrier Reef (GBR) region. Colonies were transported to the Australian Institute of Marine Science (AIMS) National Sea Simulator (SeaSIM) and placed in outdoor quarantine tanks at ambient seawater temperature (26.5°C) a week prior to spawning. Colonies spawned (i.e., release of sperm and egg bundles) at 18:45 on the 3rd of November 2020 and fertilisation was achieved following published culture methods (Quigley et al. 2016). Briefly, sperm and eggs from four individual colonies were mixed to allow fertilization before being transferred to an 800 L culture tank (density of 0.6 eggs per mL) at 27°C with aeration and a continuous flow of 1 µm filtered seawater (FSW) in continuous darkness to minimize algal growth. The culture tank was cleaned twice daily to prevent biofilm formation with larvae maintained for 9 days, at which time they displayed signs of settlement competency (detailed below). *Goniastrea retiformis*

colonies were collected in late November 2020 from Davies Reef (18°49'09.4"S 147°38'58.0"E, central GBR region) and spawned on the 4th of December 2020, with larvae cultured using the same approaches as previously detailed for *A. kenti* (Quigley et al. 2016). Every effort was made to ensure Symbiodiniaceae were not present, while no effort was made to eliminate bacteria associated with eggs, sperm or the local aquaria. Furthermore, corals were not fed for the duration of the experiment to ensure they only relied on their lipid reserves and actively sought energy sources from the surrounding seawater.

Coral settlement competence assays for both species were undertaken each day from 7 days post-spawning. Ten coral larvae were added to each well of a 6-well plastic culture plate (Thermo Scientific) containing 10 mL of FSW, after which 0.5 cm^2 of a fresh crustose coralline algae (CCA) chip was placed into 5 of the 6 wells to induce settlement (Appendix A). The well with no CCA chip was used as a control to ensure addition of a CCA chip did not induce confounding effects such as mortality. Plates were incubated at 28°C in darkness for 24 hours to allow metamorphosis. Coral larvae were considered competent when >80 % of larvae in each well had settled on a substrate (either well plate or CCA) at that time. Once competency had been confirmed (i.e., 9 days post spawning for *A. kenti*; 10 days post spawning for *G. retiformis*), aliquots of approximately 70 swimming larvae were added to each well of a 6-well plastic culture plate containing 5 mL of FSW and left to settle in the incubators following the same conditions as the settlement competence assays. After 24 hours, the CCA chip, coral juveniles that had settled at the edge of the well, and any larvae that had not settled or were not fully metamorphosed were removed. A complete seawater change was performed carefully using a pipette and each well was filled with 10 mL of new FSW, and incubation continued for a further 48 hours to allow coral juveniles to develop the basal disc and attach permanently to the well plate. The 6-well plates containing 12-days post-spawning *A. kenti* juveniles or 13-days post-spawning *G. retiformis* were randomly assigned to one of three different treatment groups, as follows: FSW as control (C), exposure to 1 mM of DMSP (D) and exposure to 1 mM acrylate (A).

For *A. kenti*, the experiment was conducted for 16 days. *Goniastrea* is a genus that is difficult to culture and settle in aquaria compared to *Acropora*; and hence during the settlement stage, a lower number of juveniles settled resulting in the duration of the *G. retiformis* experiment being reduced to 8 days (Table 2.1). A total of 5803 *A. kenti* settled juveniles were used in this study; 1828 juveniles in the Control treatment (average of 32 juveniles per well of each 6-well plate), 2037 in the DMSP treatment (~ 34 juveniles per well

of each 6-well plate) and 1938 (~ 32 juveniles per well of each 6-well plate) in the acrylate treatment. For *G. retiformis*, 894 juveniles were used (Control = 502 juveniles, ~18.6 per well; DMSP treatment = 214 juveniles, ~20.9 juveniles per well; and acrylate treatment = 178 juveniles, ~14.8 per well).

Table 2.1 Experimental timeline for *Acropora kenti* (Day 0 = 12 days post-spawning) and *Goniastrea retiformis* (Day 0 = 13 days post-spawning) depicting days when each procedure was performed.

Experimental Procedure	***A. kenti***	***G. retiformis***
Seawater change	Day 0, 1, 3, 5, 7, 9, 11, 13, 15	Day 0, 1, 3, 5, 7
Supplementation	Day 1, 3, 5, 7, 9, 11, 13, 15	Day 1, 3, 5, 7
Growth measurement	Day 0, 4, 6, 8, 10, 12, 14, 16	Day 0, 2, 4, 6, 8
Coral tissue extraction	Day 0, 2, 4, 8, 16	Day 0 **(control only)**, 8

2.3.3 Chemical supplementation

FSW in 6-well plates were exchanged on days 0, 1, 3, 5, 7, 9, 11, 13, and 15 for *A. kenti*, and for *G. retiformis*, on days 0, 1, 3, 5, and 7 (Table 2.1). A squeeze bottle was used to gently flush the coral juveniles to remove mucus residue, after which, residual seawater was carefully decanted. New FSW (10 mL) was added, the plate gently swirled, and the washing process repeated to ensure that all detritus and residual supplements were removed. Finally, 10 mL FSW was added to the wells.

In this study, the supplement concentration of 1 mM was selected for DMSP and acrylate based on the survival results of *Acropora* recruits observed during preliminary investigations of varying DMSP concentration exposures (Johns 2019), and the acrylate concentrations found across different coral genera (Tapiolas et al. 2013).

At the start of the experiment (Day 0), all wells were left for 24 hr before the addition of the treatment. Aliquots (38 µL) of 1 mM of DMSP or acrylate supplements were added to each treatment well immediately after FSW exchanges on days 1, 3, 5, 7, 9, 11, 13, and 15, for *A. kenti*, and days 1, 3, 5, 7, for *G. retiformis*. Similarly, 38 µL aliquots of FSW were added to each well of the control group. After water exchange and supplementation, the 6-well plates were returned to the incubator and maintained at 28°C in darkness.

2.3.4 Coral growth and survival measurements

Coral juveniles were photographed at two-day intervals throughout the experiment (days 0, 4, 6, 8, 10, 12, 14, and 16 for *A. kenti* and days 0, 2, 4, 6, 8 for *G. retiformis*), with the 6-well plates temporarily transported to the photography facility that was maintained at a constant temperature of 28°C. Coral juveniles were photographed using a Nikon AF-S 60mm macro lens on a Nikon D810 camera, in an Ikaite underwater housing with a 1000 luminance Weefine ring light attached to the lens port thread. The whole camera assembly was mounted on a robotic arm with 3-degrees of freedom (3 translation). The Computer Numerical Control (CNC) machine was operated according to the recorded coordinate script in Planet CNC software. The 6-well plates were positioned in the same location for photography. The programmed robotic arm ensured that the camera moved to the same coordinates for each time point, allowing coral growth to be monitored in a time-lapse series. For photography, a black, dull polystyrene foam mat was placed underneath and around the 6-well plate to reduce light reflection from the seawater and the transparent plastic well plate. To maintain consistency, all photos were taken using the same settings: manual mode with aperture f/7.1, 1/80s shutter speed, exposure comp of –1 EV, and 100 ISO in tag image file format (TIFF) with lossless compression. For determination of the total surface area, the region of the image containing the coral juveniles was cropped from the background using an automated Fuji ImageJ macro and the surface area of the coral was calculated with another automated ImageJ macro. Coral survival was established using the same image, with the number of living polyps counted per well. The percent growth per coral juvenile was determined by the change in the surface area of the basal disc per coral juvenile. To calculate this, the surface area of each juvenile was divided by its initial surface area to account for any variation in the initial size, as per the following equation:

$$Growth = \frac{\left(\frac{xf}{nf}\right)}{\left(\frac{x0}{n0}\right)} X\ 100\% - 100\%$$

Where:

xf = Total surface area of all coral juveniles per well at a specific timepoint

nf = Number of coral juveniles per well at the same specific timepoint

$x0$ = Surface area of coral juveniles per well at day 0

$n0$ = Number of coral juveniles per well at day 0

Survival was calculated for juveniles that were kept for the duration of the experiment (i.e. 16 days (n=1258) for *A. kenti* and 8 days (n= 532) for *G. retiformis*) (Table 2.2). The growth of juveniles (*A. kenti* n=5803 and *G. retiformis* n= 894) was measured on Day 0; growth measurements of *A. kenti* taken on Day 2 (n=4837) were excluded from growth analysis due to a measurement calibration problem.

Table 2.2 Experimental design denoting the number of *A. kenti* and *G. retiformis* juveniles recorded for growth approximation in each treatment.

Species	***A. kenti***				***G. retiformis***			
Treatment	Control	DMSP	Acrylate	Total	Control	DMSP	Acrylate	Total
Day 0	1828	2037	1938	5803	502	214	178	894
Day 2	1479	1747	1611	4837	217	203	158	578
Day 4	1076	1271	1227	3574	212	187	148	547
Day 6	737	806	871	2414	212	184	145	541
Day 8	735	806	869	2410	207	180	145	532
Day 10	346	431	484	1261	-	-	-	-
Day 12	346	430	484	1260	-	-	-	-
Day 14	346	429	484	1259	-	-	-	-
Day 16	346	428	484	1258	-	-	-	-

2.3.5 Coral tissue extraction

To quantify the DMSP concentration within coral tissues, coral tissue from replicates of each species (each well representing one replicate to ensure there was enough biomass for quantification) was extracted at each time point (as per Table 2.1). Growth measurements of all corals were taken immediately prior to coral tissue extraction to ensure both measurements represented the coral in the same physiological state. For *A. kenti* at each of the five time points, two 6-well plates (total of n=12 replicate wells) from controls and each treatment (days 0, 2, 4, 8, 16) were randomly selected for coral tissue extraction. For *G. retiformis*, given the lower number of settled juveniles, two 6-well plates (n=12 replicate wells) were extracted from controls on day 0 and from each of the three treatments (control, DMSP and acrylate supplement) on day 8.

Coral tissue extraction followed the detailed protocols reported in Tapiolas et al. (2013) and Raina et al. (2013), with slight modification. Briefly, each well (i.e., equivalent to one replicate) was rinsed three times with FSW to remove any residual chemical supplements.

The seawater was removed with a glass pipette and a sterile cotton bud used to soak any residue. A 200 µL aliquot of methanol was added to each well and the plate was then swirled for 30 seconds before the addition of 300 µL of Milli-Q H_2O. Each sample was gently mixed for a further 30 seconds and the extract was transferred by glass pipette to a 7 mL scintillation vial. The vial was flushed with nitrogen gas for 10 seconds to minimize hydrogen exchange, sealed with parafilm and stored at -20°C.

2.3.6 Sample preparation for chemical analyses

Coral extracts (–20°C) were thawed at room temperature and a 50 µL aliquot of each sample was transferred to a 500 µL centrifuge tube and spun for 30 seconds at 5400 rpm in a mini centrifuge (VWR; South Korea; MiniStar silverline). A 20 µL aliquot of the solute was transferred to a 2 mL amber autosampler vial (Agilent) with a 200 µL glass insert, followed by addition of 2 µL (10% volume of the sample) of 0.11 M caffeine prepared in MeOH:H_2O (2:3 V%V) as an external standard before being sealed with a septum screw cap. Immediately before the analysis, all septa were pierced with a needle to equalize the pressure inside the tube to atmospheric pressure. The same protocol was followed for *G. retiformis* samples with slight modifications: 50 µL of sample was transferred to a 200 µL glass insert and 5 µL (10% volume of sample) of 1 mM caffeine prepared in MeOH:H_2O (2:3 V%V) added as the internal standard.

LC-MS analyses were performed on a Shimadzu Nexera-I series high performance liquid chromatograph (LC-2040C 3D HPLC; Kyoto, Japan) equipped with a Photodiode-Array Detection detector (LC-2030/2040 PDA) and a Shimadzu LC-MS-2020 mass spectrometer (LC-MS; Shimadzu, Kyoto, Japan) with dual source electrospray ionization (DUIS). Reverse phase HPLC separation of DMSP was performed on a Phenomenex Ultracarb column (5 µm sphere particles, dimension: 50 x 4.6mm, part no. 00B-2134-E0) maintained at 25ºC. The following solvents were prepared to give optimal separation and peak shape; (A) HPLC grade 2 mM of ammonium formate (Fluka Analytical 17843-50G) in Milli-Q water with 0.1% formic acid (HCOOH) and (B) HPLC grade acetonitrile (Fisher Chemical A988-4) with 0.1% HCOOH. For *A. kenti* samples, 1 µL of each extract was injected into the system with a flow rate of 500 µL min^{-1}. The column was pre-equilibrated in 90% solvent A for 10 mins prior to injection. The gradient elution profile was: 10% solvent B to 50% solvent B over 5.5 mins, then ramped up to 90% solvent B over 2.5 mins, held for linear elution for 2 mins, then returned to 10% solvent B over 3 mins, and allowed the column to re-equilibrate

for 5 mins (total run time 18 min; total number of runs n= 180). For *G. retiformis* samples, the LC-MS method was optimised to reduce runtime. A 1 µL aliquot of extract was injected onto the column with an 800 µL min^{-1} flow rate. The gradient elution profile was: 10% solvent B to 50% solvent B over 2.5 mins, then ramped up to 90% solvent B over 1 min, held for linear elution for 1.5 mins, then returned to 10% solvent B over 1 min, and allowed the column to re-equilibrate for 4 mins (total run time 10 min).

The DUIS was operated in positive mode, with a target mass set to *m/z* 135 for DMSP $[M+H]^+$ (confirmed with a DMSP standard). DMSP elution occurred at retention time 3.2 min for *A. kenti* samples and 1.7 min for *G. retiformis* samples. The extracted ion chromatogram *m/z* peak signal was integrated with Shimadzu LabSolution software using the calibration curve to attain the peak's corresponding concentration. The caffeine internal standard eluted at 8.3 min for *A. kenti* and 3.7 mins for *G. retiformis* sample, with targeted mass for $[M+H]^+$ of *m/z* 195. DMSP concentrations were normalized to the integral of caffeine. In total, the DMSP concentration were determined for *A. kenti* juveniles (n=5795) in 180 replicates, and *G. retiformis* juveniles (n= 793) in 48 replicates.

2.3.7 Statistical analysis

Kaplan-Meier survival plots were constructed using R packages "survminer" and "survival" to evaluate the survival of *A. kenti* and *G. retiformis* recruits in different treatments compared to controls (Therneau 2015; Kassambara et al. 2017). Pairwise-comparison using log-rank test was performed with treatment as the only factor used to estimate the survival of coral recruits with Bonferroni correction.

A two-way repeated measure ANOVA in the R statistical program (version 4.1.0 with rstatix package) (R Core Team 2019; Kassambara 2022) was used to analyse the growth of *A. kenti* juveniles per treatment and per day. Inverse response transformation was used to provide the best fit of assumptions (Supplementary Data Figure 2.1). As mentioned above, given there was some variance in growth between recruits within the same treatment on Day 0, the growth of each individual coral juvenile measured throughout the experiment was normalized to its own initial surface area measured at Day 0 to avoid any size variation bias. Hence, Day 0 growth was considered as zero, with percentage of growth since Day 0 on subsequent days, i.e., Day 2 and onwards. DMSP concentration per *A. kenti* recruit was also analysed with a 2-way ANOVA with square root response transformation (Supplementary Data Figure 2.2). The interaction between specific treatment and day was examined with a

Bonferroni multiple measure correction method to control false positives. DMSP concentration per *G. retiformis* recruit was also analysed with a 2-way ANOVA with square root response transformation (Supplementary Data Figure 2.3). A one-way ANOVA analysis was performed on *G. retiformis* DMSP concentrations on day 8 for the best model fit (Supplementary Data Figure 2.4).

2.4 Results

2.4.1 Coral juvenile survival

High survival of *A. kenti* (> 98%) and *G. retiformis* (> 80%) juveniles was observed across all treatments over the 16 and 8 days of the respective experiments (Figure 2.1). *A. kenti* recruits supplemented with DMSP and acrylate recorded 99.3 ± 0.40% and 98.8 ± 0.49% survival, respectively, and these values did not differ statistically (p-value > 0.0167; Tukey post-hoc with Bonferroni correction level of significance is 0.0167 for n=3 in coral juveniles survival statistics) from the control (98.3 ±0.69%; Figure 2.1A). *G. retiformis* exhibited slightly higher mortality when compared to *A. kenti* across all treatments including the control (92.8 ±1.73%; Figure 2.1B). Survival of *G. retiformis* recruits supplemented with DMSP (84.6 ±2.47%) also did not differ significantly from the control (p-value =0.0185; > 0.0167), however, survival of recruits supplemented with acrylate was significantly lower than the control (81.5 ±2.91%) (p-value < 0.0167).

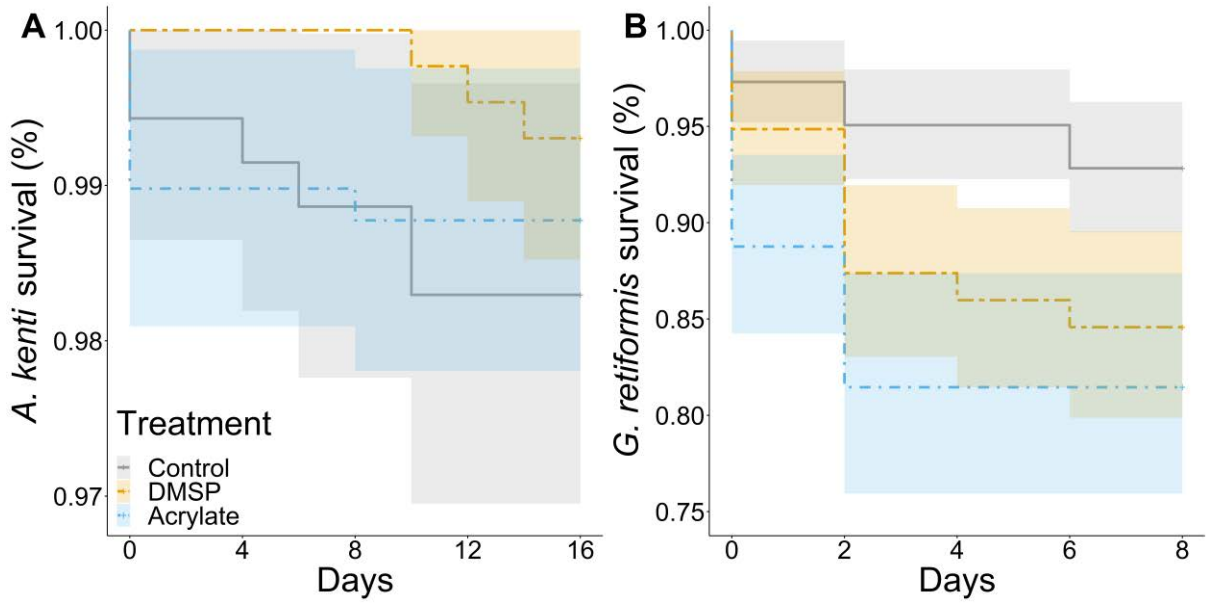

Figure 2.1 **(A)** Kaplan-Meier survival curves for *Acropora kenti* recruits over 16 days. **(B)** Kaplan-Meier survival curves for *Goniastrea retiformis* recruits over 8 days. Lines represent

averaged survival; Control (grey), DMSP (yellow), and acrylate (blue) with shade region represent 95% confidence interval.

2.4.2 Coral juvenile basal disc growth

Growth of individual *A. kenti* and *G. retiformis* juveniles was normalized to their initial size (i.e., day 0 growth equates to 0%) and therefore the size reported on subsequent treatment days represents the percent increase from day 0. Over the duration of the exposure, the growth of both *A. kenti* and *G. retiformis* juveniles supplemented with DMSP was similar to that observed in control treatments. The average size of *A. kenti* juveniles in the controls increased 20.1 ± 2.8% over the 16-day experiment, while those supplemented with DMSP were on average 21 ± 2.3% larger (Figure 2.2A). *A. kenti* juveniles supplemented with acrylate were only 14 ± 1.6% larger after 16 days (Figure 2.2A) and the interaction between treatment and time was not significant ($F_{12,132} = 1.618$, *p*-value =0.094; 2-way ANOVA *p*-value significant level is 0.05). On the other hand, there were significant differences between the treatments at each timepoint ($F_{2,22} = 4.727$, *p*-value =0.020) with the acrylate treatment displaying significantly less growth than either the control or DMSP treatments (non-pairwise post hoc comparison adjected *p*-value < 0.05). Conversely, *G. retiformis* juveniles exhibited a greater increase in size across all treatments (Figure 2B), more than doubling (~150 to 170% larger; growth pairwise comparison all treatments day 4 versus day 2, *adj p*-value < 0.05), although this growth was observed primarily in the first 4 days of the experiment (growth pairwise comparison all treatments day 6 vs day 8 *adj p*-value > 0.05). However, there was no significant difference in growth between the treatments at any timepoint (ANOVA: $F_{6, 66}$ =0.628; *p*-value = 0.707).

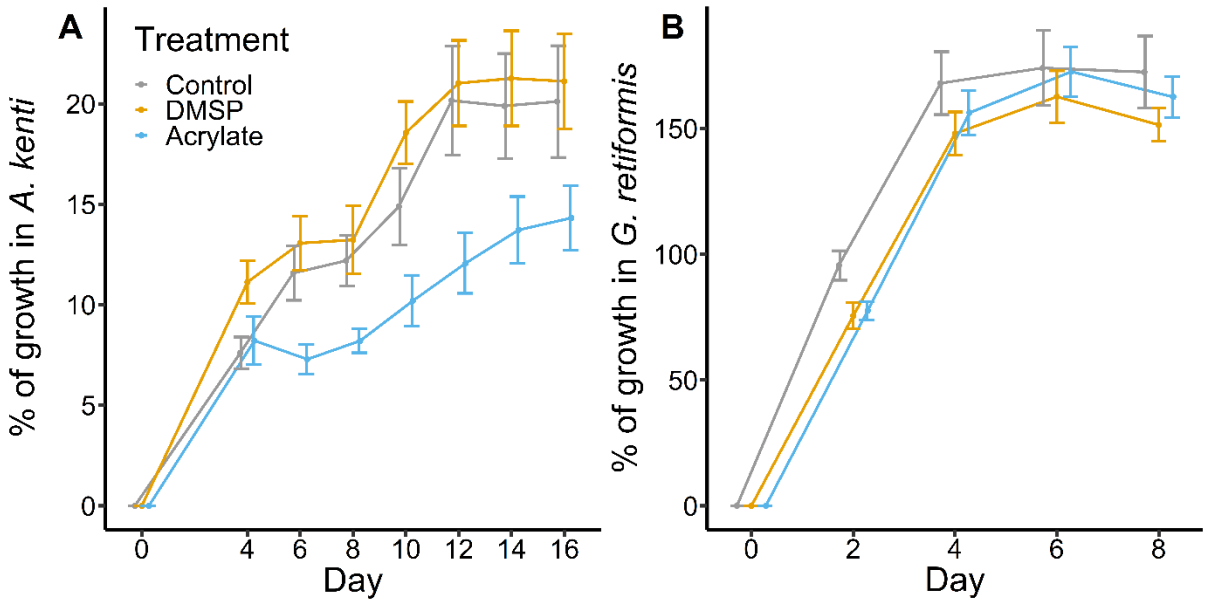

Figure 2.2 The percentage of growth per coral juvenile calculated based on the surface area measurements from repeated photographs. **(A)** The average percentage of growth in *Acropora kenti* juveniles over 16 days and **(B)** the average percentage of growth in *Goniastrea retiformis* juveniles over 8 days. Control in grey, DMSP in yellow and acrylate in blue; points represent the mean, and error bars the standard error.

2.4.3 Coral tissue DMSP concentrations

The average DMSP concentration detected within *A. kenti* juveniles varied through time and across the three different treatments (Figure 2.3A). On average, control *A. kenti* juveniles displayed the highest DMSP content (0.0295 mM), although concentrations were only slightly higher than observed for those supplemented with DMSP (0.0286 mM) and acrylate (0.0255 mM). No significant differences in DMSP concentrations were observed between treatment and time (ANOVA: $F_{4.08,44.88}$, =2.311, *p*-value = 0.071). On day 16, DMSP concentration and number of juveniles settled were positively correlated in all treatments (Figure 2.3C). Higher DMSP concentrations were measured in samples where more *A. kenti* juveniles settled and this trend was consistent between all treatments and was significant (Pearson correlation coefficient; R= 0.71-0.74, *p*-value < 0.05).

DMSP was only detected in tissues of *G. retiformis* juveniles supplemented with DMSP, having an average concentration of 0.03 mM (±0.02) DMSP per polyp (Figure 2.3B). However, a significant negative correlation was observed between DMSP concentration and

the number of juveniles (*p*-value = 0.018; Figure 2.3D). No DMSP was detectable in *G. retiformis* juveniles in either the control or acrylate treatments sampled on days 0 and 8 of the experiment. As a result, DMSP concentrations were significantly different between treatments (ANOVA; $F_{2,22}$ =10.57; *p*-value = 0.001), with pairwise t-test confirming the DMSP treatment was significantly different to the control and acrylate treatments (Bonferroni *adj p*-value = 0.002).

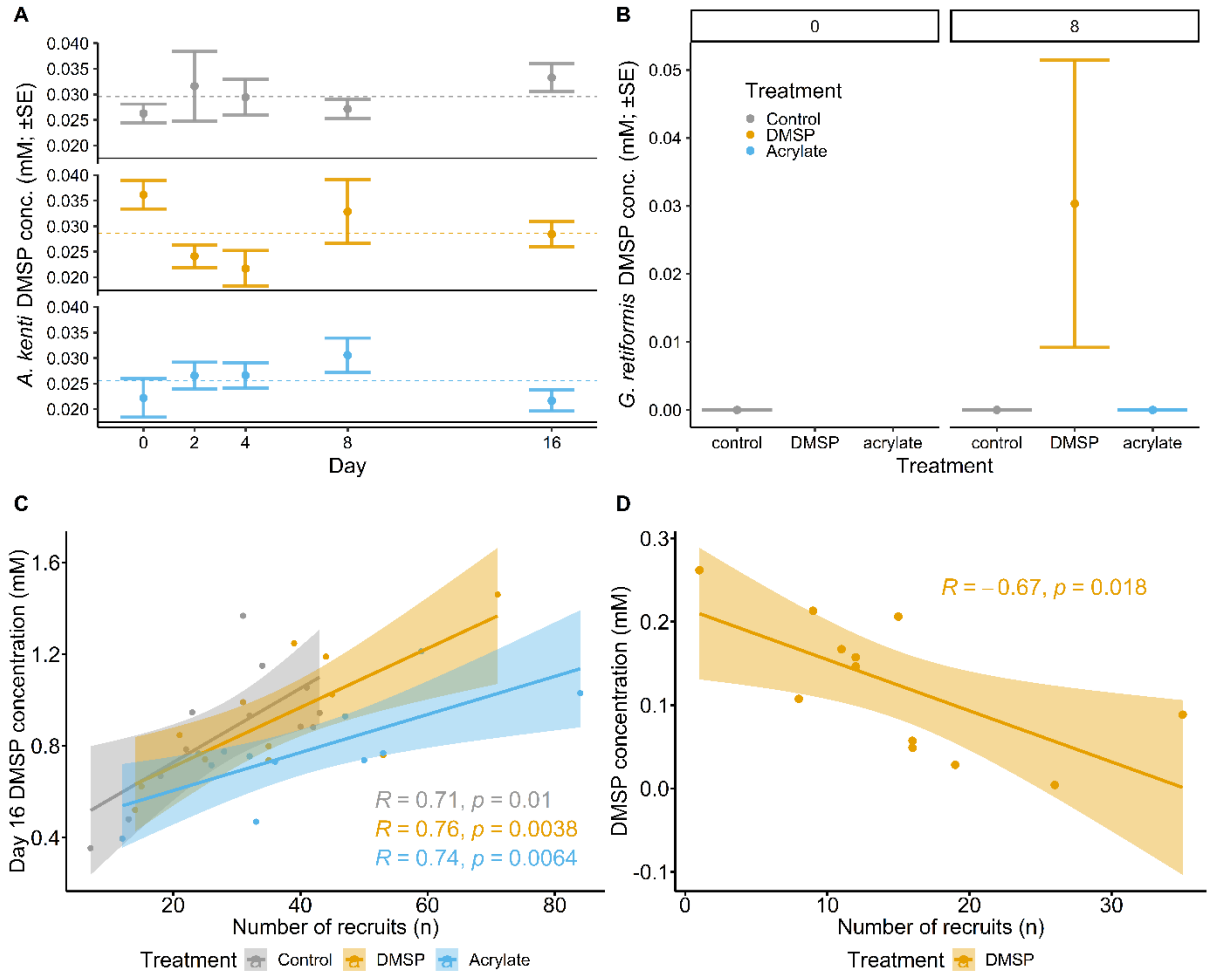

Figure 2.3 DMSP concentration per coral polyp, quantified by mass spectrometry. **(A)** DMSP concentration per *Acropora kenti* polyp (mM; ±SE) across different treatments and days. Dashed lines represent mean DMSP concentration of each treatment. **(B)** DMSP concentration (mM± SE) per *Goniastrea retiformis* polyp in different treatments on days 0 and 8. Points represent mean DMSP concentration, error bars represent standard error. Pearson correlation of DMSP concentration as a function of the number of recruits (n) settled in each well. **(C)** DMSP concentration in each treatment at day 16 as a function of the number of *A. kenti*

recruits settled in each well. **(D)** DMSP concentration at day 8 of exposure to DMSP as a function of the number of *G. retiformis* recruits settled in each well. No DMSP was detected in the control or acrylate treatments; shaded region represents 95% confidence interval.

2.5 Discussion

Some fast-growing coral species, particularly the Acroporids, have high concentrations of DMSP and acrylate within their tissues (Tapiolas et al. 2010). While the likely role of organo-sulfur compounds with the coral holobiont includes scavenging of oxygen radicals (Sunda et al. 2002; Deschaseaux et al. 2014b; Jones and King 2015), the high concentrations of acrylate are perplexing and led to the postulation that it may support coral growth. Acrylate can polymerize to polyacrylic acid, which has chemical functionality similar to that of aspartic acid-rich proteins in the coral organic matrix (Miller and Holcombe 2001; Cantaert et al. 2013b), and hence, polyacrylic acid could potentially catalyse $CaCO_3$ precipitation(Mass et al. 2013; Akiva et al. 2018a) and support skeleton deposition. Here, however, the addition of exogeneous DMSP and acrylate as supplements for *A. kenti* and *G. retiformis* juveniles did not impart any growth advantage.

2.5.1 Acrylate supplementation increases mortality in *Goniastrea retiformis* recruits

The high survival rates observed for recruits of both *A. kenti* and *G. retiformis* exposed to DMSP indicates DMSP supplementation was at an appropriate concentration. In contrast, exposure to acrylate resulted in mild toxicity to *G. retiformis*, as evidenced by the slightly lower survival rate of 81.5 ± 2.91% compared to 92.8 ±1.73% in controls. Although 10 mM of acrylate supplement was recommended from previous literature for *Acroproa* juveniles (Johns 2019; Kuek 2021), here, based on the fact that adult *Goniastrea* contain lower concentrations of acrylate (0.253 nmol mm^{-2}) as compared to adult Acroporids (15.223 nmol mm^{-2}) (Tapiolas et al. 2013), and assuming that *G. retiformis* and *A. kenti* juveniles consist of a similar metabolite profile as the species in their respective genera, recruits of both species were exposed to 1 mM acrylate, a magnitude lower. The observed toxicity indicates, however, that even at this lower acrylate concentration, *G. retiformis* juveniles may have been exposed to acrylate concentrations much higher than the natural biological level. This suggests *G. retiformis* juveniles are not equipped to effectively detoxify excess acrylate concentrations. It is also possible that since corals are more vulnerable to stressors during their early life stages (Albright 2011), the impacts on survivorship may be a result of *G. retiformis* recruits having

less well-developed cellular and molecular mechanisms to detoxify acrylate compared to mature *G. retiformis* and to *A. kenti*.

2.5.2 DMSP biosynthesis and exogeneous uptake differ between coral genera

Supplementation with DMSP did not facilitate enhanced growth in juveniles of either species relative to controls. DMSP was observed in *A. kenti* controls and in both treatments, with DMSP concentrations constant across all treatments. As such, there is no evidence of DMSP uptake. These results do, however, confirm that aposymbiotic *A. kenti* juveniles are capable of DMSP biosynthesis and can maintain intracellular concentrations for an extended period. Establishment of DMSP biosynthesis by aposymbiotic *A. kenti* controls corroborates prior findings that Acroporid species are capable of producing and storing DMSP in their tissues at relatively high levels (Raina et al. 2013). Yet, as uptake was not observed here, it is not possible to establish a link between exogenous DMSP and growth. However, the ability of *A. kenti* to produce and store DMSP is undoubtedly contributing to the strong (and linear) correlation between increased DMSP concentrations and the higher number of *A. kenti* juveniles settled per well, this trend being consistent across all treatments, including the control at day 16.

The ability of *A. kenti* juveniles to produce intracellular DMSP may negate the need to uptake exogenous DMSP. The biosynthesis of DMSP may support *Acropora* early life stage metabolism ensuring survival until they acquire Symbiodiniaceae (Hill et al. 1995). In adult corals, Symbiodiniaceae are the major producers of DMSP (Hill et al. 1995), and the positive correlation of Symbiodiniaceae cell density with DMSP concentrations (Frade et al. 2016) confirms the adult coral animal requires DMSP additional to that which it can itself produce. There are two possible scenarios to explain the lack of increase in DMSP concentrations for *A. kenti* aposymbiotic juveniles; 1) they are not capable of uptake of exogeneous DMSP from the surrounding seawater or 2) uptake occurred but the excess DMSP was rapidly metabolised.

The uptake of exogenous DMSP has been observed in diatoms and it is highly likely this process requires active transporters (Kiene and Hoffmann Williams 1998). It is possible that aposymbiotic *A. kenti* juveniles do not have the machinery to actively transport exogeneous DMSP across the cell membrane, or that acquiring exogenous DMSP is energetically costly. If this is the case, it may be more cost-efficient for *A. kenti* to instead acquire environmental sulfate (SO_4^{2-}), following a similar metabolic pathway used by

symbiotic bacteria (Raina et al. 2017), to support the biosynthesis of DMSP (Matrai and Keller 1994).

Given the presence of high concentrations of DMSP in some symbiotic corals (Broadbent et al. 2002), it is possible that aposymbiotic *A. kenti* juveniles, lacking the symbiotic algal partner to support DMSP biosynthesis, may have a high demand for DMSP. Therefore, these juveniles may uptake exogenous DMSP, which is then immediately metabolised, resulting in no measurable difference in DMSP concentrations in the coral tissue, i.e., the basal equilibrium is maintained. It has been established that marine bacteria have the ability to sequester exogeneous DMSP from the seawater and metabolize it within 24 hours (Kiene et al. 2000; Gao et al. 2020; Fernandez et al. 2021), e.g., via the action of DMSP lyases (Curson et al. 2011b). Furthermore, it has been reported that DMSP lyase genes, whose products catalyse DMSP cleavage to DMS and acrylate, have undergone expansion in members of the genus *Acropora* (Shinzato et al. 2021). Here, the intracellular DMSP concentration was measured 24 hours after supplementation, the deliberate delay in measurement providing time for coral to metabolise any absorbed DMSP. Given there was no effort to eliminate bacteria, in theory, DMSP lyases from either the bacteria or the *A. kenti* juveniles could rapidly catabolise DMSP. Future research effort should monitor changes in DMSP concentrations at earlier timepoints to establish whether uptake is occurring within *A. kenti* and/or associated bacteria.

Metabolism of DMSP via the lyase cleavage pathway produces acrylate. If this pathway is active, uptake of exogeneous DMSP would be expected to increase acrylate concentrations within the coral tissues. Here acrylate concentrations were not measured, the LC-MS method being unable to simultaneously quantify DMSP and acrylate due to the poor ionization of acrylate. Therefore, additional studies should develop a different LC-MS solvent system tailored to the ionization of acrylate. Alternatively, quantification using nuclear magnetic resonance spectroscopy (^{1}H-qNMR) could be used to detect DMSP and acrylate in coral tissues simultaneously, although this would require sample pre-concentration (Tapiolas et al. 2013). Regardless, given that the growth of *A. kenti* was not enhanced as a result of DMSP supplementation, if it was indeed taken up it is likely that both DMSP and any derived acrylate serve cellular functions other than growth.

For *G. retiformis* juveniles, no DMSP was detected in controls, but was detected in those supplemented with DMSP. The juveniles settled in treatment wells were meticulously

washed three times with FSW before solvent extraction, and therefore the DMSP detected is unlikely to be residual exogeneous DMSP. If this had occurred the concentrations of DMSP detected would be expected to be consistent across all DMSP treated wells, though no increase in basal DMSP was observed in *A. kenti* supplemented with DMSP. Further, if post-washing residual DMSP was adsorbed to the coral surface and then subsequently extracted, then more would be expected to be extracted from wells having a higher density of corals (i.e., as the surface area increases more DMSP should be extracted), though again this was not observed.

The lack of DMSP detected in aposymbiotic *G retiformis* juveniles supports previous observations that symbiotic adult *Goniastrea* colonies do not have DMSP at detectable levels (Tapiolas et al. 2013). However, acrylate was detected in these adult colonies (Tapiolas et al. 2013), and this observation is highly suggestive of the former presence or the rapid metabolism of DMSP, DMSP being the immediate precursor of acrylate. The lack of DMSP in *G. retiformis* controls establishes that, unlike *A. millepora* and *A. kenti* (Raina et al. 2013), *G. retiformis* does not have the capacity to produce DMSP and relies on its supply via symbionts. By day 8 of exposure, DMSP was detected in *G. retiformis* juveniles supplemented with DMSP, and not in the control or acrylate treatments. The concentrations detected were similar to that in *A. kenti* juveniles (~0.03 mM) and hence this observation indicates that incorporation of exogeneous DMSP to corals is possible, either passively or through active transporters. This expands our knowledge of DMSP uptake by corals, supporting a prior study on the aposymbiotic deep sea coral *Lophelia pertusa* which has been speculated to nutritionally acquire particulate DMSP (Burdett et al. 2014). Aposymbiotic *Goniastrea* is able to acquire dissolved exogeneous DMSP from the surrounding environment, yet as it is a slow-growing coral species relative to *Acropora*, the 8-day exposure may not be long enough to observe any benefit, i.e., no enhancement of growth was observed. Extending the supplementation period, i.e., beyond 51 days, is recommended to establish if uptake is beneficial (Nothdurft and Webb 2007).

The negative correlation observed between lower DMSP concentrations detected with the higher number of *G. retiformis* juveniles per well at day 8 potentially indicates an increase in DMSP catabolism when juveniles are in higher density. The genetic machinery for the breakdown of DMSP via the cleavage pathway has been shown to exist in the genus *Goniastrea* (Kitahara et al. 2016), although DMSP lyase genes have not undergone expansion in this phylogenetic group to the same extent as in *Acropora spp.* (Shinzato et al. 2021).

Therefore, it is possible that DMSP lyase activity is occurring in *G. retiformis* and that DMSP catabolism was much slower for juveniles at low density resulting in high levels of DMSP remaining in tissue during extraction. In contrast, rapid catabolism of DMSP could be result from juveniles settled at high density.

2.5.3 DMSP may serve different functions in different coral genera

The opposing results found for *A. kenti* and *G. retiformis* suggest that DMSP may serve different functions in these two coral species during their early life stages. Indeed, investigations in adult *A. millepora* and *Stylophora pistillata* (Gardner et al. 2017a) found the role of DMSP to be genus-specific. Under thermal stress, DMSP concentrations in *S. pistillata* decline, suggesting DMSP is acting as an antioxidant and being consumed during the harvesting of ROS. Yet for *A. millepora*, DMSP concentrations increase in response to thermal stress and are thus suspected to play a different metabolic role in this coral species. With the genus-specific DMSP lyase expansion in *Acropora*, and high production of DMSP (Tapiolas et al. 2013; Shinzato et al. 2021), it is possible that DMSP has acquired functions in *Acropora* spp. that it does not serve in other corals. Further research is needed to establish whether this extends to older juveniles and adults of *A. kenti* and *G. retiformis*.

2.5.4 Acrylate supplementation induces mild growth retardation in *A. kenti* recruits

Survival was not deleteriously affected by acrylate supplements, yet acrylate did not enhance growth of either species. Significant growth retardation was observed in *A. kenti* recruits exposed to acrylate; the size of polyps exposed to acrylate increased by only ~14% after 16 days compared to controls and those supplemented with DMSP, both of which were ~20% larger in size. These findings provide additional evidence of the toxicity of exogenous acrylate. Indeed, acrylate is known to be toxic to many organisms. For example, it can inhibit the growth of bacteria (Sullivan et al., 2011) and is lethal to microzooplankton (Wolfe et al. 1997b; Wang et al. 2002), although some microzooplankton do have the molecular mechanisms to detoxify acrylate, i.e., through its catabolism to acryloyl-CoA (Reisch et al. 2013). The slower coral growth observed here is surprising given that members of the genus *Acropora* are characterised by high levels of acrylate in their tissues, suggesting they have a mechanism to tolerate the inherent toxicity. However, the additional acrylate load, enhanced through uptake, may have exceeded the coral's level of tolerance, i.e., acting as an additional stressor. In essence, it may be that the concentration of exogeneous acrylate offered was far beyond normal biological levels in *Acropora* recruits and, detoxification of excess acrylate to

ensure survival may require diversion of energy reserves normally needed for maintenance and growth. The slight drop in survival of *Goniastrea* and the significant retardation of growth in *Acropora* juveniles caused by the acrylate supplement points to its toxicity and indicates it is not a suitable supplement to support and enhance early life stage coral growth.

2.5.5 Coral growth is determined by various factors

The factors that contribute to coral growth are complex, the predominant requirement is the availability of sufficient energy to translocate stored or acquired nutrients to support skeletal and tissue growth (Hoogenboom et al. 2008; Osinga et al. 2011). For example, newly settled aposymbiotic corals rely on the lipid content stored in eggs for subsequent development and metabolism (Richmond 1987; Harii et al. 2007). The coral juvenile is likely to use some of this stored lipid to support early growth. Here, *A. kenti* juveniles displayed a 20% increase in size over 16 days while the *G. retiformis* juveniles were 150% larger after 4 days post-settlement. This stored energy is limited and if energy reserves are not replenished through heterotrophic feeding or photosynthesis, deposition of $CaCO_3$ is reduced and coral growth suppressed (Houlbrèque and Ferrier-Pagès 2009; Drenkard et al. 2013). This scenario was observed, with growth of both coral species plateauing after an initial period of size increase. In natural systems, symbiosis is established early in post-settlement life and energy subsequently acquired through mixotrophy (i.e., both derived photosynthates and capture of heterotrophic nutrients). As the aposymbiotic control juveniles were maintained in FSW and deprived of both photosynthetic and heterotrophic nutrients, their ability to acquire energy as the experiment proceeded was limited and growth at the later timepoints expected to slow as stored lipids were depleted. Even for *A. kenti* that is capable of DMSP biosynthesis, supplementation with DMSP (and acrylate) was expected to extend a benefit to recruits of both species as a source of carbon and sulfur at the later timepoints. The results here confirm this was not the case.

The acquisition and subsequent precipitation of Ca^{2+} ions in the form of aragonite are energy expensive processes. In the coral calcification model, Ca^{2+} is acquired through either active or passive transport (Ip et al. 1991; Zoccola et al. 1999, 2015; Furla et al. 2000; Tambutté et al. 2011). In active transfer, energy is required to fuel an ATPase enzyme to allow Ca^{2+} to pass through coral tissue layers (Allemand et al. 1998; Osinga et al. 2011). If the energy reserves of settled juveniles are depleted, the supply of the Ca^{2+} to the site of calcification could be limited. Addition of exogeneous DMSP or acrylate to the coral juveniles was targeted at supplying an extra catalyst to enhance the calcification process,

noting that calcification would not proceed if the starting material, Ca^{2+}, was limited through this energy bottleneck (Dissard et al. 2012). It is important to note that coral juveniles in this study were not offered a food source, as phytoplankton contributes to the coral DMSP pool (Dacey and Wakeham 1986; Tang and Simó 2003). The absence of an additional food source was a deliberate choice to avoid complicating the quantification of DMSP uptake (Wijgerde et al. 2011). Future studies should consider the concomitant supply of an alternate energy and nutrient source that is DMSP free, i.e., *Artemia*, to support the development of the coral juveniles (Nothdurft and Webb 2007).

Exogenous DMSP in seawater is degraded and utilised by bacteria, with the pathway of degradation regulated by DMSP availability (Kiene et al. 2000) and the bacterial demand for carbon and sulfur (Simó 2001b; Varaljay et al. 2015; Gao et al. 2020). Yet, the degradation pathway is a function of the microbial community, which is itself a function of the environment. For example, the bacterial community present in inshore GBR waters is considered nutritionally rich and predominately degrades DMSP to DMS via the cleavage pathway, whereas offshore microbial communities, i.e., considered nutrient poor, convert DMSP to methanethiol via the demethylation pathway (Fernandez et al. 2021). As, no nutrient or food was provided to coral juveniles in this study, the juveniles were both sulfur and carbon limited. It is possible that coral juveniles have similar mechanisms as bacteria to regulate DMSP breakdown under limited nutrients, i.e., converting exogenous DMSP through demethylation pathways to attain energy and provide organic carbon and sulfur for development. Thereby, coral juveniles may obtain nutrient support from the breakdown of DMSP through demethylation pathways, instead of producing acrylate via the cleavage pathway, foregoing a potential growth benefit. Although the products of both DMSP breakdown pathways were not quantified, the survival of juveniles supplemented with DMSP matched that of controls. However, the growth of juveniles was not enhanced with exogenous DMSP and hence there is no observable evidence that products from either DMSP breakdown pathway offer any benefit.

2.5.6 Refinement of imaging analysis methods to improve coral juvenile growth estimates

Approaches such as wax dipping are often used to measure three-dimensional growth of adult corals and were initially considered here, however, reports have indicated low precision when applied to small coral juveniles (< 1 mm^2 Ø per recruit). For example, Veal et al. (2010) reported that the corals need to be > 5 cm^3 for robust assessment of growth using

wax-dipping, and computed tomography (or CT) scanning requires samples larger than 2 cm^3 to achieve a high enough resolution. As coral juveniles used here measured ~17.8 to 22.1 mm^2 for *A. kenti* and ~1.75 to 3.53 mm^2 for *G. retiformis*, neither of these three-dimensional methods were deemed to be suitable. Here, a two-dimensional method that measures the SA, i.e., derived from photographs, was able to estimate and monitor increase in the size of newly settled *A. kenti* and *G. retiformis* juveniles. While this method proved suitable for the measurement of multiple coral replicates over time, it does not account for any vertical extension and hence is at best a proxy, i.e., ballpark representation, of the impact of supplementation on growth. Quigley and Vidal Garcia (2022) recently assessed the applicability of intraoral dental scanning to measure the three-dimensional SA and volume of >1 year old coral juveniles at fine scale with significant improvement in the accuracy of size estimates. Future research should assess this three-dimensional method on newly settled juveniles (<1 month old) and determine the level of improvement in the accuracy of growth measurements.

2.6 Conclusion

This study explored the potential of supplementing coral juveniles with DMSP and acrylate to enhance their growth. Focus was on measuring the physiological response including survival, growth, and DMSP concentration, of newly settled aposymbiotic juveniles of the fast-growing branching *A. kenti* and the slower-growing massive *G. retiformis* to chemical supplementation. Quantifying DMSP in aposymbiotic recruits under control conditions revealed significant differences between the two species. Here, *A. kenti* recruits were shown to produce DMSP, corroborating previous knowledge from *Acropora* species, while there was no evidence for DMSP biosynthesis in *G. retiformis* recruits. In addition, although no substantive evidence was found to support the link between DMSP and acrylate supplementation and growth in either species, the response of coral recruits to exogeneous DMSP and acrylate did reveal further species-specific differences. Uptake of exogeneous DMSP was not observed for *A. kenti*. DMSP supplementation did not enhance DMSP concentration in the tissues, likely because the coral was already able to establish a basal DMSP concentration through host biosynthesis or it was catabolising it immediately upon uptake. Uptake was observed for *G. retiformis,* confirming that sequestration from the surrounding environment is possible, however, the elevated levels of intracellular DMSP did not enhance *G. retiformis* growth. Similarly, supplementation with acrylate resulted in a significantly slower growth in *A. kenti* and a decrease in *G. retiformis* survival, the latter

indicating a low level of toxicity and highlighting limitations in its use as a growth enhancer. The ramifications of these findings for both fast- and slow-growing coral species under various scenarios, including settlement and long-term juvenile growth under stress conditions and bleaching, should be the focus of future studies and should include assessment of gene expression regulation as well as physiological responses to DMSP uptake. Harbouring symbiotic algal partners allows coral to acquire energy through autotrophic feeding. As these two coral species form symbiotic relationships with DMSP-producing Symbiodiniaceae, monitoring DMSP and acrylate metabolism in Symbiodiniaceae-inoculated newly settled coral recruits may provide a better understanding of the possible functions of DMSP and acrylate in coral growth and calcification. To conclude, this study has revealed distinctive growth patterns between the early life stages of two species of hard coral in response to supplementation with the important coral metabolites DMSP and acrylate.

Chapter 3 Influence of species-specific Symbiodiniaceae on coral juvenile DMSP concentrations and growth characteristics.

3.1 Abstract

Within the coral holobiont, Symbiodiniaceae is the largest producer of the organic sulfur compound dimethylsulfoniopropionate (DMSP) and has been postulated to enhance coral calcification through its breakdown to acrylate and subsequent theoretical conversion to polyacrylic acid, a compound with a chemical structure that mimics the known calcification proteins that are rich in polyaspartic and polyglutamic acid domains. This study explored the role of algal-derived DMSP in the early life stage of coral by assessing the advantage imparted to newly settled aposymbiotic *Acropora kenti* and *Goniastrea aspera* juveniles by the Symbiodiniaceae, *Cladocopium* or *Durusdinium* monoculture. Differences in the cellular concentrations of DMSP were correlated with coral growth and survival dynamics. *Acropora kenti* juveniles hosting the thermally tolerant *Durusdinium* dinoflagellate (Symbiodiniaceae) displayed higher growth in early ontology (days 4 – 37) compared to juveniles hosting the more universally dominant *Cladocopium* species. *Acropora* juveniles hosting *Cladocopium* achieved similar size and DMSP concentrations as those hosting *Durusdinium* but required significantly longer time to do so. Although higher growth correlated with higher DMSP concentrations in *Acropora* juveniles suggesting DMSP may be involved in coral calcification, no direct link could be established between DMSP levels and calcification. In *G. aspera* juveniles, growth did not correlate with DMSP concentrations derived from the Symbiodiniaceae. Findings here suggest alternative species-specific roles of DMSP and adds to the fundamental understanding of the role of species-specific Symbiodiniaceae and algal-derived DMSP in coral growth.

3.2 Introduction

Corals host an assemblage of different Symbiodiniaceae species, the combination of different symbiotic partners resulting in unique phylotypic characteristics (Franklin et al. 2012; Parkinson and Baums 2014; Swain et al. 2020). This symbiotic relationship is critical to the survival of the coral holobiont; the coral host provides respiratory carbon dioxide (CO_2) to the Symbiodiniaceae, and in return the Symbiodiniaceae undergo photosynthesis providing oxygen and fixed carbon nutrient to the coral host (Muscatine et al. 1984). This shared provision of resources supports coral metabolism, growth, and survival (Davy et al. 2012).

Symbiodiniaceae species are characterized by different physiological properties and trade-offs. *Cladocopium* is the dominant symbiont species in the Indo-Pacific (LaJeunesse 2005; Chen et al. 2022), affording fast growth to coral via greater photosynthate translocation to the coral host (i.e., providing energy for growth and metabolism) (Cantin et al. 2009). Corals hosting *Durusdinium* have generally been demonstrated to display higher thermal resistance than counterparts hosting *Cladocopium*, the trade-off being slower growth (Little et al. 2004; Cunning et al. 2015) and downregulation of immune system responses and lysosomal digestion (Yuyama et al. 2018). The Symbiodiniaceae community associated with the coral host can shift in response to environmental variation which has been postulated as one mechanism by which coral can acclimate to warming oceans (Rowan and Knowlton 1995; Stat et al. 2006). For example, in response to thermal stress, the symbiont community shifts from predominantly *Cladocopium* to *Durusdinium*, with such population shifts predicted to become the norm under future climate change conditions (LaJeunesse et al. 2018; Dilworth et al. 2021; Quigley et al. 2022). However, shifting to a *Durusdinium*-dominate community has potentially serious trade-offs including a reduction in coral growth and slower recovery from physical disturbances such as cyclones and predation by crown-of-thorns starfish, while also increasing vulnerability to disease (Wakeford et al. 2008; De'Ath et al. 2012; Shore-Maggio et al. 2018; Aeby et al. 2020). Nevertheless, other studies suggest that Symbiodiniaceae shuffling is cost neutral for the coral host (Abbott et al. 2021) and that it is the regional evolutionary history of symbionts that shapes the thermal tolerance properties of Symbiodiniaceae in certain corals (Howells et al. 2016, 2020).

Coral reefs are the largest producers of dimethylsulfoniopropionate (DMSP) in the marine environment, with DMSP playing a crucial role in the global sulfur cycle (Kiene and Linn 2000). Within the coral holobiont, the Symbiodiniaceae partner is the main contributor to the environmental DMSP pool (Hill et al. 1995), with DMSP linked to important cellular

processes including osmoregulation and stress response (Lesser et al. 1990; Broadbent et al. 2002). In culture, free-living *Cladocopium* produces higher DMSP concentrations per cell than *Durusdinium* (Deschaseaux et al. 2014a). When under thermal stress, the production of DMSP by *Durusdinium* is not affected, while for *Cladocopium* it is significantly decreased, with levels dropping to match those of *Durusdinium*. This may correlate to the physiological properties of symbiont species, the less thermally tolerant *Cladocopium* utilises DMSP at a higher rate than *Durusdinium* to mitigate cellular thermal stress.

Under ambient conditions, i.e., when not experiencing thermal stress, healthy fast-growing *Acropora* species contain high levels of DMSP compared to slower-growing coral species (Tapiolas et al. 2013). DMSP can act as an antioxidant and osmoprotectant when the coral holobiont experiences environmental stress (Stefels 2000; Sunda et al. 2002; Deschaseaux et al. 2014b; Gardner et al. 2016, 2017b). In the *Acropora millepora* coral holobiont, DMSP functions as an antioxidant under hyposaline (Aguilar et al. 2017) and thermal stress (Gardner et al. 2017a), with DMSP concentrations upregulated, facilitating scavenging the excess reactive oxygen species (ROS). However, the response of coral appears to be species-specific, with DMSP concentrations decreasing in thermally stressed *Stylophora pistillata* (Gardner et al. 2017a).

In corals, DMSP conversion to dimethyl sulfide (DMS) and acrylate not only facilitates the scavenging of ROS but also offers a pathway for dissipating excess reduced sulfur (Stefels 2000). However, the acrylate by-product is, itself, toxic to many marine organisms (Wang et al. 2002), and its accumulation in the tissues of some coral species highlights the active retention of this compound and suggests it has a possible important functional role in supporting coral growth and health. The Symbiodiniaceae and bacterial partners modulate the DMSP and acrylate levels in coral. *Cladocopium* are the dominant Symbiodiniaceae species associated with adult *Acropora* colonies and, given that they produce higher DMSP concentrations per cell than *Durusdinium* in isolate-culture (Deschaseaux et al. 2014a), it is possible that harbouring *Cladocopium* promotes DMSP production and hence, through bacterial conversion, maintains high acrylate levels. As discussed in the previous chapters, acrylate has the potential to polymerise into polyacrylic acid, which has a structure reminiscent of skeletal aspartic acid-rich proteins (i.e., proteins high in aspartic and glutamic acids and rich in carboxyl functional groups [RCOO-]) that catalyse coral skeleton calcification (Ajikumar et al. 2005; Gotliv et al. 2005; Zhou et al.

2011; Cantaert et al. 2013b; Mass et al. 2013; Mummadisetti et al. 2021). The higher DMSP concentrations in *Cladocopium*-dominant coral may facilitate faster growth through the incorporation of excess acrylate into the skeleton.

Adult *Acropora* hosting predominantly *Cladocopium* are characterized by fast growth compared to those hosting *Durusdinium* (Stat et al. 2008; Matias et al. 2022). In contrast, in early ontology, *Acropora* juveniles hosting the non-dominant *Durusdinium* grow faster than those hosting the dominant *Cladocopium* (Yuyama and Higuchi 2014). Although free-living *Cladocopium* cultures produce higher DMSP concentrations than *Durusdinium* (Deschaseaux et al. 2014a), their production of DMSP could differ when hosted within coral. This is supported by differences in transcriptomic expression of free-living vs symbiotic Symbiodiniaceae (Yuyama et al. 2021), which may include DMSP metabolism. Previous studies have focused on the physiological response and DMSP levels in each isolated member of the coral holobiont (Raina et al. 2013, 2017; Deschaseaux et al. 2014a; Gardner et al. 2017a; Gao et al. 2020; Kuek et al. 2022). However, the link, if any, between the production of DMSP by coral juveniles hosting different Symbiodiniaceae species and coral growth has yet to be determined. Understanding the physiology of newly settled coral juveniles and revealing the factors that enhance newly settled polyp growth are important to overcome the juvenile size-escape threshold which is critical for coral survival in the early life stages (Raymundo and Maypa 2004; Doropoulos et al. 2012, 2017; Suzuki et al. 2012; Randall et al. 2020).

To understand the contribution of different Symbiodiniaceae to coral growth and the coral holobiont DMSP pool, *ex-situ* newly settled aposymbiotic *Acropora kenti* juveniles were inoculated with a single Symbiodiniaceae species, either *Cladocopium* or *Durusdinium*. Juveniles of the slow-growing *Goniastrea aspera* were similarly inoculated and monitored. *G. aspera* was specifically chosen as an alternate study species as adults do not accumulate detectable levels of DMSP (Tapiolas et al. 2013). Survivorship, basal disc surface area, Symbiodiniaceae cell density and intracellular DMSP concentrations within the coral holobiont were measured across multiple time points to examine the possibility that the growth of coral juveniles is a function of the symbiotic partner and the availability of intracellular DMSP.

3.3 Method

3.3.1 Coral sample collection

Two gravid colonies of *Acropora kenti* (formerly *Acropora tenuis* in GBR (Bridge et al. 2023)) were collected on October 2021 from the reefs of Yunbenun (Magnetic Island), Townsville (19°07'45.6"S 146°52'39.5"E) in the inshore central GBR region. Coral colonies were transported back to the AIMS SeaSIM a week prior to spawning and maintained as previously described in Chapter 2 Section 2.3.2. Colonies spawned at 18:06 on the 23rd October 2021, with the sperm and egg bundles separated carefully. Single parent cross fertilization from the two colonies was conducted to minimize genetic variation of the resulting larvae. Fertilised coral larvae were transferred to an 800 L culture tank maintained at 27 °C as described previously (see Chapter 2 Section 2.3.2). *Goniastrea retiformis* was originally chosen as the slow-growing coral species for this experiment. However, at the time of the experiment no *G. retiformis* colonies with pigmented mature eggs were found during field collection. Instead, *Goniastrea aspera* from the same genus was collected from Yunbenun (Magnetic Island) and spawned on 24th of October 2021. Sperm and eggs were collected from 14 individual colonies (to ensure high enough numbers given the small colony sizes; Babcock 1984) and mixed to allow fertilization before being transferred to three 80 L culture tanks that were maintained at 27°C. *A. kenti* and *G. aspera* larvae were settled 7 and 8 days post-spawning, respectively, and the experiment started 3 days later when juveniles were 10 and 11-days post spawning, respectively. Settlement methods are as reported in Chapter 2 Section 2.3.2, with slight modifications. Briefly, ~80 fertilized larvae were added into each well of a 6-well plate and settlement induced using autoclaved crustose coralline algae (CCA) for *A. kenti* and autoclaved coral rubble for *G. aspera* (Appendix A). Sterilized, non-living CCA and coral rubble was used to eliminate any potential transfer of CCA-associated symbionts, particularly Symbiodiniaceae spp., to the coral juveniles.

3.3.2 Symbiodiniaceae inoculation

Symbiodiniaceae cultures of *Cladocopium goreaui* (SCF 055-01.10, C1) and *Durusdinium trenchii* (SCF 082, D1a) were sourced from the AIMS Symbiont Culture Facility. *C. goreaui* and *D. trenchii* were originally isolated from *A. tenuis* widespread in Great Barrier Reef and *Acropora muricata*, respectively (Chakravarti et al. 2017; Chakravarti and van Oppen 2018; Matsuda et al. 2022). Cultures were maintained in a E500 environmental chamber (E500, Steridium) under constant temperature (27°C) and 10-hr:14-hr light:dark cycle with light level at 75 µmol photons m^{-2} s^{-1}. One-off single strain inoculation of either *Cladocopium* or *Durusdinium* was introduced to each treatment well on day 3 post-settlement at a density of 10,000 cells of Symbiodiniaceae per coral polyp. For *A. kenti*,

twelve 6-well plates per Symbiodiniaceae type were prepared (n=72 wells in total). For *G. aspera*, a total of 40 wells per Symbiodiniaceae type were prepared (not enough settled juveniles were remaining in some wells therefore these were excluded from the study). For both coral species, each 6-well plate was assigned to a single Symbiodiniaceae treatment type to avoid cross-contamination. All plates were maintained in darkness for 24 hrs to facilitate symbiont uptake by the settled corals after which a full seawater change was performed to remove any remaining free-living Symbiodiniaceae cells. An additional twelve plates (n=72 wells) of uninoculated aposymbiotic *A. kenti* juveniles and 40 wells for *G. aspera* were also maintained as controls.

On day 0 (i.e., 4-days post-settlement), a total of 12,621 *A. kenti* juveniles were settled, with an average of 59 juveniles per well in the control, 56 juveniles per well in the *Cladocopium* treatment and 60 juveniles per well in the *Durusdinium* treatment. A total of 3,764 *G. aspera* juveniles were settled with an average 35 juveniles per well in the control, and 30 and 29 juveniles per well in the treatments inoculated with *Cladocopium* and *Durusdinium*, respectively. The *A. kenti* experiment was run for 51 days. For *G. aspera* the experiment was only run for 16 days due to a lower settlement success rate resulting in a lower number of wells having a sufficient number of settled *G. aspera* juveniles. Therefore, the timeframe for the experiment was reduced to 16 days (Table 3.1); for coral tissue extraction, the number of replicate wells was also necessarily decreased from 12 to 10 . A complete seawater exchange was performed on days 0, 1 and then every second day until the end of the experiment (Table 3.1).

Table 3.1 Experimental timeline for *Acropora kenti* (Day 0 = 11 days post-spawning) and *Goniastrea retiformis* (Day 0 = 12 days post-spawning) depicting days when each procedure was performed.

Experimental Procedure	***A. kenti***	***G. aspera***
Symbiodiniaceae inoculation	Day -1	Day -1
Seawater change	Day 0, 1, 3, 5, 7, 9, 11, 13, 15, every second day until 51	Day 0, 1, 3, 5, 7, 9, 11, 13, 15
Growth measurement	Day 0, 2, 4, 6, 8, 10, 12, 14, 16, 18, 23, 30, 37, 44, 51	Day 0, 2, 4, 6, 8, 10, 12, 14, 16
Symbiodiniaceae Count	Day 0, 2, 4, 8, 16, 51	Day 0, 4, 8, 16

Coral tissue extraction	Day 0, 2, 4, 8, 16, 51	Day 0, 4, 8, 16

3.3.3 Coral growth and survival measurement

Coral juveniles were photographed to assess survival and to measure growth (using coral tissue surface area as a proxy). For *A. kenti*, photographs were taken every second day of the experiment (starting from day 0) until day 18 of the experiment after which photographs were taken every 7 days (i.e., days 23, 30, 37, 44 and 51) (Table 3.1). *G. aspera* survival and growth were measured every second day of the experiment (starting from day 0) until day 16 (Table 3.1). Photographs were taken using a camera mounted on robotic arm as described in Chapter 2 Section 2.3.4, with slight modifications. Briefly, each 6-well plate was gently rocked to induce coral juvenile tentacle retraction, as extended tentacles would interfere with coral basal disc surface area measurements. To maintain consistency, all photographs were taken using the same settings: aperture f/11, 1/80s shutter speed, exposure comp of 0 EV and 100 ISO with Weefine ring light 3000 (Kraken) mounted on camera housing lens port thread, operated in 25% of power in continuous white light mode and saved in tag image file format (TIFF). The machine learning program ilastik was used to identify coral juveniles within the image (Macadam et al. 2021), and the surface area of the coral juvenile calculated with an automated Fuji ImageJ macro adapted from Macadam et al. (2021) (see S2 Supplementary data for Chapter 3). Coral survival was established based on the percentage decrease in number of living polyps counted in the image compared to that counted on day 0. Coral polyps which detached from the well were recorded as suffering mortality, while any asexual reproduction (i.e., polyp budding) was defined as growth, which means % of survival cannot exceed initial % settlement. The % growth was calculated using the equations detailed below (also see Chapter 2 Section 2.3.4).

$$Growth = \frac{\left(\frac{xf}{nf}\right)}{\left(\frac{x0}{n0}\right)} X\ 100\% - 100\%$$

Where:

xf = Total surface area of all coral juveniles per well at a specific timepoint

nf = Number of coral juveniles per well at the same specific timepoint

$x0$ = Surface area of coral juveniles per well at day 0

$n0$ = Number of coral juveniles per well at day 0

3.3.4 Symbiodiniaceae density count

On days 0, 2, 4, 8, 16, and 51 of the experiment, five *A. kenti* polyps, equivalent to ~10% of settled polyps per well were carefully scraped off the well with a flat spatula and transferred to a cryovial containing 500 µL of filtered seawater (FSW) (Table 3.1). Formalin (10%; 500 µL) was added to the vials to achieve a final concentration of 5% formalin and stored at –20°C. Coral polyps were defrosted and rinsed with FSW to remove residual formalin before being transferred to a 200 µL plastic centrifuge tube with 20 µL of 1 % hydrochloric acid (HCl) for 24 hrs to decalcify the skeleton. The HCl solute was diluted with 20 µL of FSW and homogenized with an ultrasonicator (Cole-Parmer; USA) to breakdown the coral tissues and release the Symbiodiniaceae cells. An aliquot of solute was added to a hemocytometer (Blaubrand, Wertheim, Germany) and photographed with a Zeiss Axio Imager D2 microscope (Zeiss, Germany). The number of Symbiodiniaceae cells per aliquot was determined based on counts from the photograph, performed using an automated Fuji ImageJ macro, and counts normalized to the measured surface area for that exact coral polyp (cells per mm^2). For *G. aspera* three Symbiodiniaceae inoculated polyps were sampled from each well on days 0, 4, 8, and 16 (Table 3.1).

3.3.5 Determination of DMSP concentration within the coral tissues

To determine the concentration of DMSP within coral juvenile tissues, polyps were chemically extracted as per the method reported in Chapter 2 Section 2.3.5. In total, 12 replicate wells with settled *A. kenti* juveniles were extracted with methanol:water (2:3 ratio MeOH:H_2O) for each treatment on days 0, 2, 4, 8, 16, and 51 (Table 3.1). For *G. aspera,* 10 replicate wells of each treatment were extracted on days 0, 4, 8 and 16 of the experiment and all samples were stored at –20ºC.

Liquid chromatography mass spectrometry (LC-MS) was used to quantify the DMSP concentrations within coral juveniles, applying the LC-MS method developed to analyse DMSP concentrations in *G. retiformis* (as described in Chapter 2 Section 2.3.5) with modification. For *A. kenti,* frozen extracts (–20ºC) were thawed at room temperature and a 28 µL aliquot transferred into a 2 mL vial (amber autosampler HPLC; Agilent) with a 200 µL

glass insert. To maintain the sample DMSP concentration within the linear range of the calibration curve, each sample was then diluted with 72 µL of MeOH:H_2O (2:3 V%V). Finally, a 10 µL aliquot of 1 mM caffeine (prepared in MeOH:H_2O; 2:3 V%V) was added to each sample as an internal standard to give a final volume of 110 µL (i.e., 10% ratio of internal standard to solute). For *G. aspera*, 50 µL of thawed tissue extract was transferred to vials with a glass insert to which 5 µL of 1 mM caffeine was added to maintain the 10% ratio of internal standard to solute volume. Vials were sealed with a septum screw cap. Prior to analysis, all septa were pierced to normalize the pressure within the vial after which vials were vortexed for 30 seconds to ensure solutes were well mixed.

3.3.6 Statistical analysis

Kaplan-Meier survival plots were constructed in the R packages "survminer" and "survival" (Therneau 2015; Kassambara et al. 2017) to determine whether the survival rate of aposymbiotic (i.e., control) *A. kenti* and *G. aspera* juveniles differed from those inoculated with the two Symbiodiniaceae species. Log-rank Pairwise-comparison was performed using treatment as a factor to estimate the survival of coral juveniles, and the *p*-value for multiple comparisons was corrected using the Bonferroni method.

To eliminate bias resulting from variation in coral juvenile size, the growth of juveniles was normalized to its own initial surface area on day 0, i.e., 0% growth. Hence, the percentage of growth was > 0 as the experiment progressed. A two-way repeated measure ANOVA was performed in the R statistical program (version 4.1.0 with rstatix package) (Kassambara 2022) to analyse the growth of *A. kenti* and *G. aspera* with inverse response transformation and normal response, respectively, to provide the best fit of assumptions. A two-way ANOVA was also performed to analyse Symbiodiniaceae cell density in *A. kenti* using a square root response transformation and a cube root response transformation for *G. aspera*. Two-way ANOVA of Symbiodiniaceae cell density between *A. kenti* and *G. aspera* on day 8 were performed using a square root response transformation. DMSP concentrations of the coral juveniles were also analysed using a two-way ANOVA with the inverse transformation for *A. kenti* and a square root response transformation for *G. aspera*. *Post hoc* tests were further performed to examine the interaction between specific treatment and time with a Bonferroni correction when the interaction was significant.

3.4 Result

3.4.1 Survival and growth of coral recruits inoculated with Symbiodiniaceae

The survival of *A. kenti* (>92%) and *G. aspera* (>98%) juveniles was high across all treatments, including aposymbiotic controls (Figure 3.1A). For *A. kenti*, the first 44 days of the experiment showed no difference in survivability between treatments (*p*-value >0.0167; Tukey post-hoc with Bonferroni corrected *p*-value significant level is 0.0167 for n=3 in coral juveniles survival statistics). On day 51, the survival of *A. kenti* juveniles hosting *Cladocopium* and *Durusdinium* was 99%, with no significant difference between these (*p*-value >0.0167), although it was significantly higher than for aposymbiotic control juveniles (93 ±0.7%; *p*-value <0.0167).

G. aspera exhibited similar survival rates across all treatments, including aposymbiotic controls, for the 16 day experiment (Figure 3.1B; *p*-value >0.0167). The highest number of survivors was observed in *G. aspera* hosting *Cladocopium* (99 ±0.5%) and *Durusdinium* (99 ±0.4%), with aposymbiotic controls having a slightly lower, but not significantly different, survival rate (98.5 ±0.7%). Overall, there was no significant difference in survivorship observed between *G. aspera* (>98.5% CI 97.1% -100%) and *A. kenti* (>99.2 % CI 98.5%- 99.8%) at day 16 of the experiment.

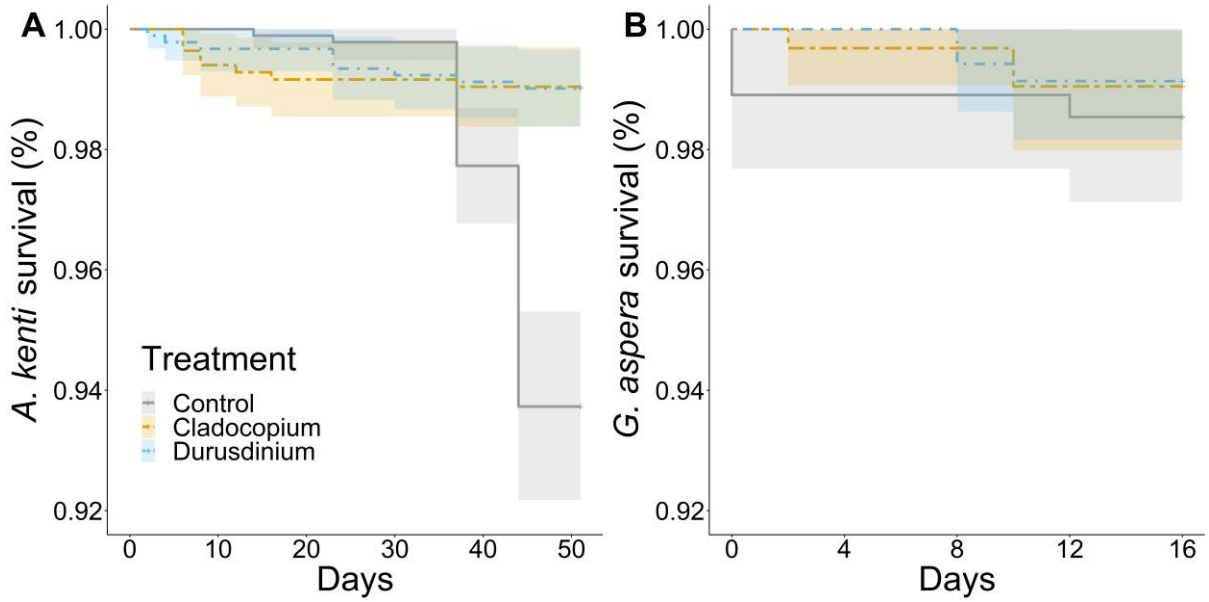

Figure 3.1**(A)** Kaplan-Meier survival curves for *Acropora kenti* juveniles inoculated with Symbiodiniaceae over 51 days post settlement. **(B)** Kaplan-Meier survival curves for *Goniastrea aspera* juveniles inoculated with Symbiodiniaceae over 16 days post settlement.

Lines represent estimate survival; Control (grey), *Cladocopium* (yellow), and *Durusdinium* (blue)

Newly settled juveniles of *A. kenti* and *G. aspera* were observed to have different growth characteristics (Figure 3.2A). *G. aspera* showed initial faster growth at the early timepoints (days 2 to 6) compared to *A. kenti*, but then plateaued with no significant change from days 6 to 16, whereas *A. kenti* showed a more linear step growth with significant difference between days 6 and 16.

A. kenti juveniles inoculated with *Durusdinium* displayed the highest growth after 51 days with a 74 ±3% increase in surface area compared to day 0. Similarly, 68 ±4% growth was observed for those inoculated with *Cladocopium*. The aposymbiotic control treatment had the least growth at 13 ±2 % and grew significantly slower than juveniles inoculated with Symbiodiniaceae (*adj p*-value *<0.05*). Infecting juveniles with either *Durusdinium* or *Cladocopium* promoted significantly higher growth in *A. kenti* compared to controls from day 2 of the experiment (non-pairwise post hoc comparison *adj p*-value <0.05). treatment In the early timepoints (days 4 to 37), *A. kenti* juveniles inoculated with *Durusdinium* grew significantly faster than those hosting *Cladocopium* (*adj p*-value *<0.05*). In the later days of the experiment, juveniles inoculated with *Cladocopium* achieved a similar size as those inoculated with *Durusdinium*. By day 44 there was no significant difference in growth between juveniles inoculated with *Cladocopium* and *Durusdinium* (*adj p*-value *>0.05*).

Inoculation of *G. aspera* juveniles with *Cladocopium* (73 ± 5%) or *Durusdinium* (55 ± 4%) did not result in significantly higher growth compared to controls (69 ±8%) (Figure 3.2B; ANOVA: $F_{2,16}$ =1.161; *p*-value = 0.338). All treatments, including controls, displayed similar growth dynamics. After an initial rapid increase in size in the first 4 days, growth plateaued. On day 16, *Cladocopium* and control treatments showed slightly higher growth than the *Durusdinium* treatment but was not significantly different (non-pairwise post hoc comparison *adj p*-value = 0.142 & 0.366; >0.05).

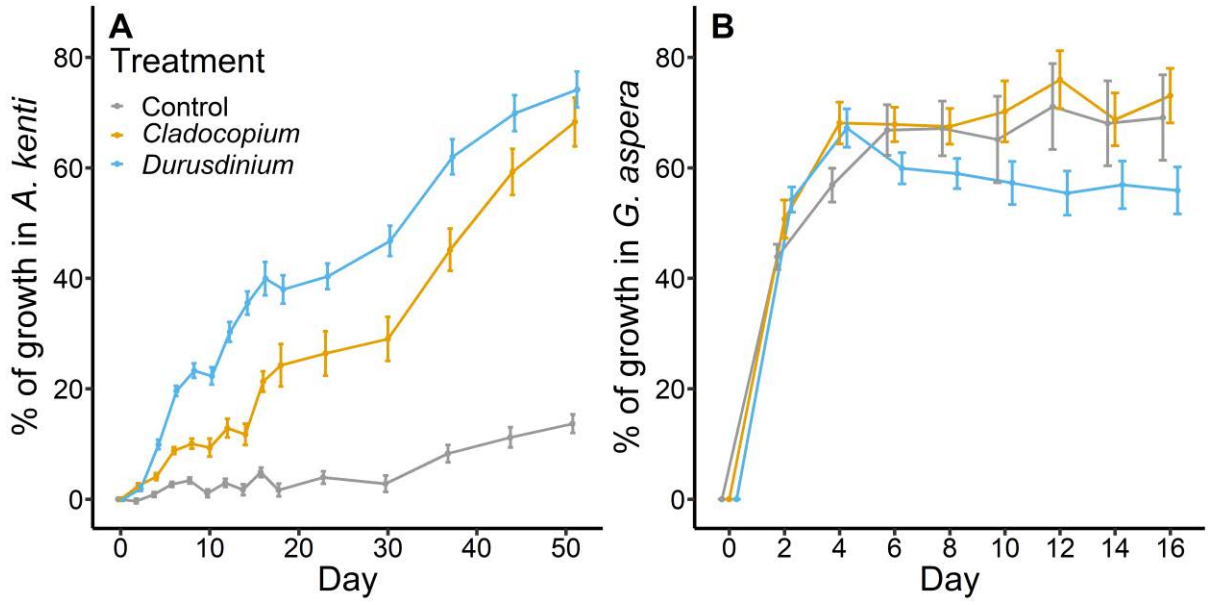

Figure 3.2: Percentage of growth of aposymbiotic juvenile corals inoculated with Symbiodiniaceae *Cladocopium* or *Durusdinium*. Percentage of growth was measured as the precent of growth of the coral juvenile from the initial surface area, with day 0 normalised to zero (initial size). Points represent average growth, error bars represent standard error (SE), treatments are staggered to facilitate interpretation. **(A)** Percentage increase in *Acropora kenti* surface area over 51 days. **(B)** Percentage increase in *Goniastrea aspera* surface area over 16 days.

3.4.2 Symbiodiniaceae cell density within coral juvenile tissues

The number of Symbiodiniaceae cells within *Acropora kenti* juvenile tissues inoculated with either *Cladocopium* or *Durusdinium* differed significantly across the 51 day experiment (Figure 3.3A). No Symbiodiniaceae cells were observed in the tissues of the uninoculated control juveniles throughout the experiment. Counts conducted on juveniles before Day 8, were inconsistent, though generally few cells were observed. On day 8, *Durusdinium* cell densities in inoculated juveniles were significantly higher (5000 ± 500 cells mm^2; non-pairwise t-test *adj p*-value <0.05) than *Cladocopium* cell densities (59 ± 8 cells mm^2). A similar pattern in cell densities was observed on day 16 of the experiment (490 ± 90 cells mm^2 *Cladocopium* vs. 1300 ± 200 cells mm^2 *Durusdinium*) although there was a slight decrease in *Durusdinium* which was not significant (*adj p*-value =0.239) and a slight increase in *Cladocopium* compared to day 8, which was significant (*adj p*-value =0.002). By day 51 this trend was reversed with cell densities in *A. kenti* juveniles harbouring *Cladocopium* increasing to 5700 ± 500 cells mm^2, while cell densities in those harbouring *Durusdinium* had declined to 1300 ± 200 cells mm^2, the difference being significant (*adj p*-value <0.05).

For *G. aspera*, at day 8, *Cladocopium* cell densities were low (300 ± 100 cells mm^2), while *Durusdinium* cell densities were significantly higher (800 ± 100 cells mm^2; pairwise t-test *adj p*-value =0.009). Though, *G. aspera* with *Durusdinium* was significantly lower than that of *A. kenti* on day 8 (non-pairwise t-test *adj p*-value < 0.05). On day 16, *Cladocopium* cell densities remain low (300 ± 90 cells mm^2) while *Durusdinium* cell densities had increased (2200 ± 400 cells mm^2) and were significantly higher than *Cladocopium* (pairwise t-test *adj p*-value < 0.05). Similar to *A. kenti* samples, cell densities in *G. aspera* inoculated with *Durusdinium* were significantly higher than those inoculated with *Cladocopium* across the 16 days experiment (non-pairwise t-test *adj p*-value < 0.05).

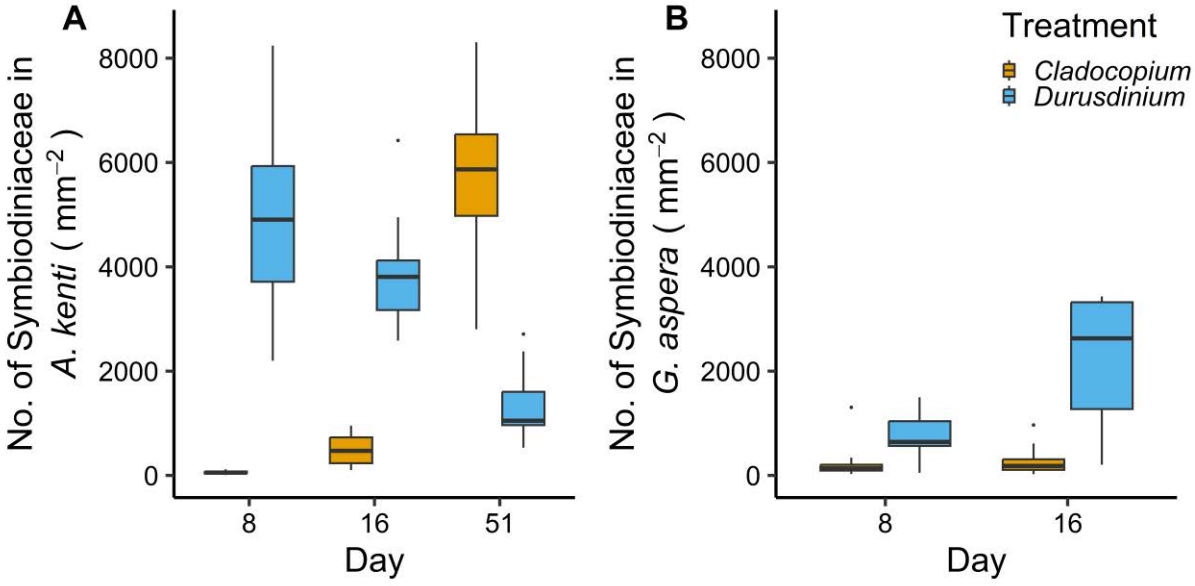

Figure 3.3 Number of Symbiodiniaceae cells within inoculated coral juveniles. Cell counts were normalized to the surface area of the juvenile (mm^{-2}). Treatments are staggered to facilitate interpretation. **(A)** Number of Symbiodiniaceae cells in *Acropora kenti* (mm^{-2}) over 51 days. **(B)** Number of Symbiodiniaceae cells in *Goniastrea aspera* (mm^{-2}) over 16 days.

3.4.3 DMSP concentrations in coral juvenile tissues

DMSP was detected throughout the experiment in the tissues of uninoculated *A. kenti* juveniles (Figure 3.4A). In these aposymbiotic *A. kenti* controls, the DMSP concentrations were highest at day 0 and declined throughout the experiment, though there was no statistical difference in DMSP concentrations for samples taken on days 16 and 51 (non-pairwise t-test *adj p*-value =0.077). DMSP concentration in the tissues of juveniles inoculated with either *Cladocopium* or *Durusdinium* on day 0 were similar to the controls. DMSP concentrations in the tissues of inoculated *A. kenti* juveniles declined over the first 8 days of the experiment (Figure 3.4A). At day 8, juveniles hosting *Cladocopium* displayed a higher concentration of

DMSP (0.022 ±0.001 mM) than juveniles inoculated with *Durusdinium* (0.015 ± 0.001 mM; *adj p*-value = 0.004). On day 16, the *Durusdinium* treatment displayed an increase in DMSP concentrations (0.021mM ± 0.0009) in recruit tissues compared to day 8 (0. 015 ± 0.001 mM), and these concentrations were significantly higher (*adj p*-value <0.05) than for juveniles inoculated with *Cladocopium* (0.016 ±0.0009 mM) or the controls (0.0106 ±0.0003 mM). DMSP concentrations in tissues of juveniles inoculated with *Cladocopium* were higher on day 51 of the experiment compared to day 16 but equivalent to those concentrations in the earlier life stages (days 0 to 8). By day 51, both *Cladocopium* and *Durusdinium* inoculated juveniles displayed similar DMSP concentrations (*adj p*-value > 0.05) and were significantly higher than the controls (*adj p*-value <0.05).

Across the 16-day experiment, no DMSP was detected in aposymbiotic *G. aspera* juveniles in contrast to Symbiodiniaceae inoculated treatments (non-pairwise t-test *adj p*-value <0.05). The DMSP concentrations in the tissues of *G. aspera* juveniles inoculated with *Cladocopium* and *Durusdinium* were similar across the first 4 days of the experiment (Figure 3.4B*; adj p*-value > 0.05). However, DMSP concentrations in the *Cladocopium* treatment ($1.7 \times 10^{-4} \pm 2.2 \times 10^{-5}$ mM) decreased by day 8 and were significantly lower than those in juveniles inoculated with *Durusdinium* ($2.6 \times 10^{-4} \pm 3.0 \times 10^{-5}$ mM; *adj p*-value = 0.015). On day 16, DMSP concentrations for *Cladocopium* inoculated juveniles had declined even further ($2.9 \times 10^{-5} \pm 1.2 \times 10^{-5}$ mM) and was significantly different to those inoculated with *Durusdinium* where the DMSP concentration remained stable ($3.3 \times 10^{-4} \pm 3.9 \times 10^{-5}$ mM; *adj p*-value < 0.05).

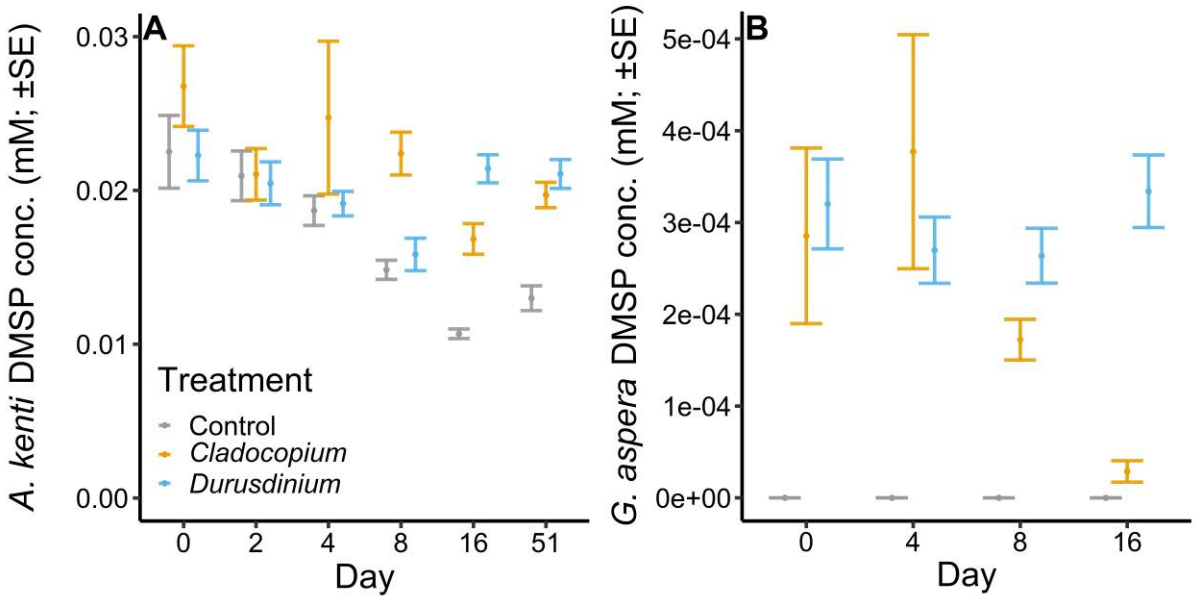

Figure 3.4 DMSP concentrations of aposymbiotic juvenile corals inoculated with Symbiodiniaceae *Cladocopium* or *Durusdinium*. DMSP concentration is normalised to per juvenile and not to Symbiodiniaceae density. Points represent average DMSP concentration (mM), error bars represent standard error (SE), treatments are staggered to facilitate interpretation. **(A)** DMSP concentration per *Acropora kenti* juvenile (mM ±SE) over 51 days. **(B)** DMSP concentration per *Goniastrea aspera* juvenile (mM ±SE) over 16 days.

3.5 Discussion

The coral holobiont is comprised of partners that form a mutualistic and symbiotic relationship to maintain system health and regulate the host response to build tolerance and adapt to environmental conditions (Dittami et al. 2021). Studies primarily report on the adult holobiont, and those that do investigate settlement often focus on the host and ignore the contribution of the other partners. To better understand the factors that promote and potentially enhance early life stage growth, this study investigated the contribution of different Symbiodiniaceae, quantifying polyp survival, growth and DMSP levels. Here, Symbiodiniaceae, the largest producer of DMSP, promoted early life stage growth of the fast-growing *A. kenti* but not of the slower-growing *G. aspera*, although it should be noted that the experimental timeframe for *G. aspera* was shorter, at 16 days, as opposed to 51-days for *A. kenti*. It is possible that the contribution from Symbiodiniaceae was not captured for *G. aspera* within the 16 days. Hosting *Durusdinium*, which is characterised as being thermally tolerant (Stat and Gates 2011), enhanced growth and increased DMSP concentrations in *A. kenti* during early ontology, however, growth of those juveniles harbouring *Cladocopium*, often the dominant Symbiodiniaceae species hosted by adult corals of the GBR, was slower

although they eventually achieved the same size. This observation is opposite to previous studies that report coral hosting *Cladocopium* grow faster when hosting *Durusdinium*, and postulate that hosting *Durusdinium* over *Cladocopium* provides thermal tolerance at the expense of slower growth (Little et al. 2004; Cunning et al. 2015). These contrasting results suggest other factors such as the difference in Symbiodiniaceae density may be driving the difference observed in growth. For the slow-growing *G. aspera*, no enhancement of growth was observed regardless of the Symbiodiniaceae species, however, hosting *Durusdinium* did result in a stable DMSP pool.

3.5.1 The influence of Symbiodiniaceae differs with coral host species

Aposymbiotic *A. kenti* juveniles were found to have overall lower survivorship, percent growth and final DMSP concentrations compared to those inoculated with Symbiodiniaceae. As the symbiotic algal partner in the coral holobiont, Symbiodiniaceae perform photosynthesis, thereby supporting the host energy requirements of oxygen and fixed carbon nutrients (Muscatine et al. 1984) underpinning coral metabolism and survival (Davy et al. 2012). Aposymbiotic juveniles only have access to a limited embryotic lipid store to support metabolism and therefore, if they are unable to establish a symbiotic relationship with Symbiodiniaceae, they will suffer from energy deprivation over time, impacting coral health and survival (Houlbrèque and Ferrier-Pagès 2009). The slow and subtle decline in survivorship of aposymbiotic *A. kenti* recruits observed on Day 51 is indicative of this. *A. kenti* juveniles hosting *Cladocopium* and *Durusdinium* both exhibited similar higher survival rates and outgrew aposymbiotic controls, confirming the symbionts are providing an essential energy source to support coral growth, including skeletal deposition.

In contrast, growth and survival of *G. aspera* recruits were not enhanced by the presence of Symbiodiniaceae in this experiment. *Goniastrea* species are slow-growing, and results indicate that monitoring over 16 days (experimental timeframe) is not sufficient to observe any substantial growth even when a symbiotic partner is present. The lack of influence of either Symbiodiniaceae species on the growth of *G. aspera*, and specifically the lack of any increase in the basal disc surface area compared to controls, suggests recruits rely solely on their embryotic lipid reserve as an energy source at this early life stage. Growth plateaued by Day 6 in all three scenarios suggesting the lipid reserves were depleted, and with no further increase in basal disc area evident, it is unclear to what end the host is utilising the

symbiont photosynthates. As neither food nor additional nutrients were provided during the experiment, it is possible that having suffered energy deprivation *G. aspera* diverted energy resources to ensure survival at the expense of establishing symbiosis and growth. Ultimately, this may adversely affect the long-term health of all partners within the holobiont, therefore, for future experiments, it is recommended an adequate heterotrophic food supply exclusive of DMSP be included and the monitoring of endpoints be extended to provide further insight into the effect of Symbiodiniaceae on *Goniastrea* survival and growth.

3.5.2 Early ontogenetic corals preferentially establish symbiosis with *Durusdinium*

For both coral species, Symbiodiniaceae densities were too low to be accurately counted in the first 4 days of the experiment. Robust Symbiodiniaceae density counts were only possible in both species at Day 8 and onwards, highlighting that the coral-algal symbiotic relationship requires time (i.e., > 4 days) to establish the intracellular Symbiodiniaceae population. Indeed, inoculation of corals with free-living cultured Symbiodiniaceae is significantly slower than if Symbiodiniaceae are acquired from conspecific adult coral through horizontal transmission (Nitschke et al. 2016).

The observation of 100-fold higher cell densities observed on Day 8 in *A. kenti* corals hosting *Durusdinium* (4832 ± 1894 cells per polyp) compared to *Cladocopium* (50.04 ± 27.15 cells per polyp) is consistent with previous studies that have reported *Durusdinium* as being a more adept opportunist than *Cladocopium*, quickly establishing symbiosis with newly settled *Acropora* juveniles (Abrego et al. 2009a). Yuyama and Higuchi (2014) reported *Durusdinium* populations were approximately 50-fold higher in *A. tenuis* juveniles at Okinawa, Japan (293.66 ± 42.02 cells per polyp in 10 days of inoculation) relative to *Cladocopium* (6.25 ± 3.03 cells per polyp). Moreover, *Cladocopium* cell density in newly settled *Acropora* was low, likely stemming from the low uptake of *Cladocopium* during the inoculation. This supports Yuyama et al. (2005) who reported that *Cladocopium* cell densities in juvenile Acropoids remained low for the first two months following settlement. A follow up study has also shown that *A. tenuis* juveniles hosting a monoculture of *Durusdinium* grew faster during the first 3 months after settlement than those hosting *Cladocopium* (Yuyama et al. 2005; Yuyama and Higuchi 2014). Together, these findings indicate *Cladocopium* is not the preferred symbiotic partner for newly settled *Acropora* juveniles. Yet, in the current study, by Day 51 the *Cladocopium* density had significantly increased compared to Day 16, which is a slightly earlier rapid rise of this population in the juvenile tissues than reported in Yuyama & Higuchi (2014) (3 months). This finding supports previous reports highlighting juveniles

switch from the initially dominant *Durusdinium* symbiont species to *Cladocopium* between one to three years after settlement with *Cladocopium* generally the preferred Symbiodiniaceae in adults (Van Oppen et al. 2001; Little et al. 2004; Gómez-Cabrera et al. 2008; Abrego et al. 2009b).

Newly settled *A. kenti* juveniles hosting *Durusdinium* grew significantly faster than when hosting *Cladocopium*, contrary to previous findings. *Cladocopium* cells provide greater photosynthate translocation to coral than *Durusdinium* thereby supporting faster growth compared to Durusdinium (Cantin et al. 2009). *Durusdinium* is capable of establishing a high cell population in newly settled coral recruits more rapidly than *Cladocopium* (Abrego et al. 2009a). It is possible that a higher density of *Durusdinium* is able to contribute a larger photosynthate pool for coral than the lower density *Cladocopium* population. Later, *A. kenti* growth accelerated in direct response to the exponential increase in *Cladocopium* symbiont density between Day 16 and 51. These results suggest that while *Durusdinium* may impart an initial benefit in the early timepoints, *A. kenti* hosting *Cladocopium* are capable of 'catching up' once sufficient cell densities are reached. This is consistent with observations of *A. tenuis*, where the growth of juveniles inoculated with *Cladocopium* eventually equals that supported by *Durusdinium* (Yuyama and Higuchi 2014). Conversely, a field study monitoring out planted *Cladocopium*-dominant *A. tenuis* juveniles (i.e., raised in aquaria from adults collected from Yunebaum; Magnetic Island) found them to have greater growth in the first 6 months of settlement than those inoculated with *Durusdinium* (Little et al. 2004), the *Cladocopium* providing a higher quality lipid-rich energy source (Cantin et al. 2009; Jones and Berkelmans 2010, 2011; Cunning et al. 2015).

The *Durusdinium* symbiont density in the *A. kenti* tissues was lower at Day 51 than the Day 16 counts. *Durusdinium* established a high cell density in *Acropora* on day 16, but by day 51 the cell density had significantly declined. This decrease in cell density could be attributed to the selfish nature of *Durusdinium*, which rapidly establishes high cell densities by retaining more photosynthate for symbiont cell replication rather than providing it to the coral host (Falkowski et al. 1993; Van Oppen and Medina 2020). Symbiotic coral juveniles can maintain health using yolk reverses for approximately 40 days, but without food or nutrient support, host Symbiodiniaceae density starts to decline (Watanabe et al. 2007). It is possible that the energy-deprived coral host no longer has the capacity to maintain the symbiotic relationship with *Durusdinium* and expels the 'greedy' symbiont, as observed on day 51 here. Therefore, future experiments should provide alternate nutrient support to

symbiotic coral juveniles to help maintain the symbiotic relationship. The energy transfer between Symbiodiniaceae and host should be monitored to account for the variations in energy allocation among different symbiont species. It is also possible the coral host relies on an external supply of CO_2 and ammonium to support the photosynthetic and metabiotic activity of Symbiodiniaceae (Furla et al. 2005). In this study, CO_2 and ammonium resources were replenished through seawater exchange every 2 days. However, it is possible that the levels of CO_2 and ammonium in the closed system (i.e., stagnant seawater) may not be sufficient to support *Durusdinium* photosynthesis. Furthermore, the production of ROS during photosynthesis may reach a level that is toxic to coral within the 2 days of stagnant water, whereby it becomes a trigger for Symbiodiniaceae expulsion. Future studies should aim to provide optimal culture conditions, including a continuous flow through of seawater.

Field-based studies have reported that *Durusdinium* is the dominant symbiont species in early *Acropora* ontology, even though other Symbiodiniaceae species are readily available (Abrego et al. 2009a; Quigley et al. 2020), i.e., *Cladocopium* is less preferred by newly settled *Acropora* and is likely outcompeted by other Symbiodiniaceae species. *Durusdinium* also tends to dominate in *Acropora* when the coral immune system is supressed, i.e., when the coral is experiencing disturbance or in degraded environments, or when attempting to re-establish the symbiont assemblages (Claar et al. 2020). The preference of early life stage *A. kenti* juveniles for *Durusdinium* observed could be a function of the thermal stress tolerance of this Symbiodiniaceae; *Durusdinium* providing an initial advantage to *Acropora* corals when settling to new habitats (Baker 2003). The parental *A. kenti* colonies originated from inshore reefs with high turbid conditions and inherently lower light availability (Reynolds et al. 2008; Finney et al. 2010; Lewis et al. 2012). Therefore, their offspring may also have traits that favour a more stress tolerant symbiotic partner to combat marginal environmental conditions for the newly settled recruits (Gabay et al. 2019; Herrera et al. 2021). However, another study found *Cladocopium* to be dominant in *Acropora* juveniles during the first month, after which it quickly switches to *Durusdinium* (Little et al. 2004). Regardless, these collective findings, and findings here, suggest the preference for symbiotic partners in *Acropora* corals varies depending on life stage and environmental conditions (Van Oppen et al. 2001; Gómez-Cabrera et al. 2008; Abrego et al. 2009b).

Similar to *A. kenti,* by Day 16 higher densities of *Durusdinium* were cultivated by *G. aspera* compared to *Cladocopium*, highlighting a preference for *Durusdinium* to form a symbiotic relationship with *G. aspera* in early ontogeny. In the 10 day post-settled *G.*

retiformis juveniles, the symbiont community quickly switches from a *Cladocopium*-dominant one to a co-dominant one with *Cladocopium* and *Durusdinium* (Terrell et al. 2023). This preference for *Durusdinium* is also observed here for the *G. aspera* parental colony, being dominated by a single Symbiodiniaceae species *Durusdinium* type D1/D4-D1u (*Durusdinium trenchii*) (Supplementary Table 3.3). Hence the preference of the juveniles reflects that of the parental colony. However, other studies have shown *Cladocopium* (C3 or C1) is usually the dominant algal partner of adult *Goniastrea* from the cooler regions such as Heron Island and Western Australia (Lajeunesse et al. 2003; Silverstein et al. 2011), suggesting the regional thermal environment may also drive symbiont preference (LaJeunesse et al. 2010).

3.5.3 DMSP biosynthesis in coral early life stages

Acropora hosting a high abundance of Symbiodiniaceae benefit from receiving photosynthates which support coral development and metabolism (Cantin et al. 2009; Abrego et al. 2012). Symbiodiniaceae also produce the majority of DMSP within the coral holobiont (Hill et al. 1995). Even so, at Day 0, DMSP was detected in aposymbiotic *A. kenti* controls, corroborating previous studies reporting that *Acropora* juveniles are capable of producing DMSP (Raina et al. 2013) (Chapter 2 Section 2.5.2). DMSP concentrations in controls were similar to those quantified in juveniles harbouring *Cladocopium* and *Durusdinium*, and even though a decrease in concentration was observed over time, DMSP was still constitutively produced by the controls throughout the experiment, confirming that the host continues to contribute to the holobiont DMSP pool.

Irrespective of Symbiodiniaceae species, *A. kenti* juveniles achieved a similar size and elevated intracellular DMSP concentration by Day 51, both of these measurements being significantly higher than for aposymbiotic controls. The *A. kenti* juveniles benefitted more so from the fast establishment of the symbiotic relationship with *Durusdinium*, growing faster and achieving a steady state concentration of intracellular DMSP earlier. For juveniles inoculated with *Cladocopium*, a similar but slower trend in growth was observed, with both polyp size and DMSP levels attaining *Durusdinium* levels by Day 51.

Higher growth in *Acropora* juveniles is correlated with higher DMSP concentrations, which aligns with the hypothesis that DMSP (and thereby acrylate) contributes to skeletal growth. However, this correlation could be an artefact of the recruits being bigger, having greater biomass and thus able to produce more DMSP. Further analysis should focus on

normalizing DMSP concentrations to coral surface area, to confirm whether higher DMSP concentration per surface area is associated with higher coral growth.

Symbiotic coral juveniles processing higher DMSP concentrations may derive, through cleavage pathways, acrylate and polyacrylic acid that is then utilized as a catalyst facilitating $CaCO_3$ deposition and promoting *Acropora* skeletal growth. However, molecular evidence to support the role of *Cladocopium* or *Durusdinium* in enhancing intracellular DMSP in coral and promoting coral growth is lacking. Alternatively, the higher growth of *A. kenti* juveniles could be independent of high DMSP concentrations, and instead be a consequence of higher photosynthate concentration resulting from the high endosymbiotic cell density. Normalizing DMSP concentrations with symbiont density may provide further insight into the portion of DMSP that is derived from hosting Symbiodiniaceae.

In the absence of a symbiotic algae partner, DMSP was not detected in *G. aspera* juveniles, consistent with that reported for *G. retiformis* (refer to Chapter 2 Section 2.5.2) and indicates *Goniastrea*, unlike *Acropora*, are not capable of DMSP biosynthesis (Tapiolas et al. 2013). In the *Goniastrea* holobiont, both *Cladocopium* and *Durusdinium* were solely responsible for the DMSP pool observed. The DMSP profiles of inoculated juveniles were initially similar, however, those hosting *Cladocopium* displayed a subtle decline in DMSP concentrations on Day 8 and a further significant decline by Day 16 with *Cladocopium* cell density remaining low throughout the experiment. Together these results suggest the initial pool of DMSP is being consumed by the holobiont at a rate that the *Cladocopium* are unable to replenish fully. In contrast, juveniles inoculated with *Durusdinium* maintained stable DMSP concentrations supported by an increasing *Durusdinium* cell density.

Goniastrea is a slow-growing coral, with an annual skeleton extension rate 16 times less than *Acropora* (Harriott 1999). Here, no difference in basal disc surface area between aposymbiotic juveniles and those inoculated with *Durusdinium* and *Cladocopium* was observed, even though DMSP levels differed. The growth metric used in this experiment is measured by the basal disc area of the coral polyp and does not account for vertical extension or the density of the $CaCO_3$ skeleton. It is possible juveniles start vertical extension after establishing the basal surface area. Therefore, future studies should consider applying the buoyant weight method to measure skeletal density (Jokiel and Maragos 1978), and micro-3D dental scanner to determine the vertical growth and the total surface area of early life stage coral juveniles (Quigley and Vidal Garcia 2022) (detailed in Chapter 2 session 2.5.5). In

contrast to *A. kenti*, the metabolic products of Symbiodiniaceae, including DMSP, did not enhance *G. aspera* growth in the early days of settlement. Evidence shows that within the first 16 days of inoculation, the Symbiodiniaceae cell density had not yet reached a level able to support enhanced growth, i.e., no differential growth from aposymbiotic coral juveniles. It is likely that slow-growing coral genera like *Goniastrea* require more established (or higher) Symbiodiniaceae populations to meet the nutritional needs of the holobiont, including the production of DMSP. *Cladocopium* densities in *A. kenti* exceeded *Durusdinium* at Day 51, correlating with an increase in coral juvenile size and DMSP concentration. Extension of the monitoring time period is needed to determine whether a similar trend occurs in *Goniastrea* at or beyond Day 51.

Gardner et al. (2017a) suggested that DMSP may have species-specific roles in coral. In further support of previous findings (in Chapter 2 session 2.5.3) that *Goniastrea* are able to uptake exogenous DMSP, *G. aspera* juveniles were able to establish a DMSP pool via the endosymbiotic algae. This finding was independent of growth suggesting DMSP may play a different role in *G. aspera* to that in *A. kenti*. Determining whether other coral genera, such as *S. pistillata* (fast-growing branching species having detectable DMSP) and *Diploastrea heliopore* (slow-growing massive species with no detectable DMSP (Tapiolas et al. 2013)), benefit from hosting a specific Symbiodiniaceae may provide additional insight into the role of DMSP in different coral genera.

3.5.4 DMSP production varies in free-living and *in-hospite* Symbiodiniaceae

Free-living *Cladocopium* produces higher DMSP concentrations per cell than *Durusdinium* (Deschaseaux et al. 2014a), however, the physiological responses of these Symbiodiniaceae can be differentially expressed between free-living cultures and those hosted within the coral holobiont (Yuyama et al. 2021). In support of this, *G. aspera* juveniles hosting *Durusdinium* displayed higher DMSP concentrations per polyp (Figure 3.4) than those hosting *Cladocopium*. Further normalizing DMSP concentration per symbiont cell might confirm the portion of DMSP contributed by inoculating specific species of Symbiodiniaceae. For *G. aspera*, evidence suggests the coral host is utilising DMSP (as levels steadily declined over time), and that *Cladocopium*, as the sole contributor of DMSP, is not able to maintain the DMSP pool. Conversely, when inoculated with *Durusdinium*, the holobiont DMSP pool is maintained. For *A. kenti*, DMSP levels were lower at Day 16 when hosting *Cladocopium*, but eventually reached the same steady-state level as juveniles hosting *Durusdinium* on Day 51. Given the significant differences in the Symbiodiniaceae cell counts,

this suggests the host is contributing to the maintenance of the holobiont DMSP pool, i.e., *A. kenti* juveniles are able to regulate production of DMSP beyond the lipid reserve period of 40 days in symbiotic coral juveniles (Richmond 1987; Watanabe et al. 2007; Graham et al. 2008). In contrast, results suggest the *Cladocopium*-*G. aspera* holobiont is utilising DMSP and not simply actively detoxifying DMSP. The regulation of DMSP catabolism in the coral holobiont is clearly complex, hence why previous studies have focussed on the individual partners (Raina et al. 2013; Kuek et al. 2022). As the production of DMSP by Symbiodiniaceae could differ depending on form, i.e., free-living vs holobiont, the function of DMSP may also vary. Although methodologically challenging, future studies should investigate the DMSP catabolism potential of all partners within a living holobiont, including associated microbes, to provide a better understanding of the function of DMSP across the holobiont.

3.6 Conclusion

This study confirms species-specific roles of the host and Symbiodiniaceae in establishing symbiosis in the early life stages of corals. The fast-growing *Acropora kenti* benefited from harbouring the heat tolerant *Durusdinium*, with a growth advantage observed concomitant to high *Durusdinium* cell densities and attainment of an elevated steady-state coral holobiont DMSP concentration. Hosting *Cladocopium*, the dominant Symbiodiniaceae in *A. kenti* adult colonies, did not impart the same initial benefit, but with time *A. kenti* juveniles did eventually attain the same size and DMSP concentrations as their *Durusdinium* counterparts. Higher Symbiodiniaceae density resulted in higher DMSP concentrations and was correlated with an increase in the size of the basal plate of *A. kenti*. These results suggest that greater concentrations of endosymbiotic-derived DMSP, and its by-product acrylate, may contribute to coral growth in *A. kenti* and may yet play a role in coral calcification. Quantifying acrylate concentrations and normalizing DMSP and acrylate concentrations to Symbiodiniaceae density is needed to better understand the effect on juvenile growth rates. In contrast, Symbiodiniaceae did not impart any measurable benefit to the slower-growing *Goniastrea aspera* juveniles. Growth was not enhanced even though Symbiodiniaceae cell densities increased and the holobiont DMSP pool was established. Swain et al (2020) highlighted the importance of understanding the effect of Symbiodiniaceae functional diversity on host fitness, and evidence here further supports this. Similarly, this study supports the findings of Gardner et al. (2017a), that the role of DMSP is coral species-specific.

However, both the role of specific Symbiodiniaceae species and of DMSP and acrylate in the growth of different coral species remains poorly understood and further investigation to identify the molecular pathways of DMSP and acrylate in coral and their function in the coral holobiont are warranted.

Chapter 4 General Discussion

Factors that enhance coral survival, skeletal formation and tissue growth are critical to the success of newly settled coral juveniles. Previous investigations have identified the organic sulfur molecule dimethylsulfoniopropionate (DMSP), and its by-product acrylate, as key metabolites in the early life (Raina et al. 2013) and adult (Tapiolas et al. 2013) stages of corals. However, there remains limited knowledge of the ecological function(s) of these compounds within the coral holobiont. In adult corals, the symbiotic partner Symbiodiniaceae is the predominate contributor to the DMSP pool (Hill et al. 1995), though newly settled *Acropora* recruits can also produce DMSP in low amounts (Raina et al. 2013). To further understand the role of DMSP and acrylate in corals, this study examined the impact of chemical dosing of these compounds, and inoculation with the two dominants endosymbiotic Symbiodiniaceae partners, *Cladocopium* or *Durusdinium* (Matsuda et al. 2022), and assessed the influence on survival, DMSP concentrations and growth of recruits. The study focused on species from two common coral genera with different life history characteristics, the fast-growing *Acropora kenti* with demonstrated high pools of DMSP and acrylate, and the slow-growing *Goniastrea retiformis* and *Goniastrea aspera*, the latter with no DMSP and only low acrylate concentrations (Tapiolas et al. 2013). Here, several key findings implicate DMSP in early-life stage coral physiology and found significant differences between the two genera, although, no conclusive evidence was found confirming a role for DMSP or acrylate in juvenile growth, regardless of whether corals were supplemented or inoculated. Higher growth and greater DMSP concentrations were found in *A. kenti* inoculated with Symbiodiniaceae, indicating DMSP might have a role in coral calcification. Future research directions and approaches to elucidate the role of DMSP and acrylate in coral calcification are suggested and discussed. Collectively, this knowledge will contribute to a better understanding of the function of DMSP and acrylate in the coral holobiont and their potential involvement in coral calcification.

4.1 Examining the potential function of DMSP and acrylate in coral calcification through chemical supplementation and Symbiodiniaceae inoculation

If left unabated, ocean acidification will lower the pH in seawater, thereby shifting the carbonate equilibrium and making it less favourable for the formation of CO_3^{2-} ions (Drake et al. 2013; Ramos-Silva et al. 2013; Von Euw et al. 2017). The reduction in the calcium carbonate ($CaCO_3$) saturation state is expected to slow the rate of coral calcification in certain Scleractinia species, as well as other marine calcifiers (Feely et al. 2004; Orr et al. 2005), with

$CaCO_3$ skeletons likely to dissolve at a faster rate than they are deposited (Marubini et al. 2008; Jokiel 2011; Steiner et al. 2018b). Improving understanding of the chemical processes involved in coral calcification could help mitigate the impact of ocean acidification on coral calcification. In coral, the deposition of the $CaCO_3$ skeleton is orchestrated by lipid and protein biomacromolecules in the skeletal organic matrix (SOM), and includes the coral acidic-rich proteins (CARPs) which contain stretches of polyaspartic acid and polyglutamic acid residues (Mitterer 1978; Ajikumar et al. 2005; Zhou et al. 2011; Mass et al. 2013; Ramos-Silva et al. 2013; Takeuchi et al. 2016). Fast-growing *Acropora* corals contain uniquely high levels of DMSP and acrylate (Tapiolas et al. 2013), yet their origin and ecological role in the *Acropora* holobiont remains unclear. In contrast, only low levels of acrylate are detected in other non-*Acropora* genera, including *Goniastrea*. Preliminary spectroscopic evidence shows polyacrylic acid, the polymerised form of acrylate, is present at the growing edge of the skeleton of newly settled *Acropora* juveniles (Kuek 2021) (Figure 1.4; Chapte1; Section 1.8). Polyacrylic acid shares the same carboxyl functional group (-COOH) as polyaspartic acid rich proteins (Drake et al. 2013; Mass et al. 2013) (Figure 1.3; Chapter 1; Section 1.8). Together these observations suggest that acrylate, and therefore polyacrylic acid, potentially has a role in facilitating calcification in fast-growing *Acropora* species. Hence, supplementation with acrylate, or its precursor DMSP, and, by extension, inoculation with Symbiodiniaceae, responsible for the majority of DMSP production in the holobiont, may help corals to calcify.

In this current study, the chemical supplementation of fast (*A. kenti*) and slow-growing (*G. retiformis*) aposymbiotic juveniles with DMSP did not impart any measurable benefit to growth (Figure 2.2 Chapter 2; Section 2.4.2). Aposymbiotic *A. kenti* juveniles were found capable of DMSP biosynthesis, establishing and maintaining basal DMSP levels, which supported the previous finding of Raina et al (2013). DMSP concentrations associated with coral juveniles did not accumulate as a result of exposure to exogenous DMSP, however, the current study could not rule out the possible uptake and rapid catabolism of this compound. Inoculation with Symbiodiniaceae demonstrated moderate enhancement of the holobiont DMSP pool in *A. kenti* juveniles. These findings suggest that *Acropora* corals (may) have a fundamental requirement for DMSP and have developed mechanisms to ensure the maintenance of the DMSP pool without relying on exogenous uptake An increase in juvenile growth correlated to the presence of Symbiodiniaceae and increasing DMSP concentrations, however, this increase could not be conclusively attributed to the enhanced DMSP

concentration. As there was no equivalent growth observed in aposymbiotic *Acropora* juveniles supplemented with DMSP, growth is likely a result of other Symbiodiniaceae functions independent of cellular DMSP concentrations.

DMSP was not detected in tissues of aposymbiotic *G. retiformis* or *G. aspera* juveniles (Chapter 2; Section 2.4.3 and Chapter 3; Section 3.4.3, respectively), but was detected in *G. retiformis* juveniles supplemented with exogenous DMSP. This suggests *Goniastrea* corals, unlike *Acropora*, are incapable of DMSP biosynthesis, but confirms they can uptake it from the environment, thereby suggesting exogenous DMSP could potentially play an ecological role in these coral juveniles. Symbiodiniaceae populations were established in *G. aspera* within 8 days of inoculation, but at a much lower density than for *A. kenti*, with significant enhancement of the holobiont DMSP pool observed. Regardless, growth of *Goniastrea* juveniles was not enhanced. After an initial rapid increase in basal disc size (Chapter 2; Section 2.4.2) growth of supplemented aposymbiotic *G. retiformis* juveniles plateaued, suggesting that the coral had depleted maternal energy reserves and was not able to utilize DMSP for tissue growth, i.e., it was energy deprived. Similar growth characteristics were observed for *G. aspera* inoculated with Symbiodiniaceae (Chapter 3; Section 3.4.1). These findings suggest that *Goniastrea* corals may also have a requirement for DMSP and have developed mechanisms to ensure maintenance of the DMSP pool through exogeneous or endosymbiotic sources, yet there is a lack of evidence to support a role for DMSP in growth enhancement. Shorter experiments were conducted for the *Goniastrea* species (8 days supplementation and 16 days inoculation experiment); hence it is possible that a longer timeframe would see DMSP levels increase. Further research effort into the DMSP flux within *Goniastrea* sp. is required, especially as symbiotic adult *Goniastrea* do not contain detectable levels of DMSP (Tapiolas et al. 2013).

Overall, the findings indicate significant differences between coral genera in their ability to biosynthesize DMSP and uptake exogenous DMSP and may contribute to the differences in coral tissue growth, i.e., fast vs. slow-growing corals. In the case of *Goniastrea*, neither DMSP supplementation nor symbiont inoculation promoted growth, and the role of DMSP in calcification remains elusive. Although symbiotic *A. kenti* juveniles showed a positive correlation between DMSP concentrations and enhanced growth, correlation does not always imply causation, hence more evidence is required to confirm their ecological causation. In addition, the suppression of growth observed in *A. kenti* and higher mortality demonstrated in *G. retiformis* individuals supplemented with acrylate confirms acrylate to be

mildly toxic. As intracellular acrylate levels were not measured in this study, it is not possible to decouple toxicity from exogeneous uptake. Consequently, future research directions are suggested below to elucidate the role of DMSP and acrylate in the coral holobiont.

4.2 Revealing the potential for DMSP uptake

The current study provides valuable insights into coral physiology, despite inconclusive results regarding the uptake of exogenous DMSP by *A. kenti*. As the occurrence of cellular uptake of DMSP was not observed here and no DMSP transportation channel is known for this genus, this study was not able to confirm *Acropora* uptake of exogenous DMSP. Paradoxically, this study could not rule out the possibility that *Acropora* possess this capability and that rapid catabolism occurred, re-establishing the equilibrium to maintain a constant DMSP pool, i.e., to levels prior to supplementation (Chapter 2; Section 2.5.2). Shinzato et al. (2021) has recently demonstrated the expansion of DMSP lyase-like (DL-L) genes in *Acropora* species, implying that DMSP is catabolised by members of this genus. Additionally, it has been observed that when marine bacteria, having prokaryotic DMSP lyase genes are supplemented with 1 mM of DMSP they are capable of its complete catabolism within 24 hours (Gao et al. 2020). Therefore, further investigation is required to determine if *Acropora* species have the cellular machinery capable of DMSP transportation into the cell and incorporation (Figure 4.1A). In coral, DMSP is unlikely to be passively transported across the cell membrane, due to its zwitterionic nature (Swan et al. 2017). Rather, DMSP uptake is likely facilitated through specific active membrane transport mechanisms, as demonstrated for diatoms (Kiene and Hoffmann Williams 1998). Genetic tools such as CISPR/Cas9 gene-editing (Cleves et al. 2018, 2020) offer an avenue for identifying similar membrane transport proteins in coral, presumably located in the epidermis layer, that are responsible for DMSP incorporation. If transport proteins are identified, the uptake of exogenous DMSP by *Acropora* could be monitored through this discrete transport protein

activity.

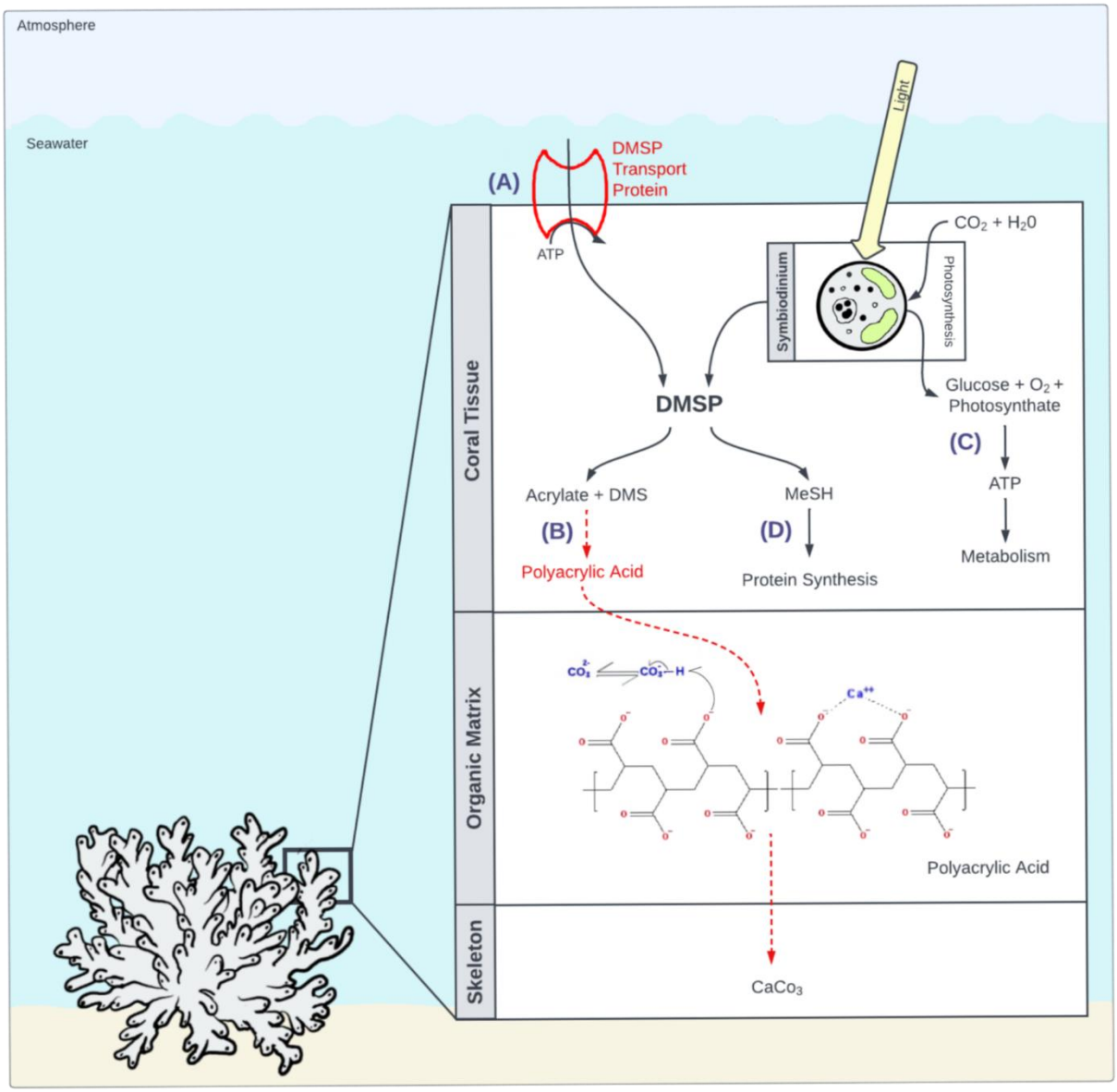

Figure 4.1 DMSP metabolism in the coral holobiont and proposed future research directions to investigate its potential role in coral calcification. **(A)** Identify the DMSP transport protein in coral. **(B)** Identify the acrylate metabolic pathway(s) and site of conversion to polyacrylic acid. **(C)** Determine photosynthate contribution to coral growth **(D)** Elucidate alternate DMSP degradation pathways. Tentative DMSP metabolism are annotated in red.

The growth of *Goniastrea* was not enhanced by either DMSP supplementation or Symbiodiniaceae inoculation. Unlike the Acroporidae, *Goniastrea* species have not experienced DMSP lyase-like gene expansion (Shinzato et al. 2021), suggesting that members of this genus have only very limited capacity to catabolize DMSP through lyase cleavage pathways. Juveniles of *G. retiformis* investigated in this study were capable of exogenous DMSP uptake, however, whether this uptake is active or passive, and whether it offers any advantage to the coral host, remains to be determined. The lack of growth enhancement suggests that its function may not be related to calcification. Identifying the proteins facilitating DMSP uptake in *Goniastrea* (Figure 4.1A) will contribute to a better understanding of its role in this slow-growing coral genus.

4.3 **DMSP cleavage metabolic pathways in coral**

Currently, there is only a limited understanding of DMSP cleavage metabolism in the coral holobiont, the acrylate metabolic pathway and site of conversion to polyacrylic acid remains unknown (Figure 4.1B). The DMSP cleavage pathway converting DMSP to DMS and acrylate has been identified in coral and is mediated by DL-L genes similar to *Alma1* (Alcolombri et al. 2015; Chiu and Shinzato 2022). A subset of DMSP lyase-like genes are highly expressed in *Acropora* juveniles indicating the production of DMS and acrylate is a critical function (Shinzato et al. 2021) (Miller personal communication). Preliminary work has detected a signal reminiscent of polyacrylic acid at the growing edge of the *Acropora* skeleton (Kuek 2021) and suggests these fast-growing corals may also have specialized mechanisms capable of converting acrylate to polyacrylic acid, yet the details of this conversion and the site at which it occurs is unknown (Figure 4.1B; putative reaction pathways in red). Therefore, to confirm the function of DMSP and acrylate in coral calcification, it is critical to establish whether there is a molecular link between the high levels of DMSP and acrylate in the tissues, the putative presence of polyacrylic acid in organic matrix and the incorporation of polyacrylic acid to the skeleton.

Anionic CARPs containing polyaspartic acid and polyglutamate acid residues are synthesised in the endoplasmic reticulum, then packaged into transport vesicles in the Golgi complex and exported extracellularly to the SOM (Pelham 1990; Gotliv et al. 2005). It is unclear whether polyacrylic acid (a polymer and not a protein) could similarly be formed

within coral cells and transported extracellularly to the SOM (Allemand et al. 1998), or alternatively, whether the polymerization occurs within the SOM. Determining whether biologically-mediated acrylate polymerisation is possible in corals, and if so where polyacrylic acid is localized, i.e., within the coral tissue or the SOM, is necessary to establish its role in coral calcification. However, tracking and visualising DMSP across multiple tissue types and the skeleton is analytical challenging.

4.3.1 Tracing DMSP and acrylate catabolism – what has been done and the next steps

Several quantitative analytical tracking techniques have the potential to track the biosynthesis and catabolism pathways of DMSP and acrylate in the coral holobiont. For example, the presence of DMSP in coral was initially confirmed by gas chromatography mass spectrometry (GC-MS) detecting the chemically-induced release of DMS gas as a proxy for DMSP (Broadbent and Jones 2004; Deschaseaux et al. 2014b, 2016, 2022; Jones and King 2015; Swan et al. 2017). Quantitative proton nuclear magnetic resonance spectroscopy (^{1}H-qNMR) subsequently enabled the simultaneous detection and quantification of DMSP and acrylate within adult coral tissue extracts (Tapiolas et al. 2010, 2013) and confirmed the production of DMSP in aposymbiotic *Acropora* juveniles (Raina et al. 2013). More recently, a combination of nanoscale secondary ion mass spectrometry (NanoSIMS), Time-of-Fight secondary ion mass spectrometry (ToF-SIMS), LC-MS and ^{1}H-NMR were used to explore pathways associated with the biosynthesis of DMSP from ^{34}S labelled inorganic sulfate by Symbiodiniaceae and its cleavage to DMS (Raina et al. 2017) and confirmed localisation within algal vacuoles, the cytoplasm and chloroplasts. Since then, the coral host has been shown to assimilate sulfate (Higuchi et al. 2021) providing the elemental precursor for host production of DMSP. LC-MS and ^{1}H-NMR have also revealed some coral-associated bacteria are capable of DMSP biosynthesis (Kuek et al. 2022).

The catabolism of DMSP has similarly been tracked. Raina et al. (2017), applied NanoSIMS to confirm bacterial uptake of ^{34}S labelled DMSP derived from Symbiodiniaceae and further confirmed its breakdown to DMS using ^{1}H-NMR. As the labelled ^{34}S is released with DMS synthesis, it is not possible to monitor the fate of the acrylate by-product, this would require ^{13}C labelling. Most recently, Raman spectroscopy detected a signal tentatively assigned as polyacrylic acid on the growth front of skeletons of juvenile corals incubated with ^{13}C labelled acrylate (Kuek 2021). Attempts to verify this by NanoSIMS were inconclusive as detection is based on a change in the electric-dipole polarizability of a chemical bond, and ultimately it proved impossible to distinguish ^{13}C labelled chemistry from the ^{12}C counterpart.

Unfortunately, many of the methods listed above are not suited to the direct detection of metabolites in the $CaCO_3$ skeleton and require decalcification with EDTA or acid, both of which will also remove water-soluble target molecules (such as DMSP and acrylate).

^{13}C labelled DMSP, where all three carbons are labelled, may provide a means to examine the production and fate of acrylate in coral (Figure 4.1B). With the uptake of DMSP confirmed for *Goniastrea*, incubation of *Goniastrea* with ^{13}C labelled DMSP should be performed. Techniques such as matrix-assisted laser desorption/ionisation imaging mass spectrometry (MALDI-MS) could be applied to the skeleton-free region of coral polyp such as tentacles. The proposed method would allow the quantification of: ^{13}C labelled DMSP uptake, cleavage to ^{13}C labelled acrylate and potentially the polymerization to ^{13}C labelled polyacrylic acid within coral tissue, as well as visualisation of the spatial distribution of target molecules within coral tissue (Figure 4.1B). It would not, however, address the question regarding the conversion of acrylate to polyacrylic acid if this occurs in the SOM. To assess *Acropora*, alternate methods to biosynthesis ^{13}C labelled DMSP are required.

If acrylate is converted to polyacrylic acid by the coral in the SOM to support calcification, then isotope labelling of acrylate should result in ^{13}C labelled polyacrylic acid being incorporated into the coral skeleton (Figure 4.1B). Methods to extract polyacrylic acid from the skeleton and confirm its structure through direct detection and/or indirectly through conversion back to acrylate should be investigated. Acid decalcification of the coral skeleton, previously chemically extracted to remove tissue-associated compounds, would potentially yield the polyacrylic acid and after neutralisation with water could be refluxed with dialkyl phthalates at 275- 325 °C for 1 to 5 hours to promote depolymerization (Haschke and Lewis 1981). LC-MS or NMR could be applied to identify the ^{13}C labelled products, and presumably ^{13}C labelled acrylate originated from ^{13}C labelled polyacrylic acid in the SOM and coral skeleton. Employing labelled isotopic markers offers a potential avenue to explore the metabolism of DMSP and its potential molecular pathways within the coral holobiont leading to the formation of acrylate and polyacrylic acid.

4.3.2 Disrupting DMSP metabolic pathways

The function of acrylate in coral calcification could be examined through the inhibition of DMSP metabolic pathways. Brominated-DMSP (Br-DMSP) inhibits *Alma1* DMSP lyase-like gene activity in *Acropora* (Alcolombri et al. 2015, 2017). The bulky bromine molecule blocks the active site of DMSP lyase thereby inhibiting the DMSP

cleavage pathway and offers a means to investigate whether coral holobiont growth could be stunted by restricting the coral's ability to source acrylate for calcification. However, toxicity needs to be considered as brominated compounds are toxic to many marine organisms (Fisher et al. 1999). Therefore establishing the appropriate concentration of Br-DMSP to be applied is critical. A preliminary study with *Acropora* coral juveniles established that supplementation with 0.1 mM Br-DMSP is lethal, while 0.01 mM of Br-DMSP shows similar survival as controls (Johns 2019). Therefore, future studies should investigate whether skeletal growth of the coral holobiont is impacted as a result of the inhibition of DMSP cleavage by Br-DMSP. Slowed or no growth would provide further evidence for the role of acrylate in calcification.

4.4 Symbiodiniaceae stimulates coral calcification through photosynthesis

A. kenti juveniles with high Symbiodiniaceae density exhibit greater growth and higher DMSP concentrations (Chapter 3; Section 3.5.2). Previous studies have shown a direct link between algal photosynthetic activity and coral tissue (Cantin et al. 2009; Hughes and Grottoli 2013; Tremblay et al. 2016) and skeletal growth (Goreau 1959; Allemand et al. 1998, 2004b). Results here further support this; coral growth was promoted by inoculating Symbiodiniaceae and receiving photosynthates that support its growth (Figure 4.1C) (Chapter 3; Section 3.5.2). Yet the contribution of photosynthates and of DMSP specifically to coral growth requires further investigation. A study of the sea anemone, *Exaiptasia diaphana*, has shown that when bleached they expel the symbionts, initially impacting growth (Gundlach and Watson 2019). Recolonisation of the symbionts can reverse this impact, feeding with brine shrimp nauplii and/or an amino acid as nutrient supplement. Enhancing coral food supplements could promote synthesis of proteins rich in the aspartic acid region and support high calcification rates (Gupta et al. 2007). Therefore, it is possible that the enhanced growth of *Acropora* juveniles with Symbiodiniaceae could be independent of the enhanced DMSP concentration and instead be reliant on other photosynthates, such as amino acids and other small metabolites produced during photosynthesis (Figure 4.1 C). Further investigation introducing DMSP along with other nutrient supplements, to better simulate the natural photosynthate, is needed to determine whether early life stage aposymbiotic coral growth can be chemically enhanced.

The Symbiodiniaceae strain has a direct impact on the growth dynamics of *Acropora* and *Goniastrea* coral juveniles (Chapter 3; Section 3.5.1). For *Acropora* recruits, both *Durusdinium* and *Cladocopium* species promoted an increase in tissue growth and established and maintained an elevated steady state DMSP pool. In *Acropora*, although coral growth was

initially slower with *Cladocopium*, as the *Cladocopium* population increased, growth similar to that as *Durusdinium* inoculated juveniles were ultimately achieved and similar to previous studies of Yuyama and Higuchi (2014). *Acropora* hosting *Durusdinium* may favour the early-life stage growth dynamics of juveniles, however, longer-term growth enhancement could not be sustained once the *Durusdinium* population dropped. Staggered introduction of *Durusdinium* and *Cladocopium* to new recruits should be investigated to determine whether growth and DMSP concentrations can be manipulated and further enhanced (Figure 4.1 C).

Goniastrea, like *Acropora*, similarly exhibited higher *Durusdinium* cell density and DMSP concentrations at the early life stages, however, this did not afford any advantage compared to aposymbiotic controls or those colonised by *Cladocopium*. This confirms that photosynthate availability, including DMSP, as provided by the algal partner, is unlikely to be the factor driving *Goniastrea* juvenile early-stage growth. This warrants further investigation.

4.5 Additional avenues of investigation to reveal the function of DMSP and acrylate in the coral holobiont

In the coral holobiont, DMSP can be degraded through various pathways. The cleavage pathway catabolises DMSP into DMS and acrylate, while the demethylation pathway metabolizes DMSP to 3-methyl-propionate (MMPA) which is further converted to methanethiol (MeSH) (Figure 4.1D) (Curson et al. 2011a; Reisch et al. 2011a; Bullock et al. 2017). MeSH contains organic sulfur and carbon and contributes to the coral energy budget and protein synthesis (Chapter 1 section 1.2.1; Chapter 2, Section 2.5.3) (Kiene et al. 1999; Kiene and Linn 2000). In bacteria, DMSP can be broken down through both pathways, possibly simultaneously, with the relative proportion dependant on DMSP concentration and metabolic condition (Gao et al. 2020; Fernandez et al. 2021). Bacteria can also convert DMSP to DMS and 3-hydropropionate (Tandon et al. 2020a). However, the mechanism that regulates DMSP metabolic pathways in the coral holobiont is unknown. Despite the enhancement of DMSP concentrations in both coral species resulting from Symbiodiniaceae colonization, the current study was unable to show any direct correlation with calcification, although it should be noted that the bacterial community was not considered, and hence microbial degradation of DMSP to a non-acrylate product cannot be discounted (Bullock et al. 2017; Tandon et al. 2020a). As a result, even though there was enhancement of the intracellular DMSP pool, production of non-acrylate by-products may have occurred re-directing physiological function to non-calcifying processes. Therefore, the observed enhanced DMSP concentration observed in *G. retiformis* and *G. aspera* (Chapter 2; Section 2.4.3 and Chapter 3; Section 3.4.3) but lack

of concomitant enhancement in growth could be attributed to other possible DMSP degradation pathways (Figure 4.1 D). To address this, it would be beneficial to examine DMSP lyase activity and quantify acrylate concentrations directly within coral tissue.

Goniastrea juveniles can uptake exogenous DMSP, at levels that exceed normal biological levels, without any impact on survival, which may benefit this early life stage. Under predicted climate scenarios conducive to coral bleaching (i.e., breakdown of the coral-Symbiodiniaceae symbiosis), bleached *Goniastrea* colonies presumably have access to limited DMSP to mitigate stress. The uptake of exogenous DMSP, with its antioxidant function (Sunda et al. 2002; Jones et al. 2007; Deschaseaux et al. 2014b; Jones and King 2015), may enable *Goniastrea* to potentially mitigate the effects of warming, salinity and oxidative stress. Therefore, further studies should investigate DMSP supplementation of *Goniastrea* under different environmental stressors and assess the various physiological (Gardner et al. 2016), chemical (Tapiolas et al. 2013), and gene expression regulation (Gao et al. 2020; Wang et al. 2022) responses.

Previous ^{1}H-NMR investigation of adult *G. aspera* fragments did not detect DMSP (Tapiolas et al. 2013). ^{1}H-NMR has inherently low detection limits, therefore DMSP quantification in adults should be repeated using a more sensitive method, such as the LC-MS method developed here, to confirm its presence, or not, and enable a more complete understanding of DMSP metabolism across the different life history stages. Regardless, it is clear DMSP metabolism mechanisms differ between *Acropora* and *Goniastrea* and suggests the function of DMSP may also vary between genera. To explore this, future studies should expand the species investigated to include *Diplastrea heilopora,* for which no DMSP or acrylate was detected in adults (Tapiolas et al. 2013), as well as other branching genera such as *Stylophora pistillata* that do accumulate DMSP but not to the same high levels as in *Acropora*. Incorporating additional coral species will provide a broader understanding of DMSP metabolism across coral genera.

4.6 Conclusion

Corals are a significant producer of DMSP in the marine system and coral reefs have a key role in the marine sulfur cycle. This study provides valuable insights into the fundamental understanding of DMSP production in coral recruits, which is crucial for predicting the future success of the coral holobiont and the resilience of coral against climate change and ocean acidification. Here, the biosynthesis of DMSP was confirmed in aposymbiotic *Acropora kenti*

coral juveniles. Biosynthesis was not observed in aposymbiotic *Goniastrea* juveniles, yet, they did uptake exogenous DMSP, achieving intracellular DMSP concentrations comparable to those produced by aposymbiotic *Acropora* corals. Symbiodiniaceae colonisation of *Acropora* resulted in enhanced DMSP concentrations and promoted coral growth, yet for *Goniastrea*, while the DMSP pool increased there was no concomitant increase in growth. These results do not provide conclusive evidence for the role of DMSP (and hence acrylate) in skeleton formation but do highlight the complexity in studying this metabolic pathway in coral. Elucidating the DMSP and acrylate metabolic pathways within the holobiont and identifying associated proteins involved in the regulation of these pathways is of high importance.

References

Abbott E, Dixon G, Matz M (2021) Shuffling between Cladocopium and Durusdinium extensively modifies the physiology of each symbiont without stressing the coral host. Mol Ecol 30:6585–6595

Abrego D, Van Oppen MJH, Willis BL (2009a) Highly infectious symbiont dominates initial uptake in coral juveniles. Mol Ecol 18:3518–3531

Abrego D, Van Oppen MJH, Willis BL (2009b) Onset of algal endosymbiont specificity varies among closely related species of *Acropora* corals during early ontogeny. Mol Ecol 18:3532–3543

Abrego D, Willis BL, van Oppen MJH (2012) Impact of Light and Temperature on the Uptake of Algal Symbionts by Coral Juveniles. PLoS One 7:e50311

Adamiano A, Goffredo S, Dubinsky Z, Levy O, Fermani S, Fabbri D, Falini G (2014) Analytical pyrolysis-based study on intra-skeletal organic matrices from Mediterranean corals. Anal Bioanal Chem 406:6021–6033

Addadi L, Joester D, Nudelman F, Weiner S (2006) Mollusk Shell Formation: A Source of New Concepts for Understanding Biomineralization Processes. Chemistry - A European Journal 12:980–987

Aeby GS, Howells E, Work T, Abrego D, Williams GJ, Wedding LM, Caldwell JM, Moritsch M, Burt JA (2020) Localized outbreaks of coral disease on Arabian reefs are linked to extreme temperatures and environmental stressors. Coral Reefs 39:829–846

Aguilar C, Raina J-B, Motti CA, Fôret S, Hayward DC, Lapeyre B, Bourne DG, Miller DJ (2017) Transcriptomic analysis of the response of Acropora millepora to hypo-osmotic stress provides insights into DMSP biosynthesis by corals. BMC Genomics 18:612

Aizenberg J, Lambert G, Weiner S, Addadi L (2002) Factors involved in the formation of amorphous and crystalline calcium carbonate: A study of an ascidian skeleton. J Am Chem Soc 124:32–39

Ajikumar PK, Low BJM, Valiyaveettil S (2005) Role of soluble polymers on the preparation of functional thin films of calcium carbonate. Surf Coat Technol 198:227–230

Akiva A, Neder M, Kahil K, Gavriel R, Pinkas I, Goobes G, Mass T (2018a) Minerals in the pre-settled coral Stylophora pistillata crystallize via protein and ion changes. Nat Commun 9:

Akiva A, Neder M, Kahil K, Gavriel R, Pinkas I, Goobes G, Mass T (2018b) Reply to: Characterizing coral skeleton mineralogy with Raman spectroscopy. Nat Commun

Albéric M, Stifler CA, Zou Z, Sun CY, Killian CE, Valencia S, Mawass MA, Bertinetti L, Gilbert PUPA, Politi Y (2019) Growth and regrowth of adult sea urchin spines involve hydrated and anhydrous amorphous calcium carbonate precursors. J Struct Biol X 1:100004

Albright R (2011) Reviewing the Effects of Ocean Acidification on Sexual Reproduction and Early Life History Stages of Reef-Building Corals. J Mar Biol 2011:1–14

Alcolombri U, Ben-Dor S, Feldmesser E, Levin Y, Tawfik DS, Vardi A (2015) Identification of the algal dimethyl sulfide-releasing enzyme: A missing link in the marine sulfur cycle. Science (1979) 348:1466–1469

Alcolombri U, Lei L, Meltzer D, Vardi A, Tawfik DS (2017) Assigning the Algal Source of Dimethylsulfide Using a Selective Lyase Inhibitor. ACS Chem Biol 12:41–46

Allemand D, Ferrier-Pagès C, Furla P, Houlbrèque F, Puverel S, Reynaud S, Tambutté É, Tambutté S, Zoccola D (2004a) Biomineralisation in reef-building corals: From molecular mechanisms to environmental control. C R Palevol

Allemand D, Ferrier-Pagès C, Furla P, Houlbrèque F, Puverel S, Reynaud S, Tambutté É, Tambutté S, Zoccola D, Allemand (D (2004b) Biomineralisation in reef-building corals: from molecular mechanisms to environmental control. C R Palevol 3:453–467

Allemand D, TambuttE E, Girard J, Jaubert J (1998) Organic matrix synthesis in the scleractinian coral stylophora pistillata: role in biomineralization and potential target of the organotin tributyltin. J Exp Biol 201 (Pt 13):2001–9

Allemand D, Tambutté É, Zoccola D, Tambutté S (2011) Coral calcification, cells to reefs. Coral Reefs: An Ecosystem in Transition. Springer Netherlands, pp 119–150

Allison N, Cohen I, Finch AA, Erez J, Tudhope AW (2014) Corals concentrate dissolved inorganic carbon to facilitate calcification. Nat Commun 5:1–6

Antao SM, Hassan I (2009) The orthorhombic structure of CaCo3, SrCo3, PbCO 3 and BaCo3: Linear structural trends. Can Mineral 47:1245–1255

Aumont O, Belviso S, Monfray P (2002) Dimethylsulfoniopropionate (DMSP) and dimethylsulfide (DMS) sea surface distributions simulated from a global three-dimensional ocean carbon cycle model.

Ayers GP, Gillett RW (2000) DMS and its oxidation products in the remote marine atmosphere: implications for climate and atmospheric chemistry. J Sea Res 43:275–286

Babcock RC (1984) Reproduction and distribution of two species of Goniastrea (Scleractinia) from the Great Barrier Reef province. Coral Reefs 2:187–195

Baker AC (2003) Flexibility and Specificity in Coral-Algal Symbiosis: Diversity, Ecology, and Biogeography of Symbiodinium. Source: Annual Review of Ecology, Evolution, and Systematics 34:661–689

Barnes DJ (1970) Coral skeletons: An explanation of their growth and structure. Science (1979) 170:1305–1308

Barnes DJ, Lough JM (1992) Systematic variations in the depth of skeleton occupied by coral tissue in massive colonies of Porites from the Great barrier reef. J Exp Mar Biol Ecol 159:113–128

Barott KL, Perez SO, Linsmayer LB, Tresguerres M (2015) Differential localization of ion transporters suggests distinct cellular mechanisms for calcification and photosynthesis between two coral species. American Journal of Physiology-Regulatory, Integrative and Comparative Physiology 309:R235–R246

Barron ME, Thies AB, Espinoza JA, Barott KL, Hamdoun A, Tresguerres M (2018) A vesicular Na+/Ca2+ exchanger in coral calcifying cells. PLoS One 13:e0205367

Bashford D, Karplus M (1990) pKa's of Ionizable Groups in Proteins: Atomic Detail from a Continuum Electrostatic Model. Biochemistry 29:10219–10225

Bellwood DR, Hoey AS, Choat JH (2003) Limited functional redundancy in high diversity systems: resilience and ecosystem function on coral reefs. Ecol Lett 6:281–285

Bopp L, Boucher O, Aumont O, Belviso S, Dufresne JL, Pham M, Monfray P (2004) Will marine dimethylsulfide emissions amplify or alleviate global warming? A model study. Canadian Journal of Fisheries and Aquatic Sciences 61:826–835

Bridge TCL, Cowman PF, Quattrini AM, Bonito VE, Sinniger F, Harii S, Head CEI, Hung JY, Halafihi T, Rongo T, Baird AH (2023) A tenuis relationship: traditional taxonomy obscures systematics and biogeography of the 'Acropora tenuis' (Scleractinia: Acroporidae) species complex. Zool J Linn Soc

Broadbent AD, Jones GB (2004) DMS and DMSP in mucus ropes, coral mucus, surface films and sediment pore waters from coral reefs in the Great Barrier Reef. Mar Freshw Res 55:849

Broadbent AD, Jones GB, Jones RJ (2002) DMSP in corals and benthic algae from the Great Barrier Reef. Estuar Coast Shelf Sci 55:547–555

Bullock HA, Luo H, Whitman WB (2017) Evolution of dimethylsulfoniopropionate metabolism in marine phytoplankton and bacteria. Front Microbiol 8:637

Burdett HL, Carruthers M, Donohue PJC, Wicks LC, Hennige SJ, Roberts JM, Kamenos NA (2014) Effects of high temperature and CO2 on intracellular DMSP in the cold-water coral Lophelia pertusa. Mar Biol 161:1499–1506

Cameron KA, Harrison PL (2020) Density of coral larvae can influence settlement, post-settlement colony abundance and coral cover in larval restoration. Sci Rep 10:

Cantaert B, Beniash E, Meldrum FC (2013a) The role of poly(aspartic acid) in the precipitation of calcium phosphate in confinement. J Mater Chem B 1:6586

Cantaert B, Verch A, Kim YY, Ludwig H, Paunov VN, Kröger R, Meldrum FC (2013b) Formation and structure of calcium carbonate thin films and nanofibers precipitated in the presence of poly(allylamine hydrochloride) and magnesium ions. Chemistry of Materials 25:4994–5003

Cantin NE, van Oppen MJH, Willis BL, Mieog JC, Negri AP (2009) Juvenile corals can acquire more carbon from high-performance algal symbionts. Coral Reefs 28:405–414

Cantoni GÁ, Anderson DG (1956) Enzymatic cleavage of dimethylpropiothetin by Polysiphonia lanosa. Journal of Biological Chemistry 222:171–177

Carpenter LJ, Archer SD, Beale R (2012) Ocean-atmosphere trace gas exchange. Chem Soc Rev 41:6473–6506

Chakravarti LJ, Beltran VH, van Oppen MJH (2017) Rapid thermal adaptation in photosymbionts of reef-building corals. Glob Chang Biol 23:4675–4688

Chakravarti LJ, van Oppen MJH (2018) Experimental evolution in coral photosymbionts as a tool to increase thermal tolerance. Front Mar Sci 5:227

Chambers ST, Kunin CM, Miller D, Hamada A (1987) Dimethylthetin can substitute for glycine betaine as an osmoprotectant molecule for Escherichia coli. J Bacteriol 169:4845–7

Charlson RJ, Lovelockt JE, Warren SG (1987) Oceanic phytoplankton, atmospheric sulphur, cloud albedo and climate.

Chen Y, Shah S, Dougan KE, van Oppen MJH, Bhattacharya D, Chan CX (2022) Improved Cladocopium goreaui Genome Assembly Reveals Features of a Facultative Coral Symbiont and the Complex Evolutionary History of Dinoflagellate Genes. Microorganisms 10:1662

Chiu Y-L, Shinzato C (2022) Evolutionary History of DMSP Lyase-Like Genes in Animals and Their Possible Involvement in Evolution of the Scleractinian Coral Genus, Acropora. Front Mar Sci 9:992

Chua C, Leggat W, Moya A (2013) Near-future reductions in pH will have no consistent ecological effects on the early life-history stages of reef corals. Marine Ecology Progress 143–151

Claar DC, Starko S, Tietjen KL, Epstein HE, Cunning R, Cobb KM, Baker AC, Gates RD, Baum JK (2020) Dynamic symbioses reveal pathways to coral survival through prolonged heatwaves. Nature Communications 2020 11:1 11:1–10

Cleves PA, Shumaker A, Lee JM, Putnam HM, Bhattacharya D (2020) Unknown to Known: Advancing Knowledge of Coral Gene Function. Trends in Genetics 36:93–104

Cleves PA, Strader ME, Bay LK, Pringle JR, Matz M V. (2018) CRISPR/Cas9-mediated genome editing in a reef-building coral. Proceedings of the National Academy of Sciences 115:5235–5240

Cohen AL (2003) Geochemical Perspectives on Coral Mineralization. Rev Mineral Geochem

Cole AJ, Lawton RJ, Pratchett MS, Wilson SK (2011) Chronic coral consumption by butterflyfishes. Coral Reefs 30:85–93

Constantz BR (1986) Coral Skeleton Construction: A Physiochemically Dominated Process. Palaios 1:152

Cunning R, Gillette P, Capo T, Galvez K, Baker AC (2015) Growth tradeoffs associated with thermotolerant symbionts in the coral Pocillopora damicornis are lost in warmer oceans. Coral Reefs 34:155–160

Curson ARJ, Burns OJ, Voget S, Daniel R, Todd JD, McInnis K, Wexler M, Johnston AWB (2014) Screening of metagenomic and genomic libraries reveals three classes of bacterial enzymes that overcome the toxicity of acrylate. PLoS One 9:

Curson ARJ, Rogers R, Todd JD, Brearley CA, Johnston AWB (2008) Molecular genetic analysis of a dimethylsulfoniopropionate lyase that liberates the climate-changing gas dimethylsulfide in several marine alpha-proteobacteria and Rhodobacter sphaeroides. Environ Microbiol 10:757–767

Curson ARJ, Sullivan MJ, Todd JD, Johnston AWB (2011a) DddY, a periplasmic dimethylsulfoniopropionate lyase found in taxonomically diverse species of Proteobacteria. ISME J 5:1191–1200

Curson ARJ, Todd JD, Sullivan MJ, Johnston AWB (2011b) Catabolism of dimethylsulphoniopropionate: microorganisms, enzymes and genes. Nat Rev Microbiol 9:849–859

Dacey JWH, Wakeham SG (1986) Oceanic Dimethylsulfide: Production During Zooplankton Grazing on Phytoplankton. Science (1979) 233:1314–1316

Davy SK, Allemand D, Weis VM (2012) Cell Biology of Cnidarian-Dinoflagellate Symbiosis. Microbiology and Molecular Biology Reviews 76:229–261

De'Ath G, Fabricius KE, Sweatman H, Puotinen M (2012) The 27–year decline of coral cover on the Great Barrier Reef and its causes. Proceedings of the National Academy of Sciences 109:17995–17999

DeCarlo TM, Comeau S, Cornwall CE, Gajdzik L, Guagliardo P, Sadekov A, Thillainath EC, Trotter J, McCulloch MT (2019) Investigating marine bio-calcification mechanisms in a changing ocean with in vivo and high-resolution ex vivo Raman spectroscopy. Glob Chang Biol 25:1877–1888

DeCarlo TM, D'Olivo JP, Foster T, Holcomb M, Becker T, McCulloch MT (2017) Coral calcifying fluid aragonite saturation states derived from Raman spectroscopy. Biogeosciences 14:5253–5269

DeCarlo TM, Ren H, Farfan GA (2018) The Origin and Role of Organic Matrix in Coral Calcification: Insights From Comparing Coral Skeleton and Abiogenic Aragonite. Front Mar Sci 5:170

Deschaseaux E, Jones G, Swan H (2016) Dimethylated sulfur compounds in coral-reef ecosystems. Environmental Chemistry 13:239

Deschaseaux ESM, Beltran VH, Jones GB, Deseo MA, Swan HB, Harrison PL, Eyre BD (2014a) Comparative response of DMS and DMSP concentrations in Symbiodinium clades C1 and D1 under thermal stress. J Exp Mar Biol Ecol 459:181–189

Deschaseaux ESM, Jones GB, Deseo MA, Shepherd KM, Kiene RP, Swan HB, Harrison PL, Eyre BD (2014b) Effects of environmental factors on dimethylated sulfur compounds and their potential role in the antioxidant system of the coral holobiont. Limnol Oceanogr 59:758–768

Deschaseaux ESM, Swan HB, Maher DT, Jones GB, Schulz KG, Koveke EP, Toda K, Eyre BD (2022) The Interplay Between Dimethyl Sulfide (DMS) and Methane (CH4) in a Coral Reef Ecosystem. Front Mar Sci 9:910441

Dilworth J, Caruso C, Kahkejian VA, Baker AC, Drury C (2021) Host genotype and stable differences in algal symbiont communities explain patterns of thermal stress response of Montipora capitata following thermal pre-exposure and across multiple bleaching events. Coral Reefs 40:151–163

Dissard D, Douville E, Reynaud S, Juillet-Leclerc A, Montagna P, Louvat P, McCulloch M (2012) Light and temperature effects on δ11B and B / Ca ratios of the zooxanthellate coral Acropora sp.: Results from culturing experiments. Biogeosciences 9:

Dittami SM, Arboleda E, Auguet JC, Bigalke A, Briand E, Cárdenas P, Cardini U, Decelle J, Engelen AH, Eveillard D, Gachon CMM, Griffiths SM, Harder T, Kayal E, Kazamia E, Lallier FH, Medina M, Marzinelli EM, Morganti TM, Pons LN, Prado S, Pintado J, Saha M, Selosse MA, Skillings D, Stock W, Sunagawa S, Toulza E, Vorobev A, Leblanc C, Not F (2021) A community perspective on the concept of marine holobionts: Current status, challenges, and future directions. PeerJ 9:e10911

Dodge RE, Brass GW (1984) Skeletal Extension, Density and Calcification of the Reef Coral, Montastrea Annularis: St. Croix, U.S. Virgin Islands.

Doney SC, Fabry VJ, Feely RA, Kleypas JA (2009) Ocean Acidification: The Other CO 2 Problem . Ann Rev Mar Sci 1:169–192

Donnet M, Bowen P, Jongen N, Lemaître J, Hofmann H (2005) Use of seeds to control precipitation of calcium carbonate and determination of seed nature. Langmuir 21:100–108

Doropoulos C, Evensen NR, Gómez-Lemos LA, Babcock RC (2017) Density-dependent coral recruitment displays divergent responses during distinct early life-history stages. R Soc Open Sci 4:170082

Doropoulos C, Ward S, Marshell A, Diaz-Pulido G, Mumby PJ (2012) Interactions among chronic and acute impacts on coral recruits: the importance of size-escape thresholds. Ecology 93:2131–2138

Drake JL, Mass T, Haramaty L, Zelzion E, Bhattacharya D, Falkowski PG (2013) Proteomic analysis of skeletal organic matrix from the stony coral stylophora pistillata. Proc Natl Acad Sci U S A 110:3788–3793

Drake JL, Mass T, Stolarski J, Von Euw S, van de Schootbrugge B, Falkowski PG (2020) How corals made rocks through the ages. Glob Chang Biol 26:31–53

Drenkard EJ, Cohen AL, McCorkle DC, de Putron SJ, Starczak VR, Zicht AE (2013) Calcification by juvenile corals under heterotrophy and elevated CO2. Coral Reefs 32:727–735

Dunn JG, Sammarco PW, LaFleur G (2012) Effects of phosphate on growth and skeletal density in the scleractinian coral Acropora muricata: A controlled experimental approach. J Exp Mar Biol Ecol 411:34–44

Falini G, Fermani S, Goffredo S (2015) Coral biomineralization: A focus on intra-skeletal organic matrix and calcification. Semin Cell Dev Biol

Falini G, Reggi M, Fermani S, Sparla F, Goffredo S, Dubinsky Z, Levi O, Dauphin Y, Cuif J-P (2013) Control of aragonite deposition in colonial corals by intra-skeletal macromolecules. J Struct Biol 183:226–238

Falkowski PG, Dubinsky Z, Muscatine L, Mccloskey L (1993) Population Control in Symbiotic Corals. 43:606–611

Feely RA, Sabine CL, Lee K, Berelson W, Kleypas J, Fabry VJ, Millero FJ (2004) Impact of anthropogenic CO2 on the CaCO3 system in the oceans. Science (1979) 305:362–366

Fernandez E, Ostrowski M, Siboni N, Seymour JR, Petrou K (2021) microorganisms Uptake of Dimethylsulfoniopropionate (DMSP) by Natural Microbial Communities of the Great Barrier Reef (GBR), Australia.

Ferrari R, Figueira WF, Pratchett MS, Boube T, Adam A, Kobelkowsky-Vidrio T, Doo SS, Atwood TB, Byrne M (2017) 3D photogrammetry quantifies growth and external erosion of individual coral colonies and skeletons. Sci Rep 7:

Findlay HS, Wood HL, Kendall MA, Spicer JI, Twitchett RJ, Widdicombe S (2011) Comparing the impact of high CO_2 on calcium carbonate structures in different marine organisms. Marine Biology Research 7:565–575

Finney JC, Pettay DT, Sampayo EM, Warner ME, Oxenford HA, LaJeunesse TC (2010) The relative significance of host-habitat, depth, and geography on the ecology, endemism, and speciation of coral endosymbionts in the genus Symbiodinium. Microb Ecol 60:250–263

Fischer E, Jones G (2012) Atmospheric dimethysulphide production from corals in the Great Barrier Reef and links to solar radiation, climate and coral bleaching. Biogeochemistry 110:31–46

Fisher DJ, Burton DT, Yonkos LT, Turley SD, Ziegler GP (1999) The relative acute toxicity of continuous and intermittent exposures of chlorine and bromine to aquatic organisms in the presence and absence of ammonia. Water Res 33:760–768

Foretich MA, Paris CB, Grosell M, Stieglitz JD, Benetti DD (2017) Dimethyl Sulfide is a Chemical Attractant for Reef Fish Larvae. Sci Rep 7:1–10

Foster T, Falter JL, McCulloch MT, Clode PL (2016) Climate Science: Ocean acidification causes structural deformities in juvenile coral skeletons. Sci Adv

Frade PR, Schwaninger V, Glasl B, Sintes E, Hill RW, Simó R, Herndl GJ (2016) Dimethylsulfoniopropionate in corals and its interrelations with bacterial assemblages in coral surface mucus. Environmental Chemistry 13:252

Franklin EC, Stat M, Pochon X, Putnam HM, Gates RD (2012) GeoSymbio: a hybrid, cloud-based web application of global geospatial bioinformatics and ecoinformatics for Symbiodinium–host symbioses. Mol Ecol Resour 12:369–373

Furla P, Allemand D, Shick JM, Ferrier-Pagès C, Richier S, Plantivaux A, Merle PL, Tambutté S (2005) The Symbiotic Anthozoan: A Physiological Chimera between Alga and Animal. Integr Comp Biol 45:595–604

Furla P, Galgani I, Durand I, Allemand D (2000) Sources and mechanisms of inorganic carbon transport for coral calcification and photosynthesis. Journal of Experimental Biology 203:3445–3457

Gabay Y, Parkinson JE, Wilkinson SP, Weis VM, Davy SK (2019) Inter-partner specificity limits the acquisition of thermotolerant symbionts in a model cnidarian-dinoflagellate symbiosis. ISME J 13:2489

Gal A, Weiner S, Addadi L (2015) A perspective on underlying crystal growth mechanisms in biomineralization: Solution mediated growth versus nanosphere particle accretion. CrystEngComm 17:2606–2615

Gao C, Fernandez VI, Lee KS, Fenizia S, Pohnert G, Seymour JR, Raina JB, Stocker R (2020) Single-cell bacterial transcription measurements reveal the importance of dimethylsulfoniopropionate (DMSP) hotspots in ocean sulfur cycling. Nature Communications 2020 11:1 11:1–11

Gardner SG, Nielsen DA, Laczka O, Shimmon R, Beltran VH, Ralph PJ, Petrou K (2016) Dimethylsulfoniopropionate, superoxide dismutase and glutathione as stress response indicators in three corals under short-term hyposalinity stress. Proceedings of the Royal Society B: Biological Sciences 283:20152418

Gardner SG, Nitschke MR, O'Brien J, Motti CA, Seymour JR, Ralph PJ, Petrou K, Raina J-B (2022) Increased DMSP availability during thermal stress influences DMSP-degrading bacteria in coral mucus. Front Mar Sci 9:1684

Gardner SG, Raina JB, Nitschke MR, Nielsen DA, Stat M, Motti CA, Ralph PJ, Petrou K (2017a) A multi-trait systems approach reveals a response cascade to bleaching in corals. BMC Biol 15:117

Gardner SG, Raina JB, Ralph PJ, Petrou K (2017b) Reactive oxygen species (ROS) and dimethylated sulphur compounds in coral explants under acute thermal stress. Journal of Experimental Biology 220:1787–1791

GESAMP (2001) Protecting the oceans from land-based activities: land-based sources and activities affecting the quality and uses of the marine, coastal and associated freshwater environment. Changes 71:

Giordano M, Norici A, Hell R (2005) Sulfur and phytoplankton: acquisition, metabolism and impact on the environment. New Phytologist 166:371–382

Goldberg WM (2001) Desmocytes in the calicoblastic epithelium of the stony coral Mycetophyllia reesi and their attachement to the skeleton. Tissue Cell 33:388–394

Gómez-Cabrera M del C, Ortiz JC, Loh WKW, Ward S, Hoegh-Guldberg O (2008) Acquisition of symbiotic dinoflagellates (Symbiodinium) by juveniles of the coral Acropora longicyathus. Coral Reefs 27:219–226

Goreau TF (1959) The physiology of skeleton formation in corals. I. A method for measuring the rate of calcium deposition by corals under different conditions. Biol Bull 116:59–75

Gotliv B-A, Kessler N, Sumerel JL, Morse DE, Tuross N, Addadi L, Weiner S (2005) Asprich: A Novel Aspartic Acid-Rich Protein Family from the Prismatic Shell Matrix of the Bivalve Atrina rigida. ChemBioChem 6:304–314

Gower LB (2008) Biomimetic Model Systems for Investigating the Amorphous Precursor Pathway and Its Role in Biomineralization. Chem Rev 108:4451–4627

Graham EM, Baird AH, Connolly SR (2008) Survival dynamics of scleractinian coral larvae and implications for dispersal. Coral Reefs 27:529–539

Greenfield EM, Wilson DC, Crenshaw MA (1984) Ionotropic Nucleation of Calcium Carbonate by Molluscan Matrix 1. academic.oup.com 24:

Gregory GJ, Boas KE, Boyd EF (2021) The Organosulfur Compound Dimethylsulfoniopropionate (DMSP) Is Utilized as an Osmoprotectant by Vibrio Species. Appl Environ Microbiol 87:1–14

Gruber N, Clement D, Carter BR, Feely RA, van Heuven S, Hoppema M, Ishii M, Key RM, Kozyr A, Lauvset SK, Monaco C Lo, Mathis JT, Murata A, Olsen A, Perez FF, Sabine CL, Tanhua T, Wanninkhof R (2019) The oceanic sink for anthropogenic CO 2 from 1994 to 2007. Science (1979) 363:1193–1199

Gundlach KA, Watson GM (2019) The effects of symbiotic state and nutrient availability on the cnidom in the model sea anemone, Exaiptasia diaphana. Mar Biol 166:1–10

Gupta LP, Suzuki A, Kawahata H (2007) Endolithic aspartic acid as a proxy of fluctuations in coral growth. J Geophys Res Biogeosci 112:1001

Harii S, Nadaoka K, Yamamoto M, Iwao K (2007) Temporal changes in settlement, lipid content and lipid composition of larvae of the spawning hermatypic coral Acropora tenuis. Mar Ecol Prog Ser 346:89–96

Harriott VJ (1999) Coral growth in subtropical eastern Australia. Coral Reefs 18:

Haschke EM, Lewis BJ (1981) Process for depolymerization of acrylic acid polymers.

Herfort L, Thake B, Taubner I (2008) Bicarbonate stimulation of calcification and photosynthesis in two hermatypic corals. J Phycol 44:91–98

Herrera M, Klein SG, Campana S, Chen JE, Prasanna A, Carlos •, Duarte M, Aranda • Manuel (2021) Temperature transcends partner specificity in the symbiosis establishment of a cnidarian. ISME J 15:141–153

Heyward AJ, Negri AP (1999) Natural inducers for coral larval metamorphosis. Coral Reefs 18:273–279

Higuchi T, Fujimura H, Yuyama I, Harii S, Agostini S, Oomori T (2014) Biotic control of skeletal growth by scleractinian corals in aragonite-calcite seas. PLoS One

Higuchi T, Tanaka K, Shirai K, Yuyama I, Mezaki T, Takahata N, Sano Y (2021) Sulfur assimilation in corals with aposymbiotic and symbiotic zooxanthellae. Environ Microbiol Rep 13:98–103

Hill RW, Dacey JWH, Krupp DA (1995) Dimethylsulfoniopropionate in Reef Corals. Bulletin of Marine Science 57:489–494

Hoegh-Guldberg O, Mumby PJ, Hooten AJ, Steneck RS, Greenfield P, Gomez E, Harvell CD, Sale PF, Edwards AJ, Caldeira K, Knowlton N, Eakin CM, Iglesias-Prieto R, Muthiga N, Bradbury RH, Dubi A, Hatziolos ME (2007) Coral reefs under rapid climate change and ocean acidification. Science 318:1737–1742

Hoffmann EH, Heinold B, Kubin A, Tegen I, Herrmann H (2021) The Importance of the Representation of DMS Oxidation in Global Chemistry-Climate Simulations. Geophys Res Lett 48:e2021GL094068

Hohn S, Merico A (2012) Modelling coral polyp calcification in relation to ocean acidification. Biogeosciences 9:4441–4454

Holm RH, Kennepohl P, Solomon EI (1996) Structural and functional aspects of metal sites in biology. Chem Rev 96:2239–2314

Hoogenboom MO, Connolly SR, Anthony KRN (2008) Interactions between morphological and physiological plasticity optimize energy acquisition in corals. Ecology 89:

Hopkins FE, Bell TG, Yang M, Suggett DJ, Steinke M (2016) Air exposure of coral is a significant source of dimethylsulfide (DMS) to the atmosphere. Sci Rep 6:1–11

Hossain FM, Murch GE, Belova I V., Turner BD (2009) Electronic, optical and bonding properties of CaCO3 calcite. Solid State Commun 149:1201–1203

Houlbrèque F, Ferrier-Pagès C (2009) Heterotrophy in Tropical Scleractinian Corals. Biological Reviews 84:1–17

House JE, Brambilla V, Bidaut LM, Christie AP, Pizarro O, Madin JS, Dornelas M (2018) Moving to 3D: Relationships between coral planar area, surface area and volume. PeerJ 2018:

Howard EC, Henriksen JR, Buchan A, Reisch CR, Bürgmann H, Welsh R, Ye W, González JM, Mace K, Joye SB, Kiene RP, Whitman WB, Moran MA (2006) Bacterial taxa that limit sulfur flux from the ocean. Science (1979) 314:649–652

Howard EC, Sun S, Biers EJ, Moran MA (2008) Abundant and diverse bacteria involved in DMSP degradation in marine surface waters. Environ Microbiol 10:2397–2410

Howells EJ, Abrego D, Meyer E, Kirk NL, Burt JA (2016) Host adaptation and unexpected symbiont partners enable reef-building corals to tolerate extreme temperatures. Glob Chang Biol 22:2702–2714

Howells EJ, Bauman AG, Vaughan GO, Hume BCC, Voolstra CR, Burt JA (2020) Corals in the hottest reefs in the world exhibit symbiont fidelity not flexibility. Mol Ecol 29:899–911

Hughes AD, Grottoli AG (2013) Heterotrophic compensation: A possible mechanism for resilience of coral reefs to global warming or a sign of prolonged stress? PLoS One

Inoue S, Kayanne H, Yamamoto S, Kurihara H (2013) Spatial community shift from hard to soft corals in acidified water. Nat Clim Chang

Ip YK, Lim ALL, Lim RWL (1991) Some properties of calcium-activated adenosine triphosphatase from the hermatypic coral Galaxea fascicularis. Mar Biol

Iwao K, Fujisawa T, Hatta M (2002) A cnidarian neuropeptide of the GLWamide family induces metamorphosis of reef-building corals in the genus Acropora. Coral Reefs 2002 21:2 21:127–129

Jiang LQ, Carter BR, Feely RA, Lauvset SK, Olsen A (2019) Surface ocean pH and buffer capacity: past, present and future. Sci Rep 9:1–11

Johns RachelG (2019) Calcification chemistry potentially links dimethylsulfoniopropionate (DMSP) metabolism and rapid skeletal growth in Acropora tenuis . James Cook University

Jokiel PL (2011) Ocean acidification and control of reef coral calcification by boundary layer limitation of proton flux. Bull Mar Sci

Jokiel PL, Maragos JE (1978) Coral growth: buoyant weight technique.

Jones A, Berkelmans R (2010) Potential Costs of Acclimatization to a Warmer Climate: Growth of a Reef Coral with Heat Tolerant vs. Sensitive Symbiont Types. PLoS One 5:10437

Jones AM, Berkelmans R (2011) Tradeoffs to Thermal Acclimation: Energetics and Reproduction of a Reef Coral with Heat Tolerant Symbiodinium Type-D . J Mar Biol 2011:1–12

Jones G, Curran M, Broadbent A, King S, Fischer E, Jones R (2007) Factors affecting the cycling of dimethylsulfide and dimethylsulfoniopropionate in coral reef waters of the Great Barrier Reef. Environmental Chemistry 4:310

Jones G, King S (2015) Dimethylsulphoniopropionate (DMSP) as an Indicator of Bleaching Tolerance in Scleractinian Corals. J Mar Sci Eng 3:444–465

Kageyama H, Tanaka Y, Shibata A, Waditee-Sirisattha R, Takabe T (2018) Dimethylsulfoniopropionate biosynthesis in a diatom Thalassiosira pseudonana: Identification of a gene encoding MTHB-methyltransferase. Arch Biochem Biophys 645:100–106

Kassambara A (2022) rstatix: Pipe-Friendly Framework for Basic Statistical Tests.

Kassambara A, Kosinski M, Biecek P, Fabian S (2017) survminer: Drawing Survival Curves using 'ggplot2.'

Kellock C, Cole C, Penkman K, Evans D, Kröger R, Hintz C, Hintz K, Finch A, Allison N (2020) the role of aspartic acid in reducing coral calcification under ocean acidification conditions. 10:12797

Kettles NL, Kopriva S, Malin G (2014) Insights into the regulation of DMSP synthesis in the diatom Thalassiosira pseudonana through APR activity, proteomics and gene expression analyses on cells acclimating to changes in salinity, light and nitrogen. PLoS One 9:

Khalifa GM, Kirchenbuechler D, Koifman N, Kleinerman O, Talmon Y, Elbaum M, Addadi L, Weiner S, Erez J (2016) Biomineralization pathways in a foraminifer revealed using a novel correlative cryo-fluorescence–SEM–EDS technique. J Struct Biol 196:155–163

Kiene RP, Hoffmann Williams LP (1998) Glycine betaine uptake, retention, and degradation by microorganisms in seawater. Limnol Oceanogr 43:1592–1603

Kiene RP, Linn LJ (2000) The fate of dissolved dimethylsulfoniopropionate (DMSP) in seawater: tracer studies using 35S-DMSP. Geochim Cosmochim Acta 64:2797–2810

Kiene RP, Linn LJ, Bruton JA (2000) New and important roles for DMSP in marine microbial communities. J Sea Res 43:209–224

Kiene RP, Linn LJ, González J, Moran MA, Bruton JA (1999) Dimethylsulfoniopropionate and Methanethiol Are Important Precursors of Methionine and Protein-Sulfur in Marine Bacterioplankton. Appl Environ Microbiol 65:4549

Kim YY, Kulak AN, Li Y, Batten T, Kuball M, Armes SP, Meldrum FC (2009) Substrate-directed formation of calcium carbonate fibres. J Mater Chem 19:387–398

Kirkwood M, Le Brun NE, Todd JD, Johnston AWB (2010) The dddP gene of Roseovarius nubinhibens encodes a novel lyase that cleaves dimethylsulfoniopropionate into acrylate plus dimethyl sulfide. Microbiology (N Y) 156:1900–1906

Kitahara M V., Fukami H, Benzoni F, Huang D (2016) The new systematics of scleractinia: Integrating molecular and morphological evidence. The Cnidaria, past, present and Future: The World of Medusa and her Sisters 41–59

Kramer N, Guan J, Chen S, Wangpraseurt D, Loya Y (2022) Morpho-functional traits of the coral Stylophora pistillata enhance light capture for photosynthesis at mesophotic depths. Communications Biology 2022 5:1 5:1–11

Kuek FW, Motti CA, Zhang J, Cooke IR, Todd JD, Miller DJ, Bourne DG, Raina J-B, Nevitt G, Shinzato C, Tandon K, Raina Jean-BaptisteRaina J-B (2022) DMSP Production by Coral-Associated Bacteria. Frontiers in Marine Scienc 9:1

Kuek FWI (2021) Dimethylsulphoniopropionate (DMSP) metabolism within the coral holobiont.

Laipnik R, Bissi V, Sun CY, Falini G, Gilbert PUPA, Mass T (2020) Coral acid rich protein selects vaterite polymorph in vitro. J Struct Biol 209:107431

LaJeunesse TC (2005) “Species” Radiations of Symbiotic Dinoflagellates in the Atlantic and Indo-Pacific Since the Miocene-Pliocene Transition. Mol Biol Evol 22:570–581

LaJeunesse TC, Everett Parkinson J, Gabrielson PW, Jin Jeong H, Davis Reimer J, Voolstra CR, Santos SR (2018) Systematic Revision of Symbiodiniaceae Highlights the Antiquity and Diversity of Coral Endosymbionts. Current Biology 28:2570-2580.e6

Lajeunesse TC, Loh WKW, Van Woesik R, Hoegh-Guldberg O, Schmidt GW, Fitt WK (2003) Low symbiont diversity in southern Great Barrier Reef corals, relative to those of the Caribbean. Limnol Oceanogr 48:2046–2054

LaJeunesse TC, Pettay DT, Sampayo EM, Phongsuwan N, Brown B, Obura DO, Hoegh-Guldberg O, Fitt WK (2010) Long-standing environmental conditions, geographic isolation and host–symbiont specificity influence the relative ecological dominance and genetic diversification of coral endosymbionts in the genus Symbiodinium. J Biogeogr 37:785–800

Lemarchand D, Wasserburg GJ, Papanastassiou DA (2004) Rate-controlled calcium isotope fractionation in synthetic calcite. Geochim Cosmochim Acta 68:4665–4678

Lesser MP, Stochaj WR, Tapley DW, Shick JM (1990) Bleaching in coral reef anthozoans: effects of irradiance, ultraviolet radiation, and temperature on the activities of protective enzymes against active oxygen. Coral Reefs 8:225–232

Lewis SE, Wüst RAJ, Webster JM, Shields GA, Renema W, Lough JM, Jacobsen G (2012) Development of an inshore fringing coral reef using textural, compositional and stratigraphic data from Magnetic Island, Great Barrier Reef, Australia. Mar Geol 299–302:18–32

Li J, Zou Y, Yang J, Li Q, Bourne DG, Sweet M, Liu C, Guo A, Zhang S (2022) Cultured Bacteria Provide Insight into the Functional Potential of the Coral-Associated Microbiome. mSystems 7:

Little AF, Van Oppen MJH, Willis BL (2004) Flexibility in algal endosymbioses shapes growth in reef corals. Science (1979) 304:1492–1494

Liu Y, Kim YK, Dai L, Li N, Khan SO, Pashley DH, Tay FR (2011) Hierarchical and non-hierarchical mineralisation of collagen. Biomaterials 32:1291–1300

Llauro MF, Loiseau J, Boisson F, Delolme F, Ladavière C, Claverie J (2004) Unexpected end-groups of poly(acrylic acid) prepared by RAFT polymerization. J Polym Sci A Polym Chem 42:5439–5462

Macadam A, Nowell CJ, Quigley K (2021) Machine learning for the fast and accurate assessment of fitness in coral early life history. Remote Sens (Basel) 13:3173

Mann S (1993) Molecular tectonics in biomineralization and biomimetic materials chemistry. Nature 365:499–505

Mansur HS, Mansur AAP, Pereira M (2005) XRD, SEM/EDX and FTIR Characterization of Brazilian Natural Coral. Key Eng Mater 284–286:43–46

Marshall AT, Clode PL, Russell R, Prince K, Stern R (2007) Electron and ion microprobe analysis of calcium distribution and transport in coral tissues. Journal of Experimental Biology 210:2453–2463

Marubini F, Ferrier-Pagès C, Furla P, Allemand D (2008) Coral calcification responds to seawater acidification: A working hypothesis towards a physiological mechanism. Coral Reefs 27:491–499

Mass T, Drake JL, Haramaty L, Kim JD, Zelzion E, Bhattacharya D, Falkowski PG (2013) Cloning and Characterization of Four Novel Coral Acid-Rich Proteins that Precipitate Carbonates In Vitro. Current Biology 23:1126–1131

Mass T, Drake JL, Peters EC, Jiang W, Falkowski PG (2014) Immunolocalization of skeletal matrix proteins in tissue and mineral of the coral Stylophora pistillata. Proc Natl Acad Sci U S A 111:12728–12733

Mass T, Giuffre AJ, Sun CY, Stifler CA, Frazier MJ, Neder M, Tamura N, Stan C V., Marcus MA, Gilbert PUPA (2017) Amorphous calcium carbonate particles form coral skeletons. Proc Natl Acad Sci U S A 114:E7670–E7678

Mass T, Putnam HM, Drake JL, Zelzion E, Gates RD, Bhattacharya D, Falkowski PG (2016) Temporal and spatial expression patterns of biomineralization proteins during early development in the stony coral *Pocillopora damicornis*. Proceedings of the Royal Society B: Biological Sciences 283:20160322

Matias AMA, Popovic I, Thia JA, Cooke IR, Torda G, Lukoschek V, Bay LK, Kim SW, Riginos C (2022) Cryptic diversity and spatial genetic variation in the coral Acropora tenuis and its endosymbionts across the Great Barrier Reef. Evol Appl 00:1–18

Matrai PA, Keller MD (1994) Total organic sulfur and dimethylsulfoniopropionate in marine phytoplankton: intracellular variations. Mar Biol 119:61–68

Matsuda SB, Chakravarti LJ, Cunning R, Huffmyer AS, Nelson CE, Gates RD, van Oppen MJH (2022) Temperature-mediated acquisition of rare heterologous symbionts promotes survival of coral larvae under ocean warming. Glob Chang Biol 28:2006–2025

McDougall C, Degnan BM (2018) The evolution of mollusc shells. Wiley Interdiscip Rev Dev Biol 7:e313

Meibom A, Cuif J-P, Hillion F, Constantz BR, Juillet-Leclerc A, Dauphin Y, Watanabe T, Dunbar RB (2004) Distribution of magnesium in coral skeleton. Geophys Res Lett 31:1–4

Meyer E, Davies S, Wang S, Willis B, Abrego D, Juenger T, Matz M (2009) Genetic variation in responses to a settlement cue and elevated temperature in the reef-building coral Acropora millepora. Mar Ecol Prog Ser 392:81–92

Miller TC, Holcombe JA (2001) Comparison and evaluation of the synthetic biopolymer poly-L-aspartic acid and the synthetic "plastic" polymer poly-acrylic acid for use in metal ion-exchange systems. J Hazard Mater 83:219–236

Mitterer RM (1978) Amino acid composition and metal binding capability of the skeletal protein of corals. Bull Mar Sci 28:173–180

Moran MA, Reisch CR, Kiene RP, Whitman WB (2012) Genomic Insights into Bacterial DMSP Transformations. Ann Rev Mar Sci 4:523–542

Morse ANC, Iwao K, Bab A M, Shimoike K, Hayashibara T, Omori M (1996) Morse, Aileen N. C. et al. 1996. "An Ancient Chemosensory Mechanism Brings New Life to Coral Reefs." The Biological bulletin 191, 149–154. https://doi.org/10.2307/1542917. Biol Bull 191:154

Morse JW, Arvidson RS, Lüttge A (2007) Calcium carbonate formation and dissolution. Chem Rev 107:342–381

Mummadisetti MP, Drake JL, Falkowski PG (2021) The spatial network of skeletal proteins in a stony coral. J R Soc Interface 18:

Muscatine L, Falkowski PG, Porter JW, Dubinsky Z (1984) Fate of photosynthetic fixed carbon in light- and shade-adapted colonies of the symbiotic coral Stylophora pistillata . Proc R Soc Lond B Biol Sci 222:181–202

Naumann MS, Niggl W, Laforsch C, Glaser C, Wild C (2009a) Coral surface area quantification–evaluation of established techniques by comparison with computer tomography. Coral Reefs 28:109–117

Naumann MS, Richter C, el-Zibdah M, Wild C (2009b) Coral mucus as an efficient trap for picoplanktonic cyanobacteria: implications for pelagic–benthic coupling in the reef ecosystem. Mar Ecol Prog Ser 385:65–76

Nevitt GA (2000) Olfactory foraging by antarctic procellariiform seabirds: Life at high Reynolds numbers. Biological Bulletin 198:245–253

Nevitt GA, Veit RR, Kareiva P (1995) Dimethyl sulphide as a foraging cue for antarctic procellariiform seabirds. Nature 376:680–682

Ni M, Ratner BD (2008) Differentiating calcium carbonate polymorphs by surface analysis techniques - An XPS and TOF-SIMS study. Surface and Interface Analysis

Nitschke MR, Davy SK, Ward S (2016) Horizontal transmission of Symbiodinium cells between adult and juvenile corals is aided by benthic sediment. Coral Reefs 35:335–344

Nothdurft LD, Webb GE (2007) Microstructure of common reef-building coral genera Acropora, Pocillopora, Goniastrea and Porites: Constraints on spatial resolution in geochemical sampling. Facies 53:1–26

Nudelman F, Lausch AJ, Sommerdijk NAJM, Sone ED (2013) In vitro models of collagen biomineralization. J Struct Biol 183:258–269

Oduro H, Van Alstyne KL, Farquhar J (2012) Sulfur isotope variability of oceanic DMSP generation and its contributions to marine biogenic sulfur emissions. Proc Natl Acad Sci U S A 109:9012–6

Omori M, Iwao K (2014) Methods of farming sexually propagated corals and outplanting for coral reef rehabilitation ; with list of references for coral reef rehabilitation through active restoration measure. Akajima Marine Science Laboratory, Okinawa, Japan

Orr JC, Fabry VJ, Aumont O, Bopp L, Doney SC, Feely RA, Gnanadesikan A, Gruber N, Ishida A, Joos F, Key RM, Lindsay K, Maier-Reimer E, Matear R, Monfray P, Mouchet A, Najjar RG, Plattner G-K, Rodgers KB, Sabine CL, Sarmiento JL, Schlitzer R, Slater RD, Totterdell IJ, Weirig M-F, Yamanaka Y, Yool A (2005) Anthropogenic ocean

acidification over the twenty-first century and its impact on calcifying organisms. Nature 437:681–686

Osinga R, Schutter M, Griffioen B, Wijffels RH, Verreth JAJ, Shafir S, Henard S, Taruffi M, Gili C, Lavorano S (2011) The Biology and Economics of Coral Growth. Marine Biotechnology 13:658–671

Parkinson JE, Baums IB (2014) The extended phenotypes of marine symbioses: Ecological and evolutionary consequences of intraspecific genetic diversity in coral-algal associations. Front Microbiol 5:445

Pauli GF (2001) QNMR - A versatile concept for the validation of natural product reference compounds. Phytochemical Analysis 12:28–42

Pearse VB (1970) Incorporation of metabolic CO2 into coral skeleton. Nature 228:383

Pelham HRB (1990) The retention signal for soluble proteins of the endoplasmic reticulum. Trends Biochem Sci 15:483–486

Preuß A, Schauder R, Fuchs G, Stichler W (1989) Carbon Isotope Fractionation by Autotrophic Bacteria with Three Different CO2 Fixation Pathways. Zeitschrift fur Naturforschung - Section C Journal of Biosciences 44:397–402

Puverel S, Tambutté E, Pereira-Mouriès L, Zoccola D, Allemand D, Tambutté S (2005) Soluble organic matrix of two Scleractinian corals: Partial and comparative analysis. Comp Biochem Physiol B Biochem Mol Biol 141:480–487

Quigley KM, Alvarez Roa C, Torda G, Bourne DG, Willis BL (2020) Co-dynamics of Symbiodiniaceae and bacterial populations during the first year of symbiosis with *Acropora tenuis* juveniles. Microbiologyopen 9:e959

Quigley KM, Ramsby B, Laffy P, Harris J, Mocellin VJL, Bay LK (2022) Symbioses are restructured by repeated mass coral bleaching. Sci Adv 8:eabq8349

Quigley KM, Vidal Garcia M (2022) A fast, precise, in-vivo method for micron-level 3D models of corals using dental scanners. Methods Ecol Evol 13:2159–2166

Quigley KM, Willis BL, Bay LK (2016) Maternal effects and symbiodinium community composition drive differential patterns in juvenile survival in the coral acropora tenuis. R Soc Open Sci 3:

R Core Team (2019) R: A Language and Environment for Statistical Computing.

Rahman MA, Oomori T (2008) Aspartic acid-rich proteins in insoluble organic matrix play a key role in the growth of calcitic sclerites in alcyonarian coral. J Biotechnol 136:S528

Raina JB, Clode PL, Cheong S, Bougoure J, Kilburn MR, Reeder A, Forêt S, Stat M, Beltran V, Thomas-Hall P, Tapiolas D, Motti CM, Gong B, Pernice M, Marjo CE, Seymour JR, Willis BL, Bourne DG (2017) Subcellular tracking reveals the location of dimethylsulfoniopropionate in microalgae and visualises its uptake by marine bacteria. Elife 6:

Raina J-B, Dinsdale EA, Willis BL, Bourne DG (2010) Do the organic sulfur compounds DMSP and DMS drive coral microbial associations? Trends Microbiol 18:101–108

Raina J-B, Tapiolas D, Willis BL, Bourne DG (2009) Coral-Associated Bacteria and Their Role in the Biogeochemical Cycling of Sulfur. Appl Environ Microbiol 75:3492–3501

Raina J-B, Tapiolas DM, Forêt S, Lutz A, Abrego D, Ceh J, Seneca FO, Clode PL, Bourne DG, Willis BL, Motti CA (2013) DMSP biosynthesis by an animal and its role in coral thermal stress response. Nature 502:677–680

Ramos-Silva P, Kaandorp J, Huisman L, Marie B, Zanella-Cléon I, Guichard N, Miller DJ, Marin F (2013) The skeletal proteome of the coral acropora millepora: The evolution of calcification by co-option and domain shuffling. Mol Biol Evol 30:2099–2112

Randall CJ, Giuliano C, Heyward AJ, Negri AP (2021) Enhancing Coral Survival on Deployment Devices With Microrefugia. Front Mar Sci 8:478

Randall CJ, Negri AP, Quigley KM, Foster T, Ricardo GF, Webster NS, Bay LK, Harrison PL, Babcock RC, Heyward AJ (2020) Sexual production of corals for reef restoration in the Anthropocene. Mar Ecol Prog Ser 635:203–232

Raymundo LJ, Maypa AP (2004) Getting bigger faster: Mediation of size-specific mortality via fusion in juvenile coral transplants. Ecological Applications 14:281–295

Raz S, Weiner S, Addadi L (2000) Formation of high-magnesian calcites via an amorphous precursor phase: Possible biological implications. Advanced Materials 12:38–42

Reisch CR, Crabb WM, Gifford SM, Teng Q, Stoudemayer MJ, Moran MA, Whitman WB (2013) Metabolism of dimethylsulphoniopropionate by Ruegeria pomeroyi DSS-3. Mol Microbiol 89:774–791

Reisch CR, Moran MA, Whitman WB (2011a) Bacterial catabolism of dimethylsulfoniopropionate (DMSP). Front Microbiol 2:172

Reisch CR, Stoudemayer MJ, Varaljay VA, Amster IJ, Moran MA, Whitman WB (2011b) Novel pathway for assimilation of dimethylsulphoniopropionate widespread in marine bacteria. Nature 473:208–11

Reynolds JMC, Bruns BU, Fitt WK, Schmidt GW (2008) Enhanced photoprotection pathways in symbiotic dinoflagellates of shallow-water corals and other cnidarians. Proc Natl Acad Sci U S A 105:13674–13678

Richmond RH (1987) Energetics, competency, and long-distance dispersal of planula larvae of the coral Pocillopora damicornis. Mar Biol 93:527–533

Ries JB, Cohen AL, McCorkle DC (2009) Marine calcifiers exhibit mixed responses to CO2-induced ocean acidification. Geology 37:1131–1134

Rocha LA, Bowen BW (2008) Speciation in coral-reef fishes. J Fish Biol 72:1101–1121

Rosset S, Wiedenmann J, Reed AJ, D'Angelo C (2017) Phosphate deficiency promotes coral bleaching and is reflected by the ultrastructure of symbiotic dinoflagellates. Mar Pollut Bull 118:180–187

Rowan B, Knowlton N (1995) Intraspecific diversity and ecological zonation in coral-algal symbiosis. Proceedings of the National Academy of Sciences 92:2850–2853

Savage C (2019) Seabird nutrients are assimilated by corals and enhance coral growth rates. Sci Rep 9:1–10

Sevilgen DS, Venn AA, Hu MY, Tambutté E, de Beer D, Planas-Bielsa V, Tambutté S (2019) Full in vivo characterization of carbonate chemistry at the site of calcification in corals. Sci Adv 5:eaau7447

Shinzato C, Khalturin K, Inoue J, Zayasu Y, Kanda M, Kawamitsu M, Yoshioka Y, Yamashita H, Suzuki G, Satoh N (2021) Eighteen coral genomes reveal the evolutionary origin of Acropora strategies to accommodate environmental changes. Mol Biol Evol

Shore-Maggio A, Callahan SM, Aeby GS (2018) Trade-offs in disease and bleaching susceptibility among two color morphs of the Hawaiian reef coral, Montipora capitata. Coral Reefs 37:507–517

Sieburth JM (1960) Acrylic Acid, an "Antibiotic" Principle in Phaeocystis Blooms in Antarctic Waters. Science (1979) 132:676–677

Sieburth JM (1961) Sieburth JM. Antibiotic properties of acrylic acid, a factor in the gastrointestinal antibiosis of polar marine animals. J Bacteriol 82:72–9

Sievert SM, Kiene RP, Schulz-Vogt HN (2007) The sulfur cycle. Oceanography 20:117–123

Silva J Da, Williams R (2001) The biological chemistry of the elements: the inorganic chemistry of life.

Silverstein RN, Correa AMS, LaJeunesse TC, Baker AC (2011) Novel algal symbiont (Symbiodinium spp.) diversity in reef corals of Western Australia. Mar Ecol Prog Ser 422:63–75

Simó R (2001a) Production of atmospheric sulfur by oceanic plankton: Biogeochemical, ecological and evolutionary links. Trends Ecol Evol 16:287–294

Simó R (2001b) Production of atmospheric sulfur by oceanic plankton: biogeochemical, ecological and evolutionary links. Trends Ecol Evol 16:287–294

Spielmeyer A, Pohnert G (2010) Direct quantification of dimethylsulfoniopropionate (DMSP) with hydrophilic interaction liquid chromatography/mass spectrometry. J Chromatogr B Analyt Technol Biomed Life Sci 878:3238–3242

Stat M, Carter D, Hoegh-Guldberg O (2006) The evolutionary history of Symbiodinium and scleractinian hosts—Symbiosis, diversity, and the effect of climate change. Perspect Plant Ecol Evol Syst 8:23–43

Stat M, Gates RD (2011) Clade D Symbiodinium in Scleractinian Corals: A "Nugget" of Hope, a Selfish Opportunist, an Ominous Sign, or All of the Above? . J Mar Biol 2011:1–9

Stat M, Morris E, Gates RD (2008) Functional diversity in coral-dinoflagellate symbiosis. Proc Natl Acad Sci U S A 105:9256–9261

Stefels J (1997) The smell of the sea : production of dimethylsulphoniopropionate and its conversion into dimethylsulphide by the marine phytoplankton genus Phaeocystis. Rijksuniversiteit Groningen],

Stefels J (2000) Physiological aspects of the production and conversion of DMSP in marine algae and higher plants. J Sea Res 43:183–197

Steiner Z, Turchyn A V., Harpaz E, Silverman J (2018a) Water chemistry reveals a significant decline in coral calcification rates in the southern Red Sea. Nat Commun

Steiner Z, Turchyn A V., Harpaz E, Silverman J (2018b) Water chemistry reveals a significant decline in coral calcification rates in the southern Red Sea. Nat Commun

Strom S, Wolfe G, Slajer A, Lambert S, Clough J (2003) Chemical defense in the microplankton II: Inhibition of protist feeding by-dimethylsulfoniopropionate (DMSP). Limnol Oceanogr 48:

Sullivan MJ, Curson ARJ, Shearer N, Todd JD, Green RT, Johnston AWB (2011) Unusual regulation of a leaderless operon involved in the catabolism of dimethylsulfoniopropionate in Rhodobacter sphaeroides. PLoS One 6:

Sulyok M, Haberhauer-Troyer C, Rosenberg E, Grasserbauer M (2001) Investigation of the stability of selected volatile sulfur compounds in different sampling containers. J Chromatogr A 917:367–374

Sunda W, Kieber DJ, Kiene RP, Huntsman S (2002) An antioxidant function for DMSP and DMS in marine algae. Nature 418:317–320

Suzuki G, Arakaki S, Suzuki K, Iehisa Y, Hayashibara T (2012) What is the optimal density of larval seeding in Acropora corals? Fisheries Science 78:801–808

Swain TD, Lax S, Backman V, Marcelino LA (2020) Uncovering the role of Symbiodiniaceae assemblage composition and abundance in coral bleaching response by minimizing sampling and evolutionary biases. BMC Microbiol 20:1–19

Swan HB, Jones GB, Deschaseaux ESM, Eyre BD (2017) Coral reef origins of atmospheric dimethylsulfide at Heron Island, southern Great Barrier Reef, Australia. Biogeosciences 14:229–239

Takeuchi T, Yamada L, Shinzato C, Sawada H, Satoh N (2016) Stepwise Evolution of Coral Biomineralization Revealed with Genome-Wide Proteomics and Transcriptomics. PLoS One 11:e0156424

Tambutté S, Holcomb M, Ferrier-Pagès C, Reynaud S, Tambutté É, Zoccola D, Allemand D (2011) Coral biomineralization: From the gene to the environment. J Exp Mar Biol Ecol 408:58–78

Tandon K, Lu C-Y, Chiang P-W, Wada N, Yang S-H, Chan Y-F, Chen P-Y, Chang H-Y, Chiou Y-J, Chou M-S, Chen W-M, Tang S-L (2020a) Comparative genomics: Dominant coral-bacterium Endozoicomonas acroporae metabolizes dimethylsulfoniopropionate (DMSP). ISME J 14:1290–1303

Tandon K, Lu CY, Chiang PW, Wada N, Yang SH, Chan YF, Chen PY, Chang HY, Chiou YJ, Chou MS, Chen WM, Tang SL (2020b) Comparative genomics: Dominant coral-bacterium Endozoicomonas acroporae metabolizes dimethylsulfoniopropionate (DMSP). The ISME Journal 2020 14:5 14:1290–1303

Tang KW, Simó R (2003) Trophic uptake and transfer of DMSP in simple planktonic food chains. Aquatic Microbial Ecology 31:193–202

Tapiolas DM, Motti CA, Holloway P, Boyle SG (2010) High levels of acrylate in the Great Barrier Reef coral Acropora millepora. Coral Reefs 29:621–625

Tapiolas DM, Raina J-B, Lutz A, Willis BL, Motti CA (2013) Direct measurement of dimethylsulfoniopropionate (DMSP) in reef-building corals using quantitative nuclear magnetic resonance (qNMR) spectroscopy. J Exp Mar Biol Ecol 443:85–89

Terrell AP, Marangon E, Webster NS, Cooke I, Quigley KM (2023) The promotion of stress tolerant Symbiodiniaceae dominance in juveniles of two coral species under simulated future conditions of ocean warming and acidification. Front Ecol Evol 11:1113357

Therneau TM (2015) A Package for Survival Analysis in S.

Todd JD, Curson ARJ, Dupont CL, Nicholson P, Johnston AWB (2009) The dddP gene, encoding a novel enzyme that converts dimethylsulfoniopionate into dimethyl sulfide, is widespread in ocean metagenomes and marine bacteria and also occprours in some Ascomycete fungi. Environ Microbiol 11:1376–1385

Todd JD, Curson ARJ, Nikolaidou-Katsaraidou N, Brearley CA, Watmough NJ, Chan Y, Page PCB, Sun L, Johnston AWB (2010) Molecular dissection of bacterial acrylate catabolism - unexpected links with dimethylsulfoniopropionate catabolism and dimethyl sulfide production. Environ Microbiol 12:327–343

Todd JD, Rogers R, You GL, Wexler M, Bond PL, Sun L, Curson ARJ, Malin G, Steinke M, Johnston AWB (2007) Structural and regulatory genes required to make the gas dimethyl sulfide in bacteria. Science (1979) 315:666–669

Tremblay P, Gori A, François Maguer J, Hoogenboom M, Ferrier-Pagès C (2016) Heterotrophy promotes the re-establishment of photosynthate translocation in a symbiotic coral after heat stress.

Van Oppen MJ, Palstra FP, Piquet AM, Miller DJ (2001) Patterns of coral-dinoflagellate associations in Acropora: significance of local availability and physiology of Symbiodinium strains and host-symbiont selectivity. Proc Biol Sci 268:1759–67

Van Oppen MJH, Medina M (2020) Coral evolutionary responses to microbial symbioses. Philosophical Transactions of the Royal Society B 375:

Varaljay VA, Robidart J, Preston CM, Gifford SM, Durham BP, Burns AS, Ryan JP, Marin R, Kiene RP, Zehr JP, Scholin CA, Moran MA (2015) Single-taxon field measurements of bacterial gene regulation controlling DMSP fate. The ISME Journal 2015 9:7 9:1677–1686

Veal CJ, Carmi M, Fine M, Hoegh-Guldberg O (2010) Increasing the accuracy of surface area estimation using single wax dipping of coral fragments. Coral Reefs 29:893–897

Venn A, Tambutté E, Holcomb M, Allemand D, Tambutté S (2011) Live Tissue Imaging Shows Reef Corals Elevate pH under Their Calcifying Tissue Relative to Seawater. PLoS One 6:e20013

Verch A, Gebauer D, Antonietti M, Cölfen H (2011) How to control the scaling of CaCO3: A “fingerprinting technique” to classify additives. Physical Chemistry Chemical Physics 13:16811–16820

Vidavsky N, Addadi S, Schertel A, Ben-Ezra D, Shpigel M, Addadi L, Weiner S (2016) Calcium transport into the cells of the sea urchin larva in relation to spicule formation. Proc Natl Acad Sci U S A 113:12637–12642

Von Euw S, Zhang Q, Manichev V, Murali N, Gross J, Feldman LC, Gustafsson T, Flach C, Mendelsohn R, Falkowski PG (2017) Biological control of aragonite formation in stony corals. Science (1979) 356:933–938

Wakeford M, Done TJ, Johnson CR (2008) Decadal trends in a coral community and evidence of changed disturbance regime. Coral Reefs 27:1–13

Walker JM, Marzec B, Nudelman F (2017) Solid-State Transformation of Amorphous Calcium Carbonate to Aragonite Captured by CryoTEM. Angewandte Chemie International Edition 56:11740–11743

Wang T, Huang Q, Burns AS, Moran MA, Whitman WB (2022) Oxidative Stress Regulates a Pivotal Metabolic Switch in Dimethylsulfoniopropionate Degradation by the Marine Bacterium Ruegeria pomeroyi.

Wang Z, Yin Y, Chen S, Fu X, Xie X, Duan S (2002) Studies on acute toxicity of acrylic acid and its esters to aquatic organisms. Journal of Jinan University(natural Science) 23:75–80

Watanabe T, Utsunomiya Y, Yuyama I (2007) Long-term laboratory culture of symbiotic coral juveniles and their use in eco-toxicological study. J Exp Mar Biol Ecol 352:177–186

Westmoreland LSH, Niemuth JN, Gracz HS, Stoskopf MK (2017) Altered acrylic acid concentrations in hard and soft corals exposed to deteriorating water conditions. FACETS 2:531–544

Whalan S, Abdul Wahab MA, Sprungala S, Poole AJ, De Nys R (2015) Larval Settlement: The Role of Surface Topography for Sessile Coral Reef Invertebrates. PLoS One 10:e0117675

Wheeler AP, Sikes CS (1984) Regulation of Carbonate Calcification by Organic Matrix. American Zoologist. pp 933–944

Wijgerde T, Diantari R, Lewaru MW, Verreth JAJ, Osinga R (2011) Extracoelenteric zooplankton feeding is a key mechanism of nutrient acquisition for the scleractinian coral Galaxea fascicularis. Journal of Experimental Biology 214:3351–3357

Wolfe G V., Steinke M, Kirst GO (1997a) Grazing-activated chemical defence in a unicellular marine alga. Nature 387:894–897

Wolfe G V., Steinke M, Kirst GO (1997b) Grazing-activated chemical defence in a unicellular marine alga. Nature 387:894–897

Xue L, Kieber DJ (2021) Photochemical Production and Photolysis of Acrylate in Seawater. Cite This: Environ Sci Technol 55:7135–7144

Yoch DC (2002) Dimethylsulfoniopropionate: Its sources, role in the marine food web, and biological degradation to dimethylsulfide. Appl Environ Microbiol 68:5804–5815

Yost DM, Mitchelmore CL (2010) Determination of total and particulate dimethylsulfoniopropionate (DMSP) concentrations in four scleractinian coral species: A comparison of methods. J Exp Mar Biol Ecol

Yuyama I, Hayakawa H, Endo H, Iwao K, Takeyama H, Maruyama T, Watanabe T (2005) Identification of symbiotically expressed coral mRNAs using a model infection system. Biochem Biophys Res Commun 336:793–798

Yuyama I, Higuchi T (2014) Comparing the Effects of Symbiotic Algae (Symbiodinium) Clades C1 and D on Early Growth Stages of Acropora tenuis. PLoS One 9:e98999

Yuyama I, Ishikawa M, Nozawa M, Yoshida M aki, Ikeo K (2018) Transcriptomic changes with increasing algal symbiont reveal the detailed process underlying establishment of coral-algal symbiosis. Scientific Reports 2018 8:1 8:1–11

Yuyama I, Nakamura T, Higuchi T, Hidaka M (2016) Different stress tolerances of juveniles of the coral Acropora tenuis associated with clades C1 and D Symbiodinium. Zool Stud 55:

Yuyama I, Ugawa N, Hashimoto T (2021) Transcriptome analysis of durusdinium associated with the transition from free-living to symbiotic. Microorganisms 9:1560

Zhang X-H, Liu J, Liu J, Yang G, Xue C-X, Curson ARJ, Todd JD (2019) Biogenic production of DMSP and its degradation to DMS—their roles in the global sulfur cycle. Sci China Life Sci 62:1296–1319

Zhou H, Gao Y, Hwang S-G, Lee D-Y, Park J-Y, Lee J-B (2011) A Novel Approach to Controlling $CaCO_3$ Crystalline Assembly by Changing the Concentration of Poly(aspartic acid). Bull Korean Chem Soc 32:4027–4034

Zoccola D, Ganot P, Bertucci A, Caminiti-Segonds N, Techer N, Voolstra CR, Aranda M, Tambutté E, Allemand D, Casey JR, Tambutté S (2015) Bicarbonate transporters in corals point towards a key step in the evolution of cnidarian calcification. Sci Rep 5:1–11

Zoccola D, Tambutté E, Kulhanek E, Puverel S, Scimeca JC, Allemand D, Tambutté S (2004) Molecular cloning and localization of a PMCA P-type calcium ATPase from the coral Stylophora pistillata. Biochim Biophys Acta Biomembr 1663:117–126

Zoccola D, Tambutté E, Sénégas-Balas F, Michiels JF, Failla JP, Jaubert J, Allemand D (1999) Cloning of a calcium channel α1 subunit from the reef-building coral, Stylophora pistillata. Gene 227:157–167

Supplementary data

S1 Supplementary data for Chapter 2

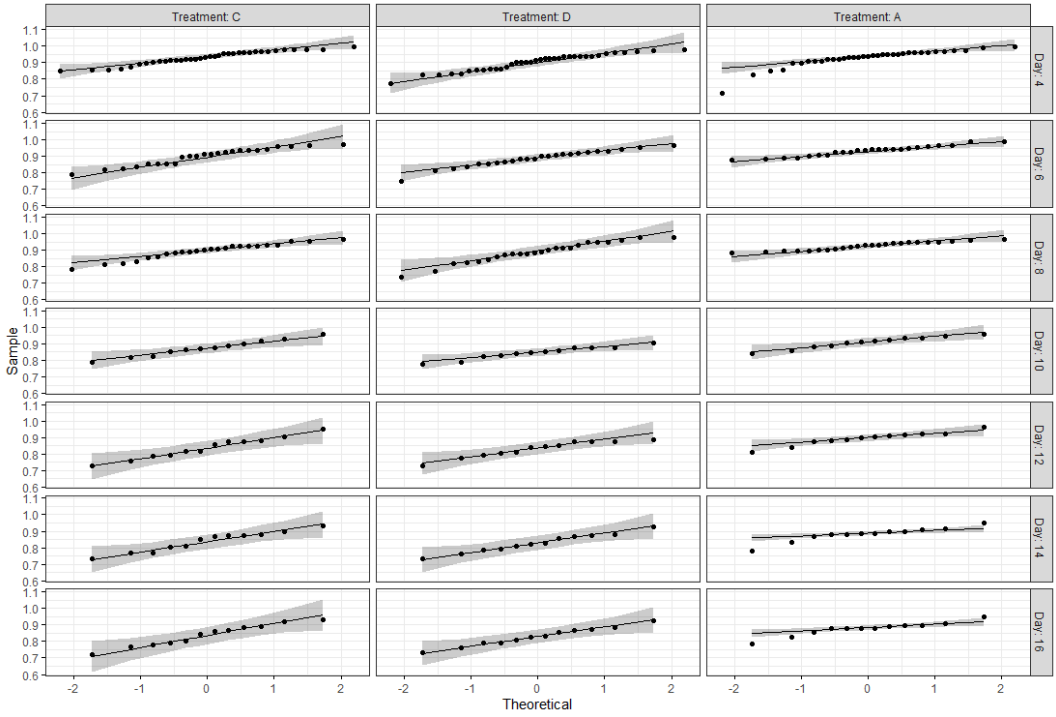

Supplementary Data Figure 2.1 *Acropora kenti* Inverse transformed growth rate QQ plot ANOVA normality validation, ANOVA was performed on days 4 to 16; day 0 is excluded due to normalization resulting in the same variance between samples.

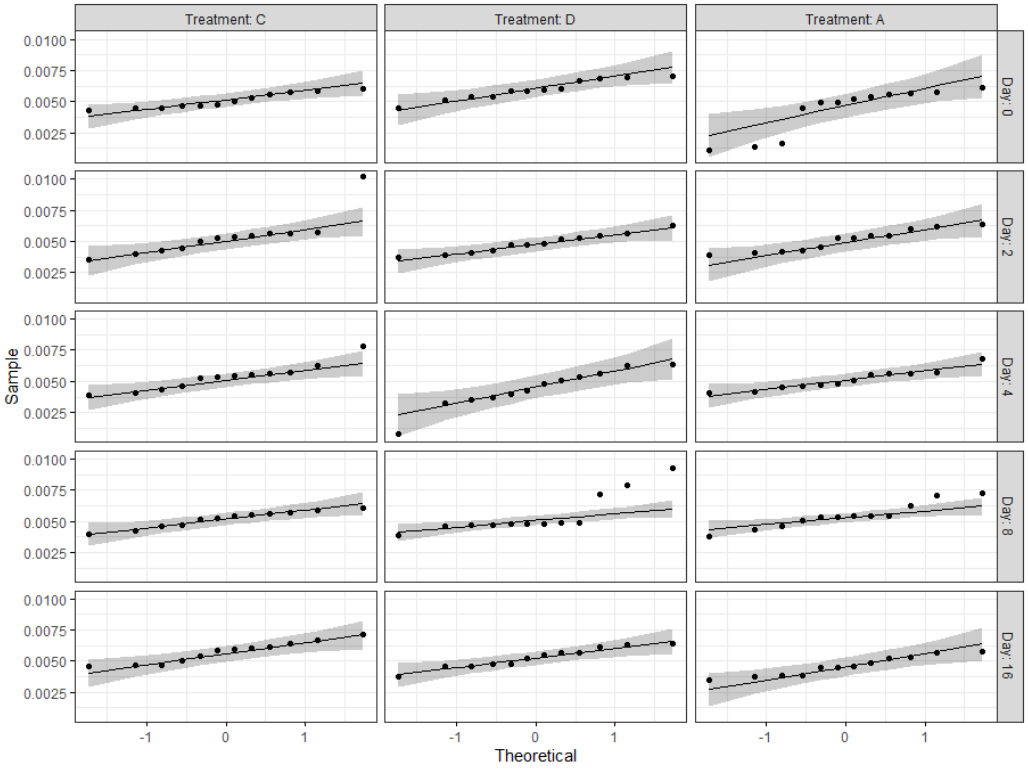

Supplementary Data Figure 2.2 *Acropora kenti* DMSP concentration per polyp in different treatments over 16 days of exposure. QQ plot of square root transformed.

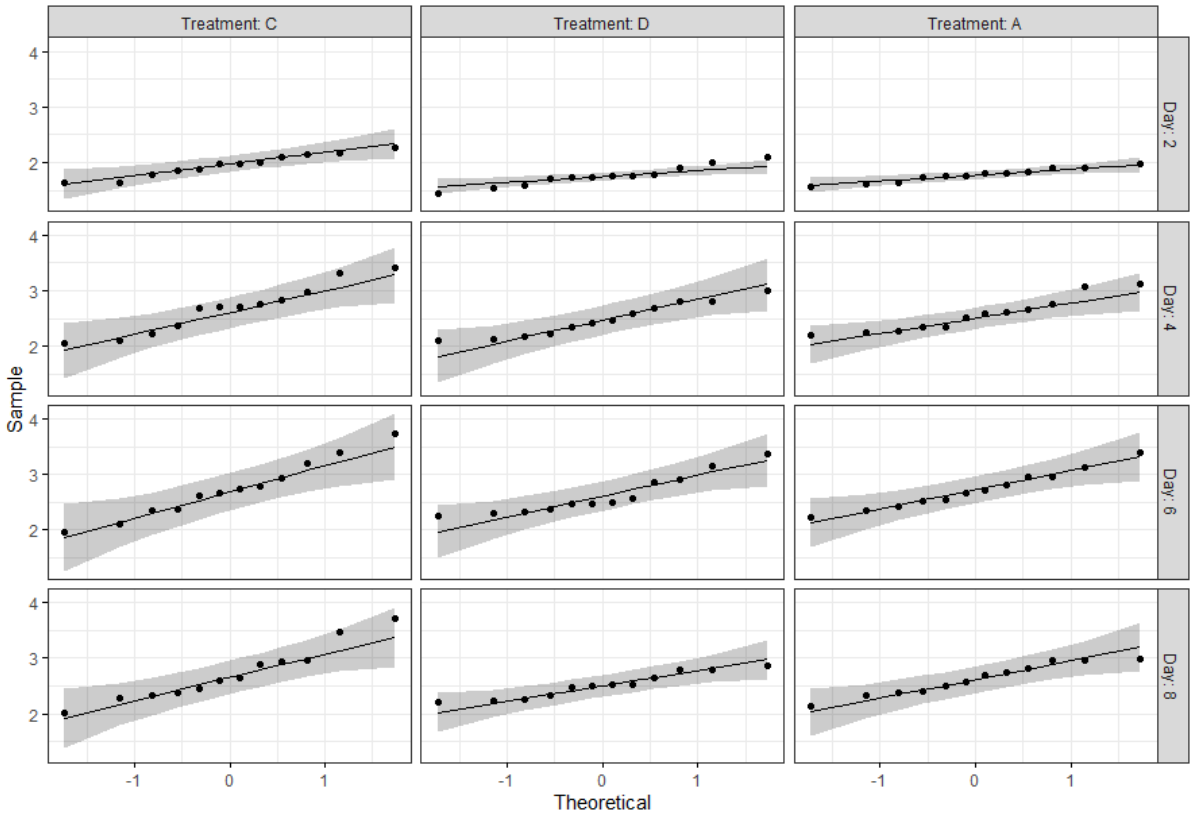

Supplementary Data Figure 2.3 *Goniastrea retiformis* square root transformed growth rate QQ plot ANOVA normality validation, ANOVA is performed on days 2 to 8; day 0 is excluded due to normalization resulting in the same variance between samples.

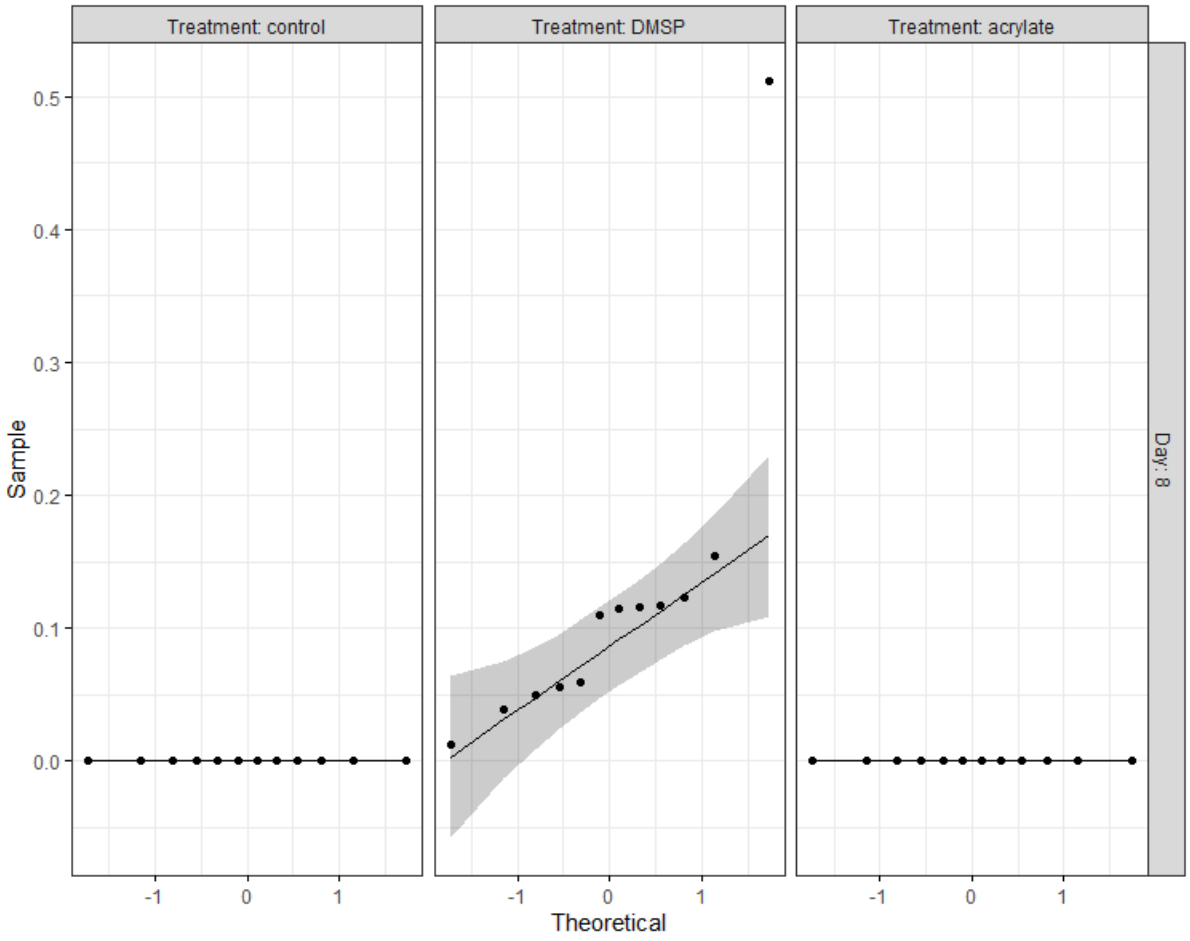

Supplementary Data Figure 2.4 QQ plot of *Goniastrea retiformis* DMSP concentration per polyp in different treatments

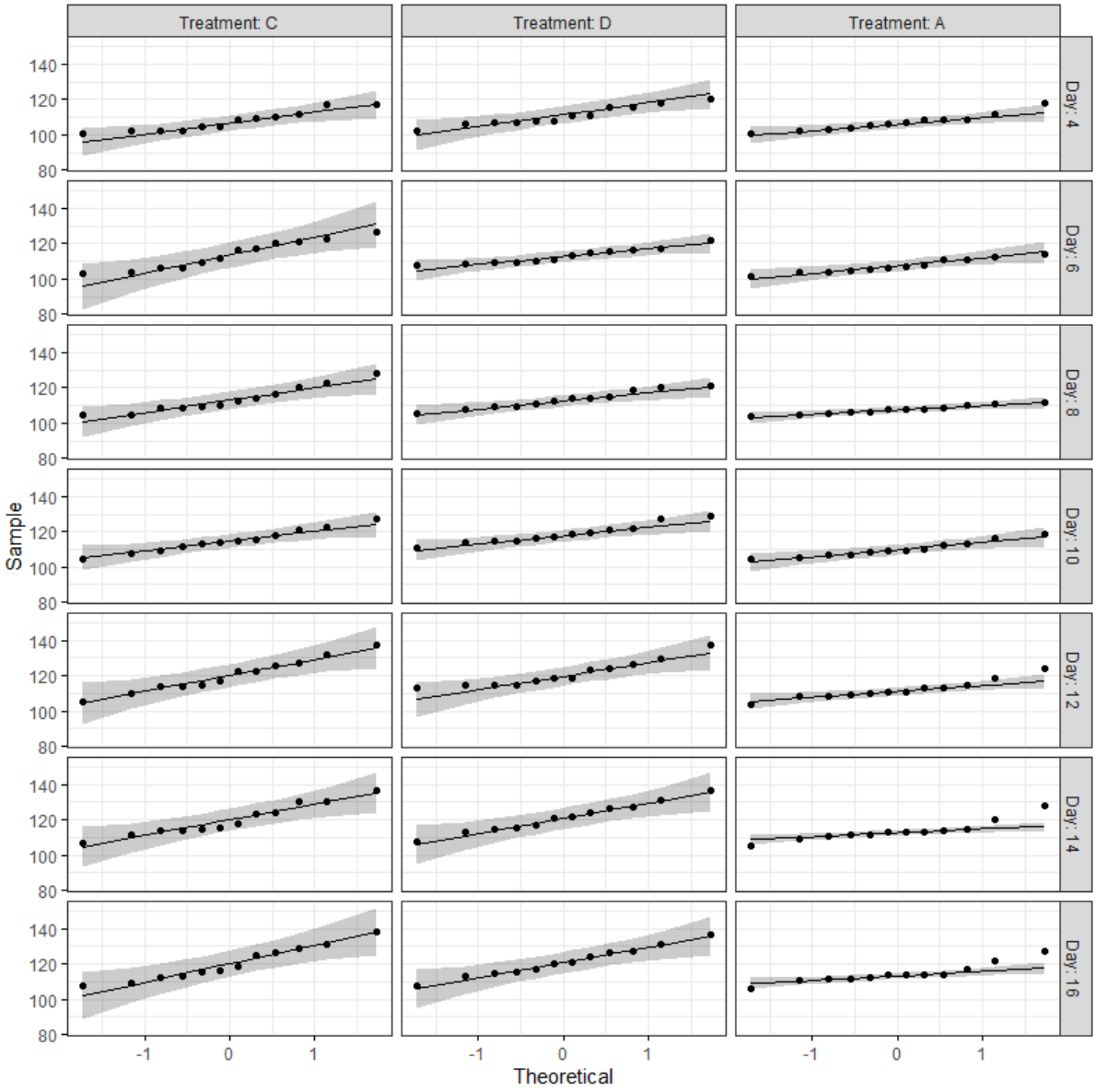

Supplementary Data Figure 2.5 QQ plot for percentage of growth of *Acropora kenti* juvenile reared 16 days in different treatments.

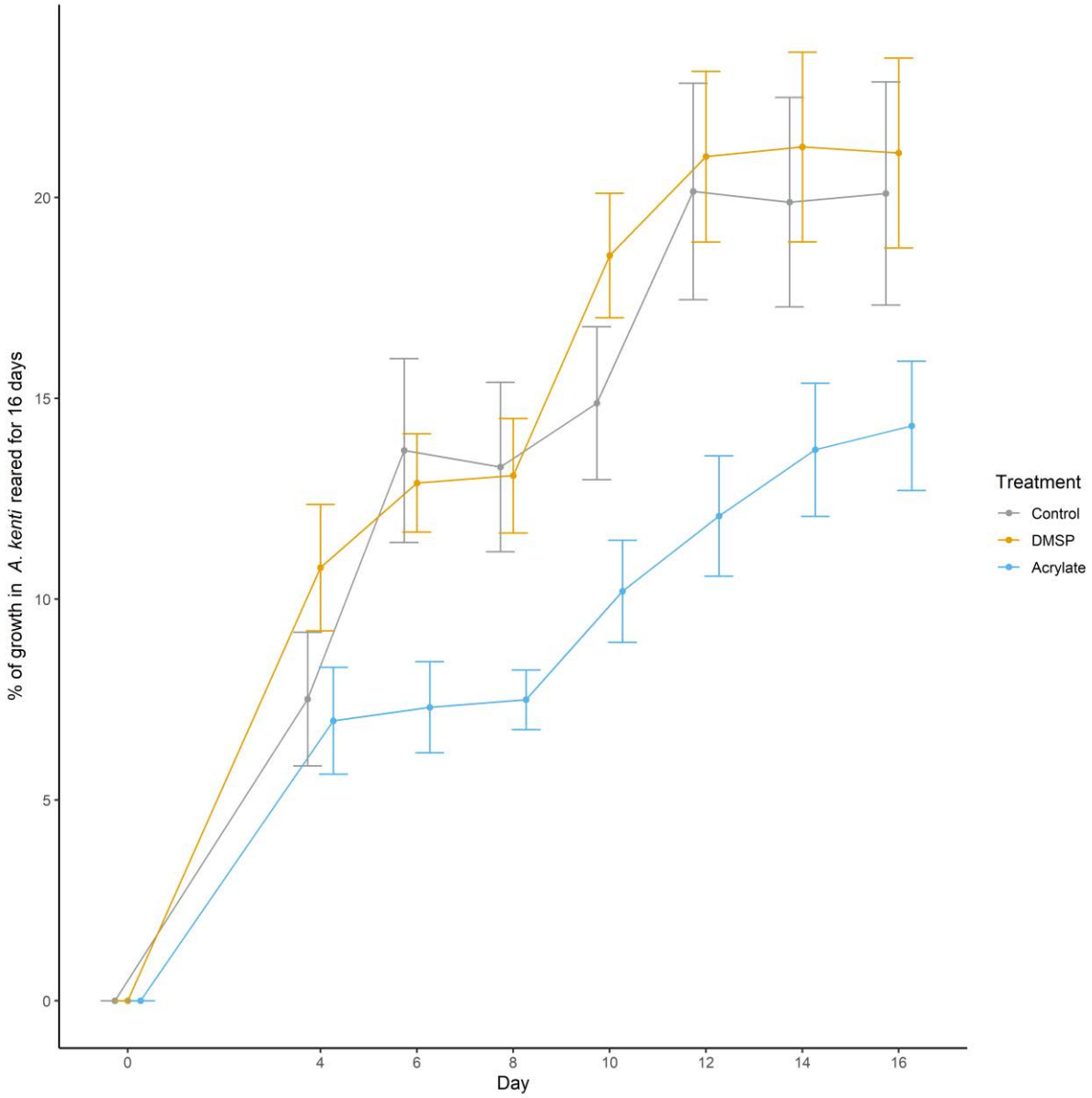

Supplementary Data Figure 2.6 Percentage growth of aposymbiotic *Acropora kenti* juveniles (%)reared for 16 days in the three different treatments: dimethylsulfoniopropionate (DMSP), acrylate and control. Points represent mean and error bar represents ± SE.

For *A. kenti* juveniles that were maintained for the full 16 days of the experiment, for coral growth there is significant interaction between treatments, as determined by a 2-way ANOVA ($F_{12,132}$ =3.547; p= .00014; Supplementary Data Figure 2.6). The effect of treatment was also analysed at each earlier time point, with Day 10 the only time point where there was a significant difference in growth between treatments (adj-p = .028). Simple time effect shows that by Day 16 there is significant growth in all treatments compared to Day 0 ($p<.05$). Pairwise comparison shows significant differences in the growth rates in DMSP and acrylate treatments from Day 6 to Day 12 ($p<.05$). The growth trend of *A. kenti* juveniles that were maintained for the full 16 days of the experiment was similar to that when including the

growth measurement of coral juveniles extracted from all timepoints (Figure 2.2), therefore those data were included to provide a larger data set and more robust statistical result.

S2 Supplementary data for Chapter 3

Coral surface area measurement ImageJ script

```
//masks="Training Set_Simple Segmentation__.tif";
//training="Training Set.tif";
//roiDir="C:\\Temp\\"

run("Options...", "iterations=1 count=1 black");

fs=File.separator;
roiManager("Associate", "false");
roiManager("Centered", "false");
roiManager("UseNames", "false");


dir=getDirectory("Select Source Directory");
list=getFileList(dir);
roiDir=dir+"ROIs"+fs;
File.makeDirectory(roiDir);
saveDir=dir+"Output"+fs;
File.makeDirectory(saveDir);

Dialog.create("Analysis Settings");
Dialog.addNumber("How Many Pixels is 10mm?", 1180); //1180
Dialog.addNumber("Size Cutoff for Positive Count (mm^2)",
0.550);
Dialog.addNumber("Circularity Cutoff for Positive Count (0-
1.0)", 0.05);
Dialog.addNumber("Live Coral Mask Number", 1);
Dialog.addNumber("Starting Point of Background Ring from Coral
(px)",5);
Dialog.addNumber("Width of Background Ring (px)",3);

Dialog.show();

howLong10mm=Dialog.getNumber();
sizeCutoff=Dialog.getNumber();
circCutoff=Dialog.getNumber();
maskNumber=Dialog.getNumber();
ringStart=Dialog.getNumber();
ringWidth=Dialog.getNumber();


tableTitle="[Coral Analysis]";
if (isOpen("Coral Analysis")){
      print("Table already open");}

      else{
```

```
                run("Table...", "name="+tableTitle+" width=1200
height=250");
                print(tableTitle, "\\Headings:Image Name\tLive Coral
ID Number\tArea (mm^2)\tPerimeter (mm)\tCoral Red Mean\tCoral Green
Mean\tCoral Blue Mean\tBackground Red Mean\tBackground Green
Mean\tBackground Blue Mean\tCoral Hue Mean\tCoral Saturation
Mean\tCoral Brightness Mean\tBackground Hue Mean\tBackground
Saturation Mean\tBackground Brightness Mean");
           }

           setBatchMode(true);

           fileCount=1;

     roiManager("reset");
     for(i=0;i<list.length;i++){
           roiManager("reset");
           run("Set Measurements...", "area mean perimeter display
redirect=None decimal=3");
           fileName=dir+list[i];
           if(endsWith(fileName, "tif")){
                print("Processing file "+fileCount+" of
"+(list.length/2));
                open(fileName);
                origImage=getTitle();
                saveName=File.getNameWithoutExtension(fileName);
                maskName=dir+list[i+1];
                open(maskName);
                maskImage=getTitle();
                print(origImage);
                print(maskImage);

                selectWindow(maskImage);
                setThreshold(maskNumber,maskNumber);
                run("Clear Results");
                run("Measure");

                if(nResults>=1){
                     run("Create Mask");

                     selectWindow("mask");
                     run("Set Scale...", "distance="+howLong10mm+"
known=10 unit=mm");

                     run("Analyze Particles...",
"size="+sizeCutoff+"-Infinity circularity="+circCutoff+"-1.00
show=Masks display clear");

                     if(nResults>=1){

                          selectWindow("Mask of mask");
                          rename("Live Mask");
                          run("Invert LUT");
                          run("Fill Holes");
```

```
                            selectWindow("mask");
                            close();
                            //selectWindow("Live Mask");
                            //run("Duplicate...", "title=[For
Dilate]");
                            //run("Options...",
"iterations="+(ringStart+ringWidth)+" count=1 black do=Dilate");

                            //selectWindow("Live Mask");
                            //run("Duplicate...", "title=[For
Dilate2]");
                            //run("Options...",
"iterations="+ringStart+" count=1 black do=Dilate");

                            //imageCalculator("Subtract create", "For
Dilate","For Dilate2");
                            //selectWindow("Result of For Dilate");
                            //rename("Background Ring");

                            //selectWindow("For Dilate");
                            //close();
                            //selectWindow("For Dilate2");
                            //close();

                            selectWindow(origImage);
                            run("Duplicate...", "title=[For HSB]");
                            selectWindow(origImage);
                            run("RGB Stack");
                            run("Make Composite",
"display=Composite");

                            selectWindow("For HSB");
                            wait(200);
                            run("HSB Stack");

     wait(200);

                            selectWindow("Live Mask");
                            getDimensions(width, height, channels,
slices, frames);
                            run("Analyze Particles...", "add");
                            roiManager("Save", roiDir+origImage+" -
Live Rois.zip");

                            numROIs=roiManager("count");
                            //roiManager("reset");
                            //wait(200);

                            //selectWindow("Background Ring");
                            //run("Analyze Particles...", "add");
                            //roiManager("Save", roiDir+origImage+" -
Ring Rois.zip");

                            //roiManager("reset");
                            //wait(200);
```

```
                              //print(numRois);

                              newImage("Background Ring", "8-bit
black", width, height, 1);

                              for(r=0;r<numROIs;r++){
                                   print("Measuring Coral "+(r+1)+" of
"+numROIs);
                                   run("Set Measurements...", "area
mean perimeter display redirect=["+origImage+"] decimal=3");
                                   selectWindow("Live Mask");
                                   //roiManager("Open",
roiDir+origImage+" - Live Rois.zip");

                                   selectWindow(origImage);
                                   setSlice(1);
                                   run("Set Scale...",
"distance="+howLong10mm+" known=10 unit=mm");

                                   selectWindow("Live Mask");
                                   roiManager("Select", r);
                                   run("Analyze Particles...",
"display");
                                   coralArea=getResult("Area");
                                   coralPerimeter=getResult("Perim.");
                                   coralRed=getResult("Mean");
                                   selectWindow(origImage);
                                   setSlice(2);

                                   selectWindow("Live Mask");
                                   run("Analyze Particles...",
"display");
                                   coralGreen=getResult("Mean");
                                   selectWindow(origImage);
                                   setSlice(3);

                                   selectWindow("Live Mask");
                                   run("Analyze Particles...",
"display");
                                   coralBlue=getResult("Mean");

                                   run("Set Measurements...", "area
mean perimeter display redirect=[For HSB] decimal=3");

                         //              selectWindow("For HSB");
                         //              setSlice(1);
                         //              run("Set Scale...",
"distance="+howLong10mm+" known=10 unit=mm");

                         //              selectWindow("Live Mask");
                         //              roiManager("Select", r);
                         //              run("Analyze Particles...",
"display");
                         //              coralHue=getResult("Mean");
                         //              selectWindow("For HSB");
                         //              setSlice(2);
```

```
                //              selectWindow("Live Mask");
                //              run("Analyze Particles...",
"display");
                //              coralSaturation=getResult("Mean");
                //              selectWindow("For HSB");
                //              setSlice(3);

                //              selectWindow("Live Mask");
                //              run("Analyze Particles...",
"display");
                //              coralBrightness=getResult("Mean");


                                selectWindow("Live Mask");
                                roiManager("select", r);
                                run("Enlarge...",
"enlarge="+(ringStart+ringWidth)+" pixel");
                                run("Create Mask");
                                selectWindow("Mask");
                                rename("Outer Ring");

                                selectWindow("Live Mask");
                                roiManager("select", r);
                                run("Enlarge...",
"enlarge="+ringStart+" pixel");
                                run("Create Mask");
                                selectWindow("Mask");
                                rename("Inner Ring");

                                imageCalculator("Subtract", "Outer
Ring","Inner Ring");
                                selectWindow("Inner Ring");
                                close();

                                run("Set Measurements...", "area
mean perimeter display redirect=["+origImage+"] decimal=3");

                                selectWindow(origImage);
                                setSlice(1);
                                selectWindow("Outer Ring");
                                run("Analyze Particles...",
"display");
                                backgroundRed=getResult("Mean");
                                selectWindow(origImage);
                                setSlice(2);
                                selectWindow("Outer Ring");
                                run("Analyze Particles...",
"display");
                                backgroundGreen=getResult("Mean");
                                selectWindow(origImage);

                                setSlice(3);
                                selectWindow("Outer Ring");
                                run("Analyze Particles...",
"display");
```

```
                                backgroundBlue=getResult("Mean");

                //              run("Set Measurements...", "area
mean perimeter display redirect=[For HSB] decimal=3");

                //              selectWindow("For HSB");
                //              setSlice(1);
                //              selectWindow("Outer Ring");
                //              run("Analyze Particles...",
"display");
                //              backgroundHue=getResult("Mean");
                //              selectWindow("For HSB");
                //              setSlice(2);
                //              selectWindow("Outer Ring");
                //              run("Analyze Particles...",
"display");
                //
     backgroundSaturation=getResult("Mean");
                //              selectWindow("For HSB");

                //              setSlice(3);
                //              selectWindow("Outer Ring");
                //              run("Analyze Particles...",
"display");
                //
     backgroundBrightness=getResult("Mean");

                                imageCalculator("Add", "Background
Ring","Outer Ring");
                                selectWindow("Outer Ring");
                                close();


                                print(tableTitle,
origImage+"\t"+(r+1)+"\t"+coralArea+"\t"+coralPerimeter+"\t"+coralRe
d+"\t"+coralGreen+"\t"+coralBlue+"\t"+backgroundRed+"\t"+backgroundG
reen+"\t"+backgroundBlue

     //+"\t"+coralHue+"\t"+coralSaturation+"\t"+coralBrightness+"\t"
+backgroundHue+"\t"+backgroundSaturation+"\t"+backgroundBrightness
                                );


                           }

                           //roiManager("reset");
                           selectWindow("Background Ring");
                           run("Select None");
                           run("Subtract...", "value=150");
                           run("Select All");
                           run("Copy");
                           selectImage(origImage);
                           run("Add Slice", "add=channel");
                           Stack.setChannel(4);
                           run("Paste");
                           run("Cyan");
```

```
                              run("RGB Color");
                              selectWindow(origImage+" (RGB)");
                              roiManager("show all with labels");
                              run("Flatten");
                              selectWindow(origImage+" (RGB)-1");

                              saveAs("Tiff", saveDir+saveName+" - Live
Selection.tif");
                              run("Close All");

                              selectWindow("Results");
                              run("Close");

                         }
                         run("Close All");
                         }
     }
                         i=i+1;
                         fileCount=fileCount+1;


                         }

     selectWindow("Coral Analysis");
     saveAs("Results", saveDir+"Coral Analysis.csv");
     run("Close");

     print("FINISHED!!!");
```

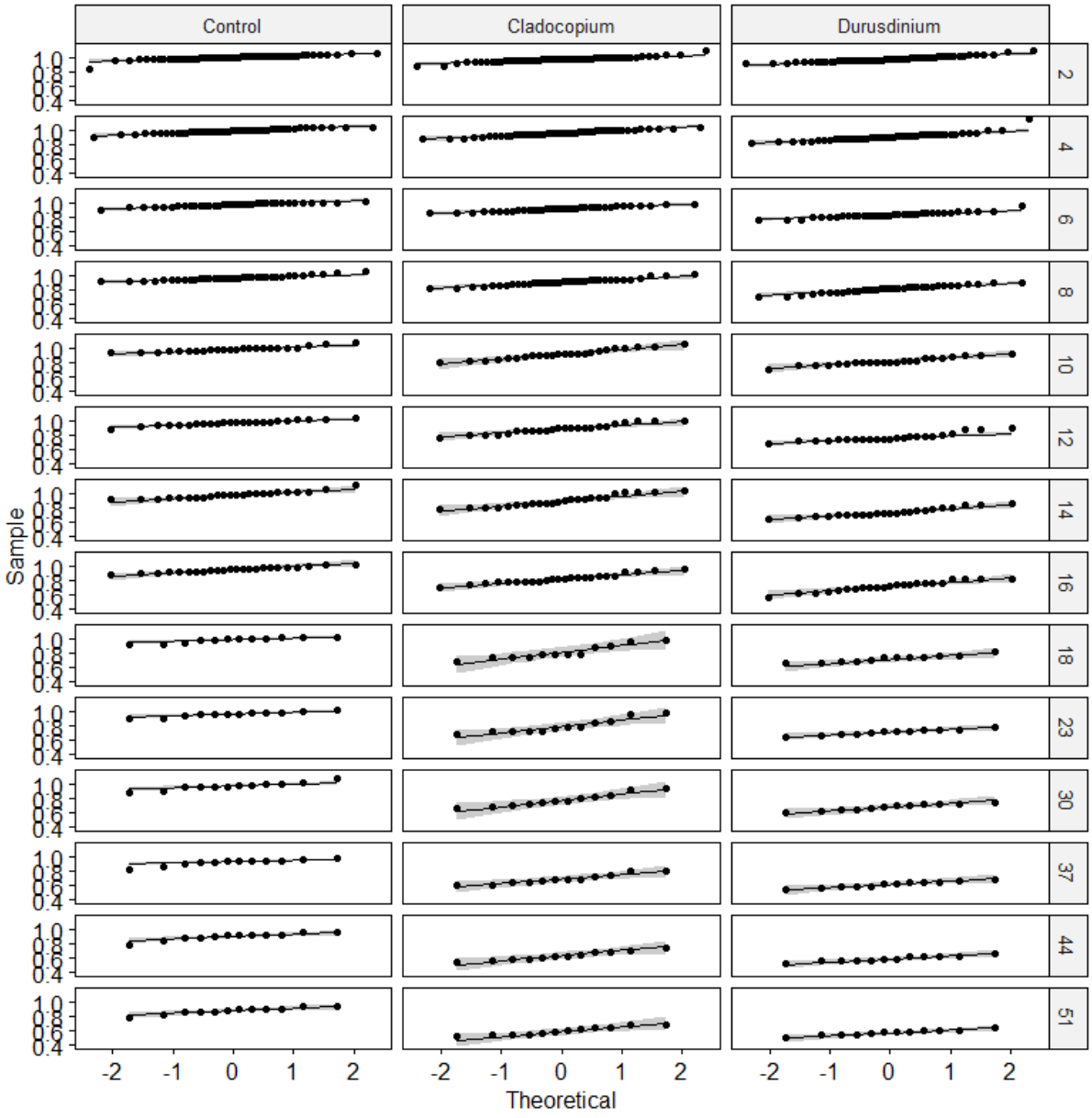

Supplementary Data Figure 3.1 QQplot for *Acropora kenti* growth per polyp in the different treatments and at different times in inverse response transformation

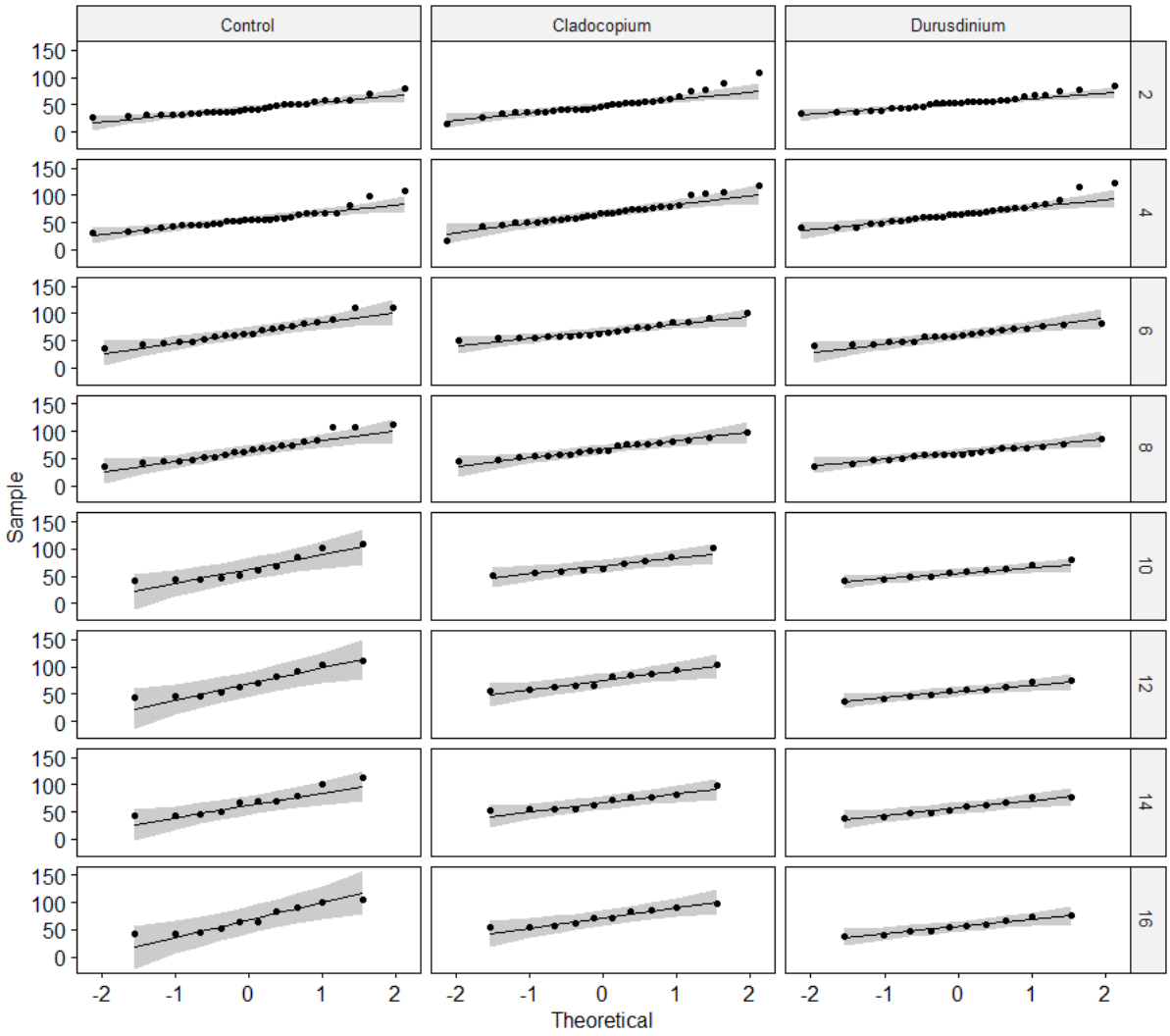

Supplementary Data Figure 3.2 QQ plot of *Goniastrea aspera* growth in normal response

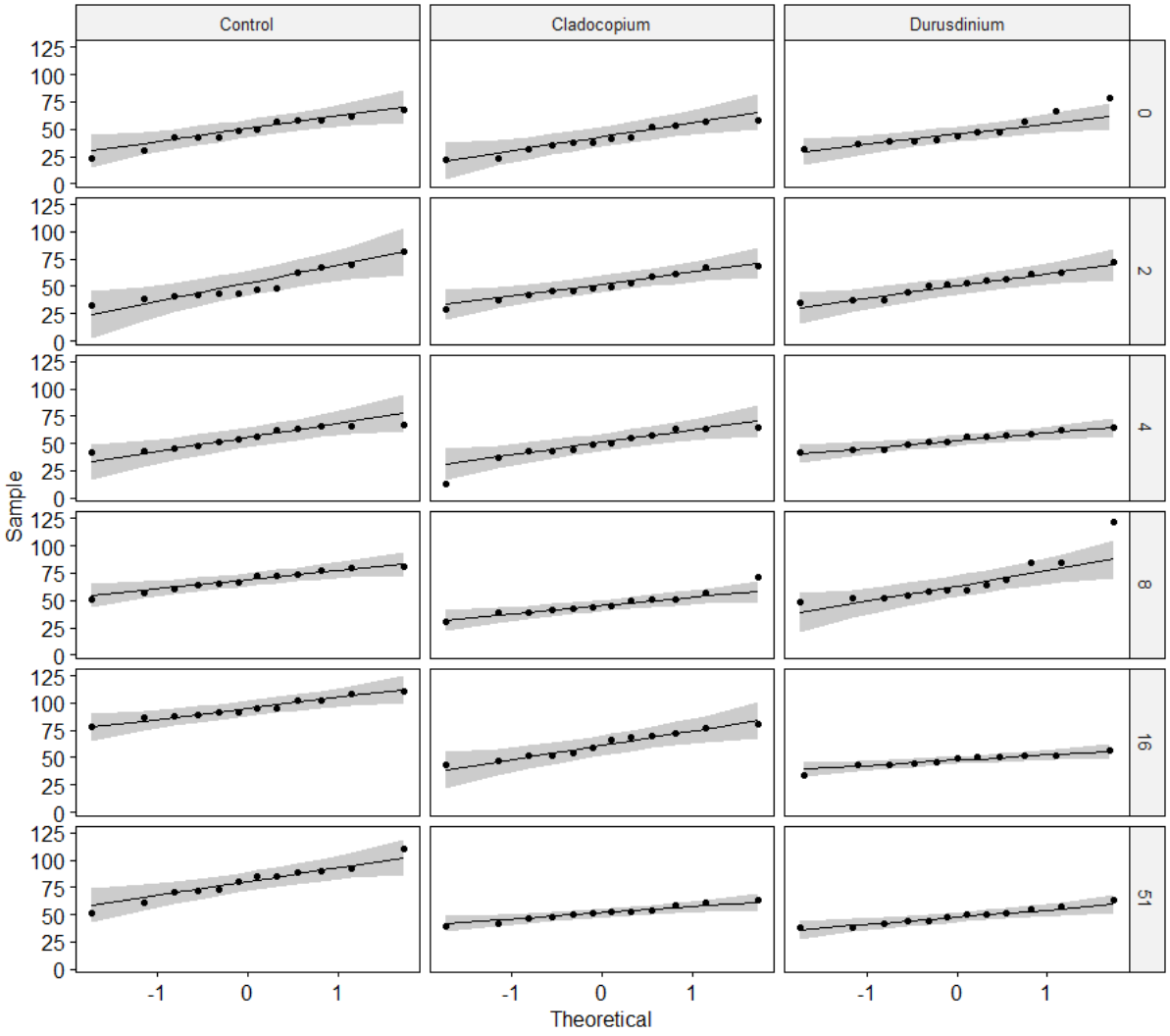

Supplementary Data Figure 3.3 QQ plot for *Acropora kenti* DMSP concentration per polyp in Inverse response transformation

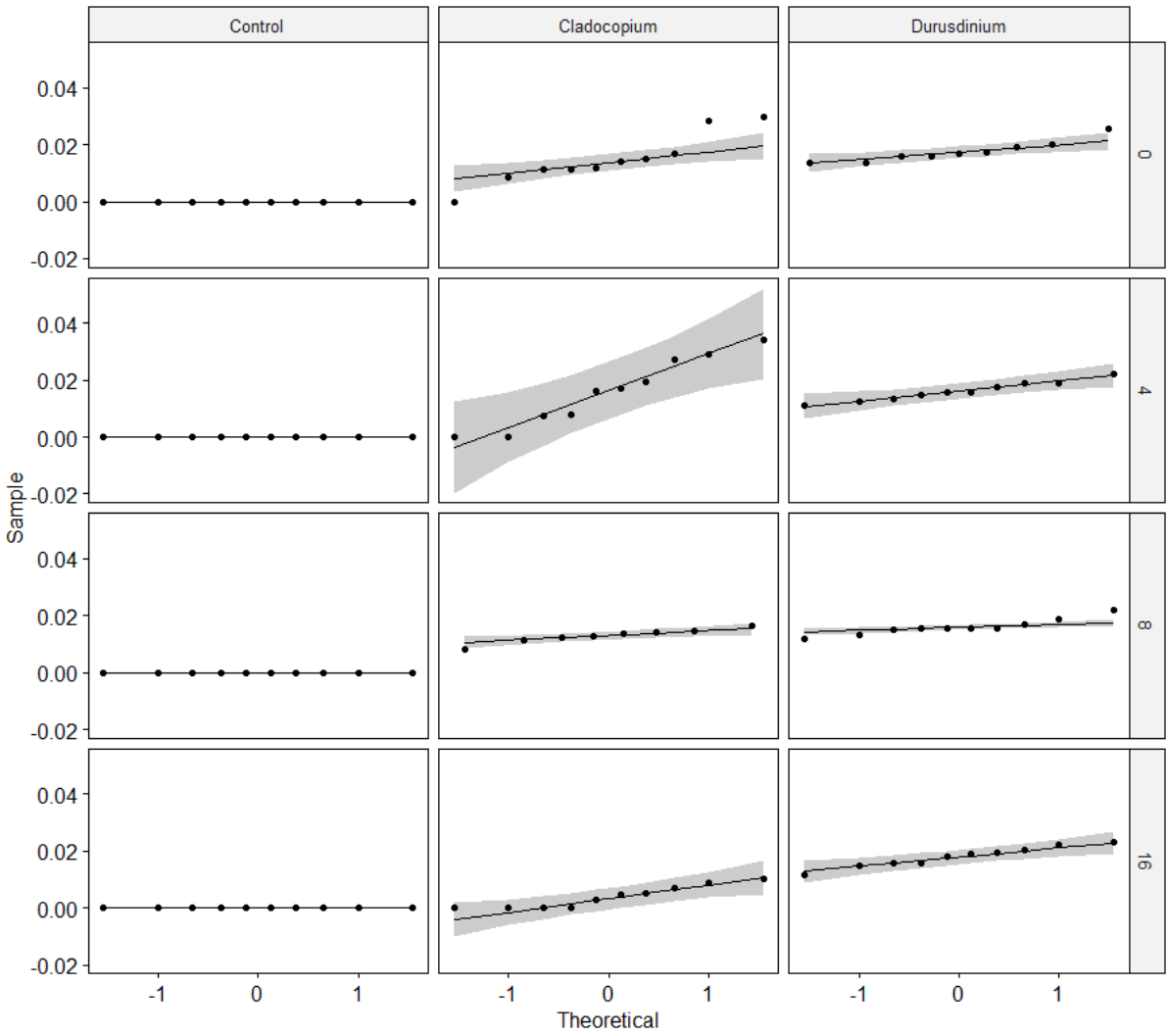

Supplementary Data Figure 3.4 QQ plot for *Goniastrea aspera* DMSP concentration per polyp in square root response transformation

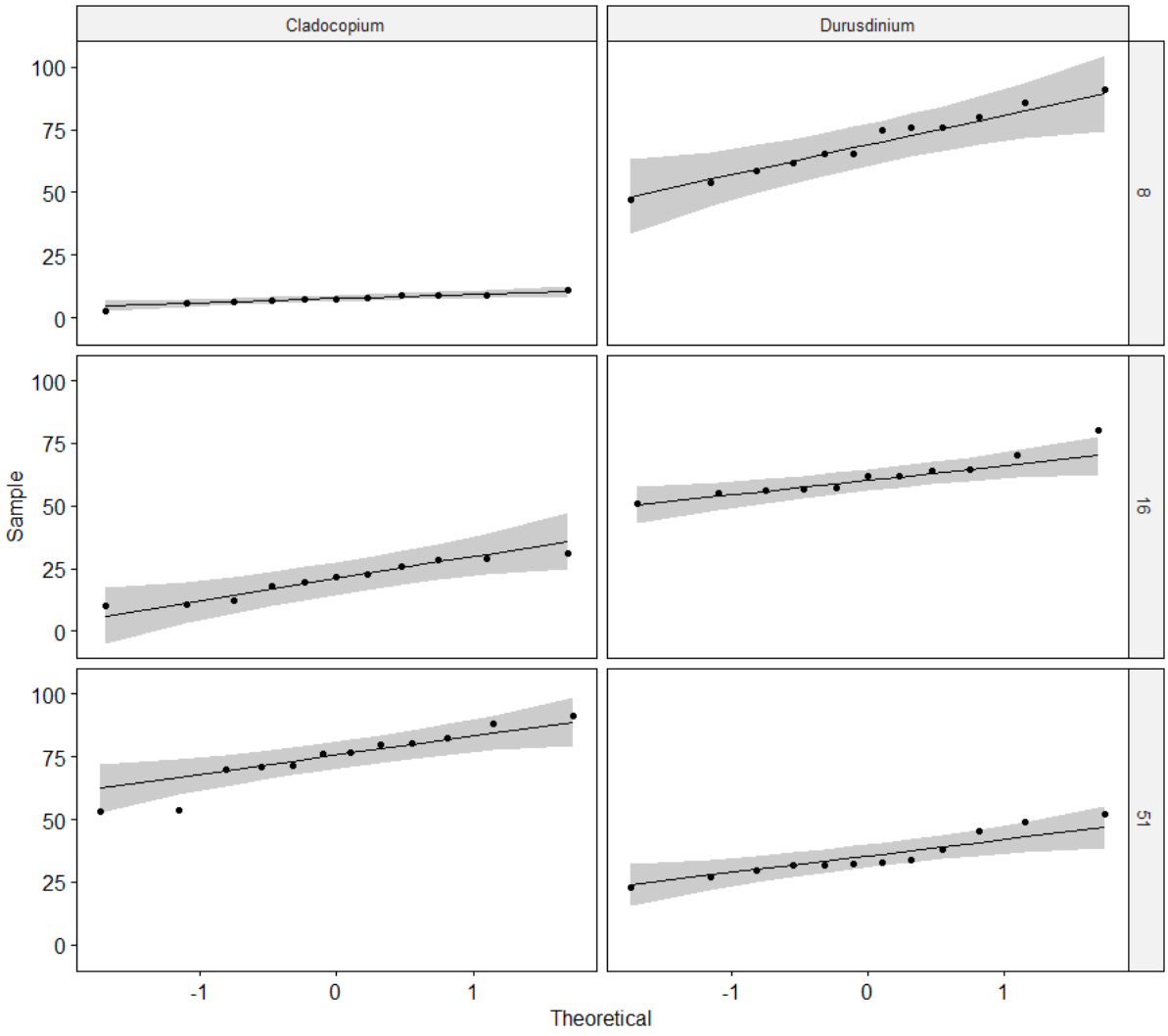

Supplementary Data Figure 3.5 QQ plot of *Acropora kenti* Symbiodiniaceae cell density in square root transformation

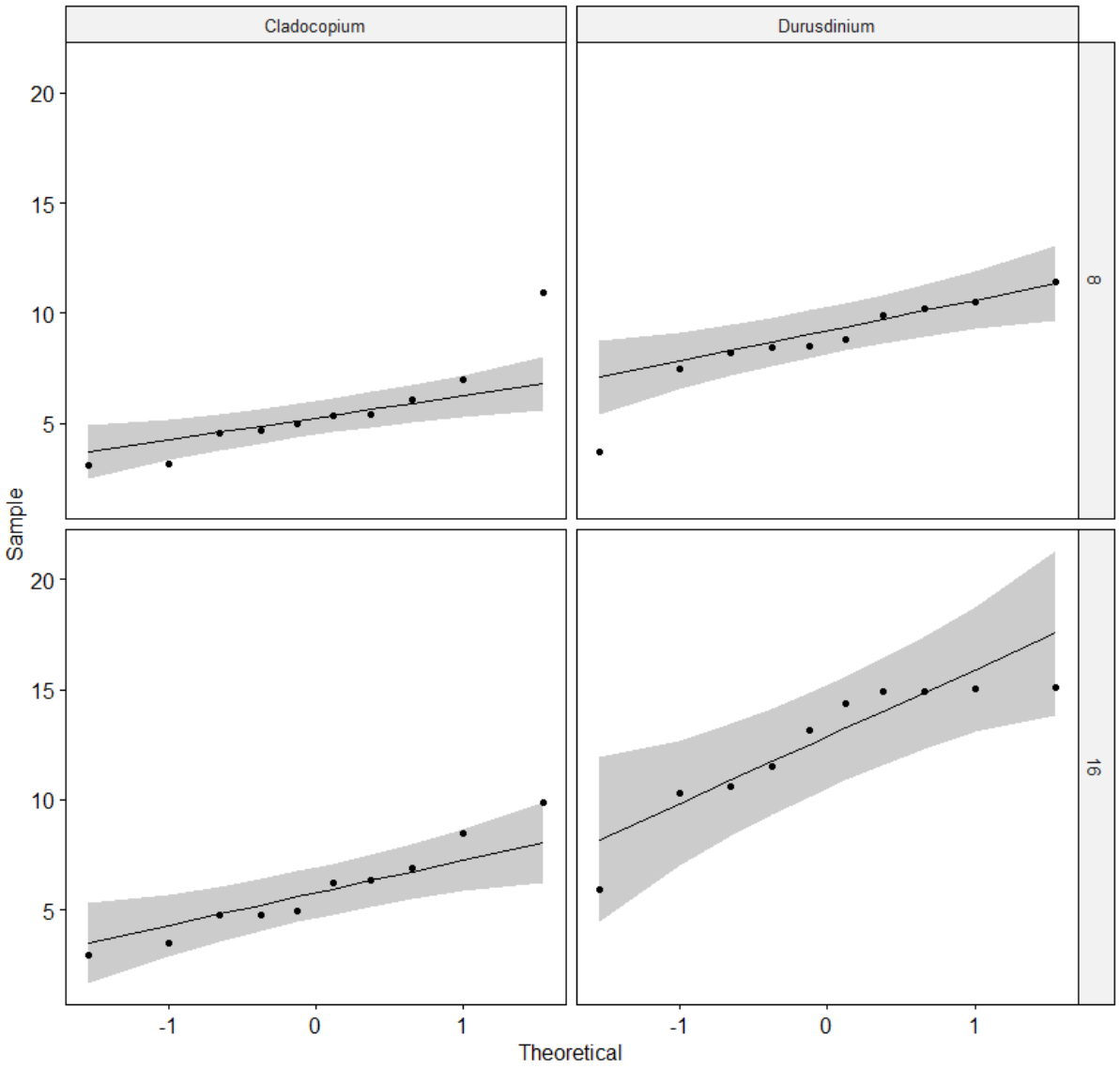

Supplementary Data Figure 3.6 QQ plot of *Goniastrea aspera* Symbiodiniaceae cell density in cube root transformation

Supplementary Table 3.1 Kaplan-Meier survival plot analysis of *Acropora kenti* survivability on different days and treatments

Treatment=Control

time	n.risk	n.event	survival	std.err	lower 95% CI	upper 95% CI
14	925	1	0.999	0.00108	0.997	1.000
23	924	1	0.998	0.00153	0.995	1.000
37	923	19	0.977	0.00490	0.968	0.987
44	904	37	0.937	0.00797	0.922	0.953

Treatment=*Cladocopium*

time	n.risk	n.event	survival	std.err	lower 95% CI	upper 95% CI
6	836	3	0.996	0.00207	0.992	1.000
8	833	2	0.994	0.00267	0.989	0.999
12	831	1	0.993	0.00292	0.987	0.999
16	830	1	0.992	0.00315	0.985	0.998
37	829	1	0.990	0.00337	0.984	0.997

Treatment=*Durusdinium*

time	n.risk	n.event	survival	std.err	lower 95% CI	upper 95% CI
2	913	1	0.999	0.00109	0.997	1.000
4	912	1	0.998	0.00155	0.995	1.000
8	911	1	0.997	0.00189	0.993	1.000
23	910	3	0.993	0.00267	0.988	0.999
30	907	1	0.992	0.00289	0.987	0.998

37	**906**	**1**	**0.991**	**0.00308**	**0.985**	**0.997**
44	**905**	**1**	**0.990**	**0.00327**	**0.984**	**0.997**

Supplementary Table 3.2 Kaplan-Meier survival plot analysis of *Goniastrea aspera* survivability on different days and treatments

Treatment=Control

time	**n.risk**	**n.event**	**survival**	**std.err**	**lower 95% CI**	**upper 95% CI**
0	**274**	**3**	**0.989**	**0.00629**	**0.977**	**1**
12	**271**	**1**	**0.985**	**0.00725**	**0.971**	**1**

Treatment=*Cladocopium*

time	**n.risk**	**n.event**	**survival**	**std.err**	**lower 95% CI**	**upper 95% CI**
2	**315**	**1**	**0.997**	**0.00317**	**0.991**	**1**
10	**314**	**1**	**0.994**	**0.00448**	**0.985**	**1**
14	**313**	**1**	**0.990**	**0.00547**	**0.980**	**1**

Treatment=*Durusdinium*

time	**n.risk**	**n.event**	**survival**	**std.err**	**lower 95% CI**	**upper 95% CI**
8	**347**	**2**	**0.994**	**0.00406**	**0.986**	**1**
10	**345**	**1**	**0.991**	**0.00497**	**0.982**	**1**

Supplementary Table 3.3 Symbiodiniaceae assemblage of *Goniastrea aspera* parental colony

ITS2 type profile UID	**317921**
Clade	D
Majority ITS2 sequence	D1
Associated species	None
ITS2 profile abundance local	1
ITS2 profile abundance DB	11
ITS2 type profile	D1/D4-D1u
159086	0.923474428
Sequence accession / SymPortal UID	853-854-10613
Average defining sequence proportions and [stdev]	0.618[nan]-0.346[nan]-0.036[nan]

Appendix A

Conditions conducive to coral larval settlement

Individual coral juveniles contain low levels of DMSP and detection requires the use of high-resolution techniques such as LC-MS; for other methods such as ^{1}H-qNMR pre-concentration is required. Here, the experiment was designed to ensure adequate recruit density to produce high enough levels of DMSP for detection. Similarly, to account for variability in growth between individuals within the same treatment and same well, a higher number of recruits are required to improve the reliability of the size measurements. The challenge here is that high settlement densities may increase intraspecific competition for food resources (Suzuki et al. 2012; Cameron and Harrison 2020), therefore, optimising recruit densities to exceed analytical detection limits while maintaining healthy experimental corals was critical to this study.

A preliminary trial was conducted and found that 20 or more *Acropora kenti* recruits were required per well to extract sufficient material from the sample to quantify intracellular DMSP; smaller species, such as *Goniastrea,* may need more live tissue. Here, the desired settlement density chosen was ~30 recruits per well; on average, 3 recruits per cm^2 was achieved. This density is higher than the 0.5-1.5 recruits per cm^2 used to explore restoration methods (Omori and Iwao 2014; Cameron and Harrison 2020) but less than that for *Acropora* species settling on preconditioned tiles, with 10 recruits per cm^2 deployed *in situ* (Doropoulos et al. 2017). Regardless, as the experiment duration was short, i.e., only 16 days, the effect of the density-dependent competition is likely to be negligible. In addition, as seawater was exchanged regularly, recruits experienced optimal environmental conditions. The high survival rate (*A. kenti* 98.3%; *G. retiformis*: 92.8%) indicates the coral juveniles are not suffering lethal stress (Cameron and Harrison 2020; Randall et al. 2021).

The choice of settlement method was dictated by the need to eliminate the introduction of an additional DMSP or acrylate source into the experiment while preferentially settling larvae on the base of the well to facilitate fine-scale growth measurements. Traditional settlement methods use preconditioned settlement tiles. These routinely return a high settlement rate. The predominate biofouling species on these, CCA, acts as the larval settlement inducer (Morse et al. 1996) and is widely used in laboratory settlement studies, including in 6-well plates. CCA “fairy dust” (Meyer et al. 2009) and a synthetic peptide GLW-amide (Iwao et al. 2002) were also considered here. During settlement

trials of *A. kenti*, both of these settlement inducers resulted in high coral recruit settlement rates. However, recruits tended to settle at the edges of the well, which is not suitable for later growth measurement. Instead, a CCA chip was placed in the centre of the well to directionally induce recruit settlement around the chip and was established to be the most optimal settlement cue. As CCA can produce DMSP, the live CCA chips were removed 24 hours after settlement to minimize any uptake (Burdett et al. 2014). The settlement of *G. retiformis* larvae was previously achieved with coral rubble (Heyward and Negri 1999), and this physical structure is favoured over the smoother edge of the plate well (Whalan et al. 2015). Based on observations from settlement trials, *G. retiformis* larvae preferred to settle beneath the rubble on the bottom of the well plate. Therefore, 2 to 3 cm^2 of concave-shaped rubble is recommended to create a spacious sheltered area under which *G. retiformis* larvae will settle, i.e., at the centre of the well plate.